IN SITU MEASUREMENTS BY INSTRUMENTED GREY SEALS (*HALICHOERUS GRYPUS*) REVEAL FINE-SCALE OCEANOGRAPHIC PROPERTIES AND ENVIRONMENTAL INFLUENCES ON MOVEMENT PATTERNS

by

Bernadette Victoria Rose Nowak

Submitted in partial fulfilment of the requirements
for the degree of Master of Science

at

Dalhousie University
Halifax, Nova Scotia
March 2019

I dedicate this thesis to my dad, who has been a constant example of how to work hard and be excited about life, and to my mom and nana, for never letting me believe there was something I couldn't do.

TABLE OF CONTENTS

LIST OF TABLES

LIST OF FIGURES

ABSTRACT

The influence of oceanographic conditions on the movements of large marine predators has been demonstrated in diverse taxa. However, obtaining subsurface data that are spatio-temporally relevant to the decisions made by benthically-foraging species can be challenging. Between the years 2009 and 2015, 117 grey seals (*Halichoerus grypus*) were captured on Sable Island, NS and instrumented with Mk10-AF Fastloc^{TM} GPS devices. A bio-optical model for the estimation of chlorophyll-*a* using light attenuation was developed by performing a replicated experiment in the Bedford Basin. This model was applied to data collected *in situ* by grey seals and, along with other oceanographic conditions, mapped across the Scotian Shelf, providing high spatio-temporal coverage. Behavioural states were estimated from location data using the hidden Markov movement model. Generalized linear mixed-effects models indicated that grey seal behaviours are influenced by the fine-scale chlorophyll-*a* and environmental conditions they encounter across the oceanographically heterogeneous Scotian Shelf.

LIST OF ABBREVIATIONS USED

A_{CDOM}	CDOM absorbance
$A_{CDOM}(465)$	absorbance of CDOM at 465 nm
$a_{CDOM}(465)$	spectral absorption coefficient of CDOM at 465 nm
AIC	Akaike Information Criterion
ARS	area-restricted search
AUV	autonomous underwater vehicle
BB	Bedford Basin
CDOM	coloured dissolved organic matter
chl-*a*	chlorophyll-*a*
CSS	central Scotian Shelf
DCRWS	first-difference correlated random walk switching
E_d	downwelling irradiance (W m^{-2})
ESS	eastern Scotian Shelf
F_{CDOM}	CDOM fluorescence (V)
$F_{chl\text{-}a}$	chl-*a* fluorescence (V)
GLMM	generalized linear mixed-effects model
GSL	Gulf of St. Lawrence
HMMM	hidden Markov movement model
K_d	diffuse attenuation coefficient of downwelling irradiance (m^{-1})
$K_d(465)_{chl\text{-}a}$	K_d estimated using chl-*a* at 465 nm (m^{-1})
$K_d(465)_{HyperPro}$	K_d estimated by the HyperPro at 465 nm (m^{-1})
LA	light attenuation (m^{-1})
LA_{HP}	light attenuation estimated by the HyperPro at 465 nm (m^{-1})
LL	light level
LME	Large Marine Ecosystem
$MAPE$	mean absolute percentage error
MCP	minimum convex polygon
MLD	mixed layer depth (m)

NPQ	non-photochemical quenching
NSC	Nova Scotia Current
PQL	penalized quasilikelihood
RMSE	root mean square error
SS	Scotian Shelf
SST	sea surface temperature (ºC)
T_{50}	upper-water column temperature (ºC)
TDLR	time-depth-light recorder
WC-DAP	Wildlife Computers Data Analysis Program
WSS	western Scotian Shelf

ACKNOWLEDGEMENTS

There have been many people in my life, both during this degree and in the years leading up to it, that have made this thesis possible. I must first acknowledge the continued support of my supervisor, Dr. Don Bowen, who has been extremely patient throughout this entire process, willingly offering as much time and resources as I needed. Thank you for inspiring me to be curious and ask big questions, and more importantly look for ways to answer them. To my other supervisor, Dr. Sara Iverson, for being an excellent role model in communicating science and encouraging me on countless occasions to follow in her footsteps. Most importantly, to both of them for allowing me the opportunity to do field work on Sable Island, which has been one of the most incredible and exciting things I will ever do. I would like to thank Dr. Joanna Mills Flemming for serving on my committee and taking to time to provide honest advice throughout my degree. I would also like to thank Dr. Jinyu Sheng for serving on my committee and Dr. Rob Harcourt for acting as my external examiner. Thank you to Dr. Katja Fennel for her role in the inception of this project.

This degree would not have been possible without the financial support from OTN Canada (NSERC and CFI), NSERC Discovery Grants of Don Bowen and Sara Iverson, Dalhousie University and the Nova Scotia Graduate Scholarship, and the Department of Fisheries and Oceans Canada. I would like to acknowledge MEOPAR and Dalhousie University for facilitating and providing data collected in the Bedford Basin. In particular, I would like thank Richard Davis and Anna Haverstock for their continued assistance and patience in helping me explore this dataset. This research would not have been possible without the incredibly hard work of everyone involved in the Sable Island Field Team. I would especially like to thank Dr. Damian Lidgard for his integral role in collecting data for my project as well as being an exceptional labmate, bunkmate, and most of all, friend. Thank you to everyone at the Ocean Tracking Network, who made this more than just a degree and provided me with a platform to share my research.

To all the friends I have made during my time in Halifax: Kim, Fran, Diane, Cailum, Scott, Sarah, Noor, Jacob, Daryl, Marion, and many others. Thank you all for building a community for me here that has made this place my home. Diane, you have

been my family here and listened and laughed with me every step of the way. I would like to thank Fran for reminding me to stay spontaneous and excited about life. There is not even a single chance I would have been able to get through this degree without the emotional, moral, and statistical support from Kim. For listening to every single question or complaint I had, and never showing even a sliver of judgement. Thank you to the many other people who offered statistical advice during my many crises, in particular Sebastian, Steph, and Scott. I would also like to thank my close friends who supported me during my undergraduate degree, namely Jacob and Elyse, who encouraged me to follow my passion for seals wherever it took me.

To my parents, who have been unbelievably supportive in every possible sense of the word. Thank you for teaching me to be determined, resilient, and independent and for always encouraging me to do what makes me happy. To my brothers, Alex and Maks, for keeping me grounded. Thank you to my nana, for giving me my attitude and always reminding me to use it. I would like to acknowledge my friends, who have been so understanding throughout this degree. Tina, you are the most supportive friend I could have asked for and I would not have made it without you and every nine o'clock call. To Emma and Iman, both of you have shown me so much love and support and it means so much to me. Michelle, thank you for always understanding my humour. Vic, for never letting me to take myself too seriously and knowing just how to make me laugh. Cole, thank you for giving me someone to talk to about anything and nothing.

You all mean so much to me and I could have never done it without you.

Benia

CHAPTER 1: INTRODUCTION

1.1 THE GREY SEAL (*HALICHOERUS GRYPUS*) IN CANADA

The grey seal (*Halichoerus grypus*) is a continental shelf phocid species found on both sides of the North Atlantic Ocean. In Canadian waters, this species has been subdivided into three management groups based on breeding colony locations: Gulf of St. Lawrence, coastal Nova Scotia, and Sable Island (Hammill et al. 2017a). Sable Island is the largest breeding colony of grey seals in the world (Bowen et al. 2007) and contributes 85% of pup production for these groups (den Heyer et al. 2017; Hammill et al. 2017b). This population has increased exponentially in size over the past five decades, from an estimated 15,000 individuals in the 1960s (Mohn and Bowen 1996) to approximately 424,300 in 2016 (Hammill et al. 2017a).

Grey seals are sexually size-dimorphic, with males being approximately 1.5 times the size of females (Beck 2002), reaching up to 230 cm and 350 kg in size and 200 cm and 250 kg, respectively (DFO 2014). Grey seals are an iteroparous species, with females producing one pup per reproductive cycle. Breeding occurs between mid-December and late-January and the fertilized egg is implanted after three to four months (Boyd 1984). Gestation lasts seven to eight months and parturition occurs during the following winter (Hewer and Backhouse 1968). Females give birth between December and January and nurse a single pup for approximately 17 days before breeding and abruptly returning to sea (Iverson et al. 1993). In order to support these metabolic demands, females employ a capital breeding strategy, in which they rely on previously acquired energy stores (Iverson et al. 1993). Males either drastically reduce foraging or do not forage at all, and in this respect, are also considered capital breeders (Beck et al. 2003c; Lidgard et al.

2005). Grey seals undergo another period of mass loss during the spring moult in May (females) and June (males) (Beck et al. 2003c). While females accumulate energy stores to prepare for each period of mass loss, male body size continuously declines until after the moult (Beck et al. 2003c). Females exhibit a prolonged period of preparation for the breeding period, with increased dive effort and acquisition of energy stores immediately following the moult. While dive effort temporarily declines between late-summer and early-fall, energy stores gained over the seven-months leading up to the breeding period are similar to those that will be depleted. Males instead gradually accumulate mass, with energetic stores gained in the three months prior reflecting those required for the breeding period (Beck et al. 2003a; Beck et al. 2003c). These differences may, in part, be owed to sex-specific differences in the fitness consequences of unsuccessful preparation for the fasted breeding period, as females must also successfully provision offspring (Mellish et al. 1999; Beck et al. 2003c; Lidgard et al. 2003; Lidgard et al. 2005; Bowen et al. 2015). This intraspecific seasonality is also reflected by their foraging behaviours (Beck et al. 2003a; Beck et al. 2003b; Austin et al. 2006), diet (Beck et al. 2007; Bowen and Harrison 2007; Tucker et al. 2007), and movement patterns (Austin et al. 2004; Breed et al. 2006; Breed et al. 2009).

1.2 MOVEMENT PATTERNS ACROSS THE SCOTIAN SHELF

This species mainly forages throughout continental shelf ecosystems, such as the Scotian Shelf (SS) (Stobo et al. 1990; Breed et al. 2006; Breed et al. 2009). During the 7-8 month pre-breeding period, movements predominantly occur over the eastern Scotian Shelf (ESS) and lower Gulf of St. Lawrence (GSL) (Beck et al. 2003b; Breed et al. 2006;

Lidgard et al. 2014). The SS is topographically complex and comprised of a series of banks and basins. These waters are stratified due to density gradients, with a cooler, fresher layer originating from the GSL and a warmer, more saline bottom layer originating from the shelf-slope; in summer, heating of the upper layer results in an additional warm surface layer (Smith & Schwing 1991; Loder et al. 1997; Loder et al. 1998; Han et al. 1999; Hannah et al. 2001). Circulation patterns across the SS are dynamic both horizontally and vertically (Ohashi et al. 2009), resulting in optically complex conditions (Beck 2016; Dever et al. 2016, Ross et al. 2017, Laliberté et al. 2018).

1.3 BIO-PHYSICAL CONDITIONS DRIVE MOVEMENT PATTERNS

Heterogeneous structuring of the marine environment results in a patchy distribution of prey species available to large marine predators (Springer et al. 1984). Optimal foraging theory predicts that individuals should seek to maximize their net energy intake relative to the effort expended foraging (MacArthur and Pianca 1966). This should be especially important in times of high energetic demands, such as leading up to the breeding season. Concentration of foraging efforts in areas of high prey density may result in more efficient foraging, as less energy will be expended searching for prey and the quantity of prey that can be consumed may be higher (Gende et al. 2006; Boyd et al. 2016). Oceanographic conditions and processes have been linked to foraging and movement patterns of diverse marine taxa (Cox et al. 2018), including sea turtles (Eckert et al. 2008; Bailey et al. 2012; Dodge et al. 2014), large bony fishes (Block et al. 2001; Thys et al. 2015; Sousa et al. 2016), elasmobranchs (Croll et al. 2012; Jaine et al. 2014;

Miller et al. 2015), seabirds (Holm and Burger 2002; Bon et al. 2015), cetaceans (Bailey and Thompson 2010; Citta et al. 2018), and pinnipeds (McConnell et al. 1992; Guinet et al. 2001; Ream et al. 2005; Campagna et al. 2006; Bailleul et al. 2007; Biuw et al. 2007; Dragon et al. 2010; McIntyre et al. 2011; Heerah et al. 2013; Sterling et al. 2014; Vacquié-Garcia et al. 2015; Malpress et al. 2017; Jonsen et al. 2018). However, obtaining sub-surface oceanographic data at spatio-temporal scales that are relevant to decisions made by benthic marine predators can be extremely challenging (O'Toole et al. 2014). Large marine predators instrumented with biologging devices can provide highly accurate location data along with oceanographic data that are contemporaneous with movements along an animal's path (Biuw et al. 2007; O'Toole et al 2015). With the improvement of statistical methods available, these data have been incorporated into analyses of estimated behavioural states (Bestley et al. 2013; O'Toole et al. 2015; Jonsen et al. 2018). Sampling performed by instrumented animals have also been used as a resource in areas where oceanographic data collection is sparse, particularly in polar regions where pinnipeds are abundant and satellite coverage is improved (Charrassin et al. 2008; Padman et al. 2010; Patterson et al. 2010; Dujon et al. 2014; O'Toole et al. 2014; Roquet et al. 2014).

1.4 RATIONALE AND RESEARCH OBJECTIVES

Oceanographic conditions within the SS ecosystem have undergone dramatic changes as a result of a globally changing climate (Loder et al. 2013). Due to added pressures from commercial fisheries, several groundfish stocks have markedly declined or collapsed (Frank et al. 2005; Worcester and Parker 2010; Shackell et al. 2012; Loder et al. 2013; Brennan et al. 2016). The grey seal has been the subject of controversy over its

role in the depression of these populations (Mohn and Bowen 1996; Trzcinski et al. 2006; Bundy et al. 2009; Benoit et al. 2011; O'Boyle and Sinclair 2012; Sinclair et al. 2015; Neuenhoff et al. 2018), yet minimal research on the bottom-up forcing of oceanographic conditions has been performed to date. Despite the importance of topographical features for foraging distributions within this population (Breed et al. 2009), these features are permanent in space and time. Grey seals show sex-specific seasonal differences in movement patterns, suggesting some other or combination of factors relevant to prey distributions may be of interest. An understanding of the influence of productivity patterns and environmental conditions on movements and foraging by a highly abundant, large marine predator is important, especially in light of climate change.

The primary objective of this thesis was to investigate the role of fine-scale oceanographic conditions on sex-specific seasonal movement patterns using environmental data measured *in situ* by instrumented grey seals. To accomplish this, an oceanographic dataset was formed and a case study on the potential for using grey seals as bioprobes to monitor primary productivity patterns and other oceanographic conditions within their habitat range was performed. To utilise primary productivity data that were contemporaneous with grey seal movements, a bio-optical model for the estimation of subsurface chl-*a* for these waters was developed.

1.5 THESIS OVERVIEW

This thesis is divided into three chapters to accomplish these objectives and is ordered sequentially by the data processing required to complete the final chapter and overall goal. In Chapter 2, I discuss the challenges of forming a bio-optical model for

these waters and relevance to habitat features heavily used by grey seals. A seasonally-specific bio-optical model for the estimation of chl-*a* was developed using replicated experiments in the Bedford Basin over the duration of the study period. This study highlights the value of repurposing light attenuation data collected from bio-logging devices. In Chapter 3, the spatio-temporal distribution of sampling by grey seals using highly accurate location data is addressed. The ability of grey seals to collect oceanographic data, including primary productivity estimates derived from the bio-optical model, and monitor ecologically important areas are demonstrated. In Chapter 4, I analyse location data collected by grey seals to estimate behavioural states along tracks using the hidden Markov movement model (HMMM). The influence of oceanographic and primary productivity data that may be relevant to grey seal foraging decisions, taking into account potential for sex-specific and seasonal differences, were assessed using generalized linear mixed-effects models (GLMMs). In summary, grey seals showed predictable sex-specific seasonal differences in foraging behaviours. Area-restricted search (ARS) behaviours by grey seals were able to be predicted by season-specific chlorophyll-*a* conditions, and sex-specific effects of upper-water column temperatures. The influence of bottom conditions (i.e., bottom temperature, dive depth, and bottom duration) was significant and showed some sex-specific variation. This study demonstrates the value of instrumented grey seals as oceanographic samplers and the importance of these conditions on their foraging behaviours and movement patterns across the Scotian Shelf.

CHAPTER 2: A BIO-OPTICAL MODEL FOR THE ESTIMATION OF CHLOROPHYLL-*A* USING ANIMAL-BORNE INSTRUMENTS IN AN OPTICALLY COMPLEX CONTINENTAL SHELF ECOSYSTEM

2.1 INTRODUCTION

The oceans provide nearly half of the earth's net primary productivity, with phytoplankton species playing a fundamental role in global carbon cycling (Falkowski et al. 1998; Field et al. 1998; Behrenfeld et al. 2001). Monitoring the spatial and temporal patterns of primary productivity is of considerable interest, particularly in the face of climate change (Sarmiento et al. 1998; Behrenfeld et al. 2006; Blondeau-Patissier et al. 2014; Behrenfeld et al. 2016; Moore et al. 2018). Marine primary productivity is typically inferred from phytoplankton biomass expressed by phytoplankton abundance (cells m^{-3}), organic carbon concentration (mg m^{-3}), or chlorophyll-*a* (chl-*a*) concentration (mg m^{-3}). However, chl-*a* is considered to be the best proxy for phytoplankton biomass (Strickland 1965; Banse 1977; Cullen 1982; Behrenfeld and Falkowski 1997). Measurements of chl-*a* are traditionally made aboard research vessels as well as by the use of moorings, floats (Roemmich et al. 2009; Riser et al. 2016), and autonomous underwater vehicles (AUVs) (Wynn et al. 2014). These platforms are generally costly, and often do not provide data at large spatial scales. Remote sensing of chl-*a* using ocean colour algorithms has proven useful in the detection of phytoplankton blooms and monitoring of primary productivity patterns (Platt and Herman 1982; Blondeau-Patissier et al. 2014). There are several limitations associated with these methods, including missing data under cloud cover or heavy ice conditions (Ackerman et al. 1998; Friedl et al. 2002; Friedl et al. 2010) and the necessity for atmospheric correction (Prince and Goward 1994; Hu et al. 2000; Remer et

al. 2005; Schroeder et al. 2007; Wang and Shi 2007; Moses et al. 2009). For these reasons, data are also often patchy, both spatially and temporally. Remote sensing is also restricted to the first optical depth, below which subsurface chl-*a* may be missed (Gordon and McCluney 1975; Cullen 1982; Cullen and Lewis 1995).

Several studies have shown that instrumented, large marine species can serve as "bioprobes" to collect valuable oceanographic data throughout their ranges (Costa 1993; Boehlert et al. 2001; Hooker and Boyd 2003; Charrassin et al. 2008; Costa et al. 2008; Padman et al. 2010; Roquet et al. 2014). The use of animal-borne sensors is an alternative method for the remote estimation of chl-*a* using wide-ranging, deep-diving species (Teo et al. 2009; Jaud et al. 2012; Xing et al. 2012; Guinet et al. 2013; O'Toole et al. 2014; Bayle et al. 2015). This approach can provide fine-scale estimation of chl-*a* within the water column along an animal's path. Two types of animal-borne instruments have been used to estimate chl-*a*: miniaturized fluorometers (e.g., Xing et al. 2012; Guinet et al. 2013) and light level (*LL*) sensors embedded in biologging tags (e.g., Teo et al. 2009; Jaud et al. 2012; O'Toole et al. 2014). The use of miniaturized fluorometers are burdened by several constraints, including correction for non-photochemical quenching (NPQ) and inaccuracies related to phytoplankton physiology and community composition (Cullen 1982; Behrenfeld et al. 2009; Xing et al. 2012; Jaud et al. 2012; Guinet et al. 2013; Bayle et al. 2015; Lander et al. 2015). An alternative method is to repurpose *LL* sensors that are designed for light-based geolocation in biologging tags to measure light attenuation (*LA*) within the water column. *LA* provides a relative measure of the diffuse attenuation coefficient of downwelling irradiance (K_d) using measurements of downwelling irradiance (E_d) that are commonly made by optical profiling platforms. Biologging

devices are limited to blue-range transmittance to maximize light detection at depth, as the attenuation of pure water is at a minimum in this range (Morel and Prieur 1977; Prieur and Sathyendranath 1981; Morel and Maritorena 2001). The majority of *LA* attributable to phytoplankton also falls within this range, making these devices suitable for inferring chl-*a* (Morel and Prieur 1977; Morel and Bricaud 1981; Loisel and Morel 1988; Morel and Maritorena 2001).

In open ocean waters, phytoplankton and optically active by-products that covary with it dominate *LA* in the water column (referred to as case 1 waters) (Smith and Baker 1978; Baker and Smith 1982; Morel et al. 2006). This has allowed for the formation of empirical global algorithms for the estimation of chl-*a* (Morel and Prieur 1977; Loisel and Morel 1998; O'Reilly et al. 1998; Morel and Maritorena 2001; Lee et al. 2005a). However, these algorithms may not be suitable where the pigment concentrations of the local phytoplankton community differ or where substantial non-algal optically active constituents are present (Bowers et al. 1996; Babin et al. 2003; Darecki et al. 2003; Siegel et al. 2005; Moore et al. 2009). Continental shelf regions are shallow (typically < 200 m) with close proximity to landmasses; as a result, freshwater inputs containing additional contributions of coloured dissolved organic matter (CDOM) may influence the optical properties of these waters (Prieur and Sathyendranath 1981). These exogenous sources of CDOM vary independently from phytoplankton biomass (referred to as case 2 waters) (Smith and Baker 1978; Baker and Smith 1982; Rochelle-Newall and Fisher 2002). The absorption of light by CDOM poses a challenge as it falls within the same range of the spectrum as that of chl-*a* (Bricaud et al. 1981). Modifications to empirical chl-*a* algorithms to account for the presence of CDOM is therefore necessary in these systems

(Doerffer and Schiller 2007). To date, studies involving the use of biologging tags for the estimation of chl-*a* have omitted continental shelf regions (i.e., case 2 waters) due to the confounding effects of optically active constituents in these waters (Jaud et al. 2012). Though this is not surprising, as the formation of uniform predictive algorithms to accommodate the presence of both case 1 and case 2 waters poses a major challenge for both remote sensing and the deployment of AUVs (Devred et al. 2005; Fuentes-Yaco et al. 2015; Beck 2016). This is problematic in the context of animal-borne instruments, as the species studied often forage in coastal or continental shelf areas (Campagna et al. 2006; Campagna et al. 2007; Bailleul et al. 2010; Jaud et al. 2012; Lowther et al. 2013; Hindell et al. 2016). These areas are especially important in terms of monitoring phytoplankton biomass, as the primary productivity here exceeds that of the open ocean, especially at higher latitudes (Behrenfeld et al. 2009). Locally-validated algorithms for the estimation of chl-*a* specific to case 2 ecosystems are needed for the reliable application to animal-borne data.

The Scotian Shelf (SS) is a highly productive and economically valuable continental shelf ecosystem. This region is home to the world's largest population of grey seals (*Halichoerus grypus*), with an increasing and currently estimated population of 424,300 individuals (Hammill et al. 2017a). Grey seals are primarily benthic foragers, diving frequently to near the ocean floor, making this species a good candidate for monitoring chl-*a* throughout the water column (Thompson et al. 1991; Beck et al. 2003a). Since grey seals have been intensively studied in this region using telemetry, they represent a potential resource for *LL* data that would otherwise go unused. Between 2009 and 2015 over 100 individuals were successfully equipped with time-depth-light

recorders (TDLRs). The Sable Island breeding component of this population is centrally located near the edge of the SS and previous telemetry studies have shown that the continental shelf is a primary foraging area (Austin et al. 2006; Breed et al. 2006; Breed et al. 2009), with movements concentrated in the eastern Scotian Shelf (ESS) and lower Gulf of St. Lawrence (GSL) during the pre-breeding period (Lidgard et al. 2014). While the SS may exhibit optical properties characteristic of case 1 waters at some times (i.e., spring bloom), the proximity to coastal areas, presence of numerous shallow banks, and immediate inflow of GSL waters result in waters more representative of case 2 conditions (Han et al. 1999; Xie et al. 2012; Beck 2016; Dever et al. 2016; Ross et al. 2017; Laliberté et al. 2018).

The development of regionally-specific, bio-optical models or algorithms must be validated against *in situ* measurements of chl-*a*. Approaches have included deployment of biologging devices paired with measurements of chl-*a* along a cruise track (Teo et al. 2009) or using satellite-derived chl-*a* estimates that are concurrent with animal locations (O'Toole et al. 2014). In this case, the logistical challenges of ship-based data collection and potential inaccuracies of remote sensing data coincident with *LA* collected by grey seals would be unlikely to provide sufficient observations for a robust predictive algorithm over multiple seasons and years. Therefore, a replicated experiment in the Bedford Basin (BB) was conducted. The BB is a coastal inlet connected to the SS by a long (10 km), shallow (20 m) sill (Li and Harrison 2008). These waters are part of the same large-scale physical regime (Loder 1998) and analysis of temperature data have shown that the BB experiences the same environmental perturbations as the continental shelf (Bundy et al. 2014). At even small time scales, the BB exhibits climatologies of the

SS, losing ecological autonomy after only three days (Lewis and Platt 1982; Li and Dickie 2001). Water exchange between the BB and SS occurs via Ekman transport and is heavily influenced by the Nova Scotia Current (NSC) (Greenberg et al. 1997; Shan et al. 2011; Shan and Sheng 2012; Dever et al. 2016). Like coastal areas of the SS, the BB is optically complex and can be classified as a case 2 water body (Bundy et al. 2014). Results of multi-year time series analyses within the BB and across the SS indicate that both nutrient concentrations and, at a given time of year, phytoplankton abundances are within the same range (Platt et al. 1972; Petrie et al. 1999; Li et al. 2006; Li et al. 2010).

The primary objective of this study was to determine whether a bio-optical relationship between *LA* measurements applicable to TDLR data and chl-*a* could be resolved for a case 2 component of the SS. In addition, to quantify the influence and variability of CDOM inputs for this system to better understand the optical conditions of these waters. To accomplish the objectives, several steps were taken to:

(i) calculate the mixed layer depth using TDLRs and determine whether chl-*a* and CDOM fluorescence show a relationship with *LA* measured by TDLRs,

(ii) validate *LA* measurements made by TDLRs against a standard oceanographic sampling instrument,

(iii) determine whether indicators of optically active constituents near-surface show relationships with *LA* measurements,

(iv) develop a long-term bio-optical model within the BB for the estimation of chl-*a* using *LA* measured by a standard oceanographic sampling instrument that is applicable to data collected by grey seals, and

(v) quantify the influence and variability of exogenous non-algal optically active constituents to assess the suitability of a bio-optical model for application on the SS.

2.2 METHODS

2.2.1 Experimental Procedure

This study took advantage of weekly sampling of several oceanographic properties in the BB, allowing for replicate observations within a single experimental system. Sampling and sample processing was performed by the Marine Environmental Observation Prediction and Response Network (MEOPAR) and Dalhousie University in conjunction with the Department of Fisheries and Oceans Canada as part of the Bedford Basin Monitoring Program on Wednesday of each week at the Compass Buoy Station (44° 41' 37" N, 63° 38' 25" W) (Li and Dickie 2001). The instrument package included a Micro CTD (conductivity-temperature-depth) system (AML Oceanographic, www.amloceanographic.com) mounted with a WET Labs ECO Triplet-*W* fluorometer (Sea-Bird Scientific, www.seabird.com). The CTD system was lowered at a targeted rate of 0.5 m s^{-1} to a maximum depth of 60 m. The fluorometer measured both chl-*a* ($F_{chl\text{-}a}$) and CDOM (F_{CDOM}) fluorescence intensity with depth (m) which were detected using 470/695 and 370/460 nm filter pairs, respectively. Since the fluorometer was not calibrated to measure chl-*a* and CDOM concentrations, data are reported in volts (V) and these data serve as proxies for chl-*a* and CDOM concentrations. Data were collected at a frequency of 1 Hz and binned at a resolution of 0.5 m. An optical profiling platform equipped with a Satlantic hyperspectral OCR-3000, referred to as the HyperPro (Sea-Bird

Scientific, www.seabird.com) was deployed immediately after the CTD system. Three casts were performed on each date: the first to a maximum depth of 60 m, followed by two casts to depths where usable light was no longer detected. The HyperPro collected E_d using a 256-channel silicon photodiode array with a bandwidth of 350 to 800 nm at a resolution of 10 ± 0.3 nm with less than 0.001 W m^{-2} of stray light detected. Sampling was performed at a maximum frequency of 12 Hz with a data rate of 57600 baud. Niskin bottle collections were made at 1 m, 5 m, and 10 m depths for the measurement of near-surface chl-*a* concentration (mg m^{-3}) and CDOM absorbance (A_{CDOM}). Samples were prepared for chl-*a* measurement by passing 39 mL through 25 mm glass fibre filters and were extracted in 90% acetone for 24 hours. They were processed using the Welschmeyer non-acidification technique (Welschmeyer 1994) to account for interfering pigments, and then read on a Turner Designs Fluorometer (www.turnerdesigns.com). Chl-*a* was measured using a 436/685 filter pair within a range of 0 to 300 ± 0.025 mg m^{-3}. A_{CDOM} was measured by filtration through a nucleopore filter and run on a Cary spectrophotometer in a 10 cm long cuvette; filtrate was kept in a glass bottle, the filter was discarded with the sample, and nanopure was used to blank. Measurements were taken within a bandwidth of 250 to 800 nm and one replicate was performed for each depth.

For 12 of the weekly sampling dates over the spring and early summer of 2012, five Mk10-AF Fastloc™ GPS TDLRs (Wildlife Computers, www.wildlifecomputers.com) (11A0091, 11A0214, 11A0254, 11A0256, and 11A0257), the same instruments as those used on grey seals, were attached to the CTD system. TDLRs recorded temperature (ºC), depth (m), corrected depth (m), and *LL*. Temperature was

measured using a fast-response external thermistor with a range of -40 to 60 ºC at a resolution of 0.05 ± 0.1 ºC. Depth was measured within a range of 0 to 1000 m at a resolution of 0.5 m ± 1% of depth reading. The *LL* sensor is comprised of a Hamamatsu silicon S2387 photodiode and a blue window transmittance filter, resulting in a peak sensitivity of 465 nm with a range of 400 to 490 nm and half band width of 50 nm (Vacquié-Garcia et al. 2017). Light intensity (W cm^{-2}) is approximately converted onboard TDLRs to a three-digit *LL* value specific to the manufacturers to enhance resolution at lower light intensities using the equation:

$$LL = 250 + 20 \log_{10} (\textit{light intensity}) \quad \text{(Equation 1)}$$

(Fig. 2.1). *LL* data are collected within a range of 25 to 225, which corresponds approximately to 5 x 10^{-12} to 5 x 10^{-2} W cm^{-2}. Calibrations were performed by instrument manufacturers at light intensity values of 10^{-5}, 10^{-7}, and 10^{-9} W cm^{-2}, resulting in *LLs* of 150, 110, and 70, respectively (Fig. 2.1). Deviations in *LL* profiles of TDLRs were evident at the surface for two of the deployment dates and were removed from these analyses; it is possible that these were due to the presence of passing clouds (Beck 2016).

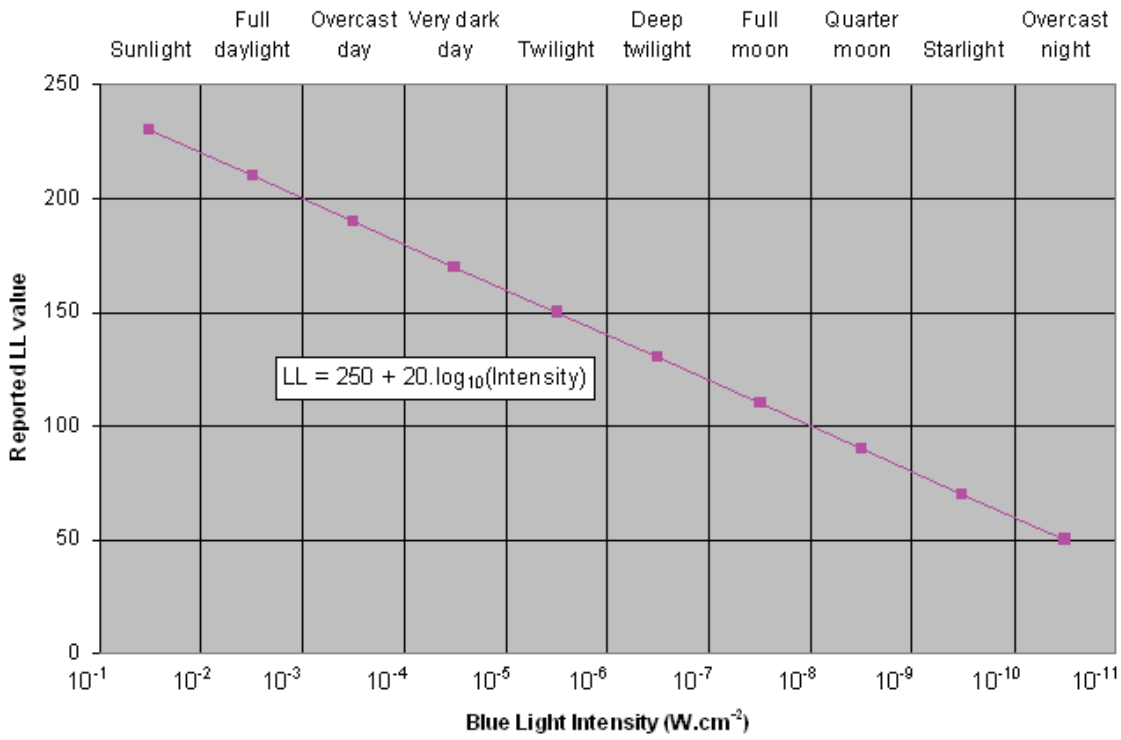

Figure 2.1 Logarithmic conversion of light intensity (W cm^{-2}) within the blue range of the visible spectrum to light level (*LL*) values measured by Mk10-AF™ GPS tags (Wildlife Computers, www.wildlifecomputers.com).

2.2.2 Data Analysis

The analysis of chl-*a* in the water column should be performed over the mixed layer depth (MLD) so that the majority of phytoplankton present in the water column are represented. To determine the MLD using data collected by TDLRs and the CTD, the thermocline was estimated using the finite-depth criterion method (de Boyer Montégut et al. 2004); this method is particularly well-suited for this region, as seasonal stratification is driven by temperature gradients (Li and Harrison 2008). A criterion value of 0.5 ºC was chosen as it has been used in both the global ocean and specific to the North Atlantic (de Boyer Montégut et al. 2004). A near-surface reference depth of 15 m was used to remove the influence of diurnal increases in surface temperature, as they were observed

below 10 m on several dates of the study (Xing et al. 2012) (Fig. 2.2). Although not essential for the estimation of MLD, temperature readings of tags were corrected to maintain consistency with *in situ* measurements where both MLD and water temperature data were collected (see Chapter 3). As tags were not calibrated at the time of deployment, 0.05 ºC was subtracted for all readings according to recommendations for these thermistors (Simmons et al. 2009). To assess differences in MLD estimates made using TDLRs (MLD_{TDLR}) and the CTD (MLD_{CTD}), the root mean square error (*RMSE*) was calculated over the ten sampling dates using the following equation:

$$RMSE = \sqrt{\frac{1}{10}\sum_{i=1}^{10}\left(MLD_{TDLR,i} - MLD_{CTD,i}\right)^2}. \quad \text{(Equation 2)}$$

Correlation tests were performed to assess the ability of the TDLRs to detect changes in the MLD over time.

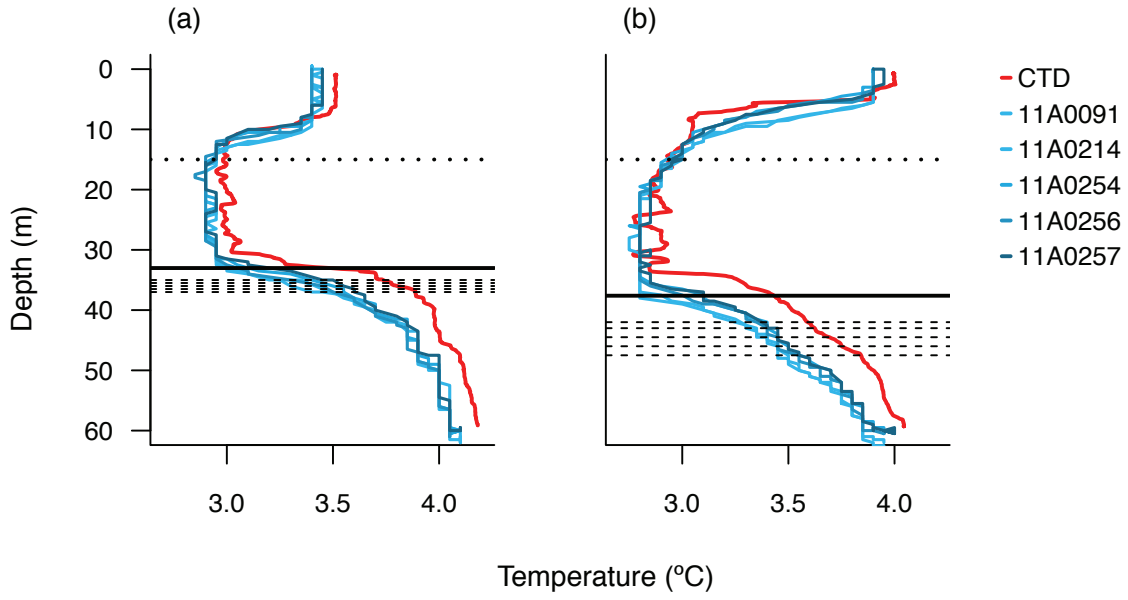

Figure 2.2 Temperature profiles and mixed layer depths estimated using time-depth-light recorders (dashed lines) and the CTD (solid line) using the reference depth of 15 m (dotted line) on (a) March 14, 2012 and (b) April 2, 2012.

The coefficient K_d is an apparent optical property commonly related to chl-*a* that can be calculated by linearly regressing log-transformed E_d with depth (Smith and Baker 1981; Kirk 1994; Lee et al. 2005b). Recent work using animal-borne instruments has highlighted the use of *LA*, a related parameter specific to *LL* data collected by TDLRs (O'Toole et al. 2014). As *LL* is already a log-transformed function of light intensity (W cm^{-2}) and therefore E_d (W m^{-2}), *LA* can be calculated using the following equation (O'Toole et al. 2014):

$$LA = -\frac{LL_1 - LL_2}{z_2 - z_1}, \quad \text{(Equation 3)}$$

where LL_1 represents the *LL* at the surface depth z_1 and LL_2 represents the *LL* at the depth within the water column z_2. *LA* was estimated using TDLRs and compared to $F_{chl\text{-}a}$ and F_{CDOM} within the MLD to assess whether detectable relationships were present within the optically complex waters of the BB; MLD was taken as that of the CTD on each date of the study. The correction of non-photochemical quenching (NPQ) was performed on $F_{chl\text{-}a}$ profiles prior to the analysis by extrapolating the maximum fluorescence intensity between the MLD and the surface (Xing et al. 2012; Guinet et al. 2013; Biermann et al. 2015). $F_{chl\text{-}a}$ and F_{CDOM} were taken as a per meter average by numerical integration within the MLD using the composite trapezoidal rule with the freely available R package *caTools* (Zhou et al. 2013; Blain et al. 2013; Tuszynski 2014). Correlation analyses for per meter $F_{chl\text{-}a}$ and F_{CDOM} were performed against *LA* estimates made within the MLD.

As TDLRs were only successfully deployed on 10 sampling dates, *LA* estimates were validated against those of the HyperPro so that any long-term bio-optical relationship formed using the standard oceanographic instrument could be applied to data collected *in situ* by grey seals. E_d data from the HyperPro were restricted to 465 nm,

corresponding to the peak sensitivity of TDLRs. These data were then converted to *LL* as the constant denoted by 250 is slightly variable among tags and may result in incorrect conversions for TDLRs (Eq. 1; personal communication, Wildlife Computers). Analyses performed using the HyperPro are constrained by the accuracy of *LL* measurement at depth. A previous study noted that the HyperPro is limited by approximately 118 *LL* units (log-scaled irradiance of -6), while these data suggest that this is closer to 150 (Lagman 2013). Measurements made below these values, referred to as the noise equivalence irradiance (NEI), should be regarded as electronic noise and excluded from analyses (Fig. 2.3; personal communication, MEOPAR). The NEI was determined using only the first cast to maximum depth to obtain a single NEI for each date of the study. The depth of the NEI was determined by ordering *LL* measurements according to increasing depth and using a threshold at which the first increase in *LL* was detected, with respect to both depth and time. While this method provides a conservative estimate of the NEI, there may still be reductions in the sensitivity of the HyperPro compared to TDLRs approaching these depths (e.g., Fig. 2.3b). To assess agreement between the *LA* of the HyperPro ($LA_{HyperPro}$) and TDLRs (LA_{TDLR}) at the deepest depth possible, the *RMSE* and mean absolute percentage error (*MAPE*) were calculated above the NEI depths for each of the ten sampling dates using the equations:

$$RMSE = \sqrt{\frac{1}{10}\sum_{i=1}^{10}\left(LA_{\mathrm{TDLR,i}} - LA_{\mathrm{HyperPro,i}}\right)^2}, \quad \text{(Equation 4)}$$

$$MAPE = \frac{100}{10}\sum_{i=1}^{10}\left|\frac{LA_{\mathrm{TDLR,i}} - LA_{\mathrm{HyperPro,i}}}{LA_{\mathrm{TDLR,i}}}\right|. \quad \text{(Equation 5)}$$

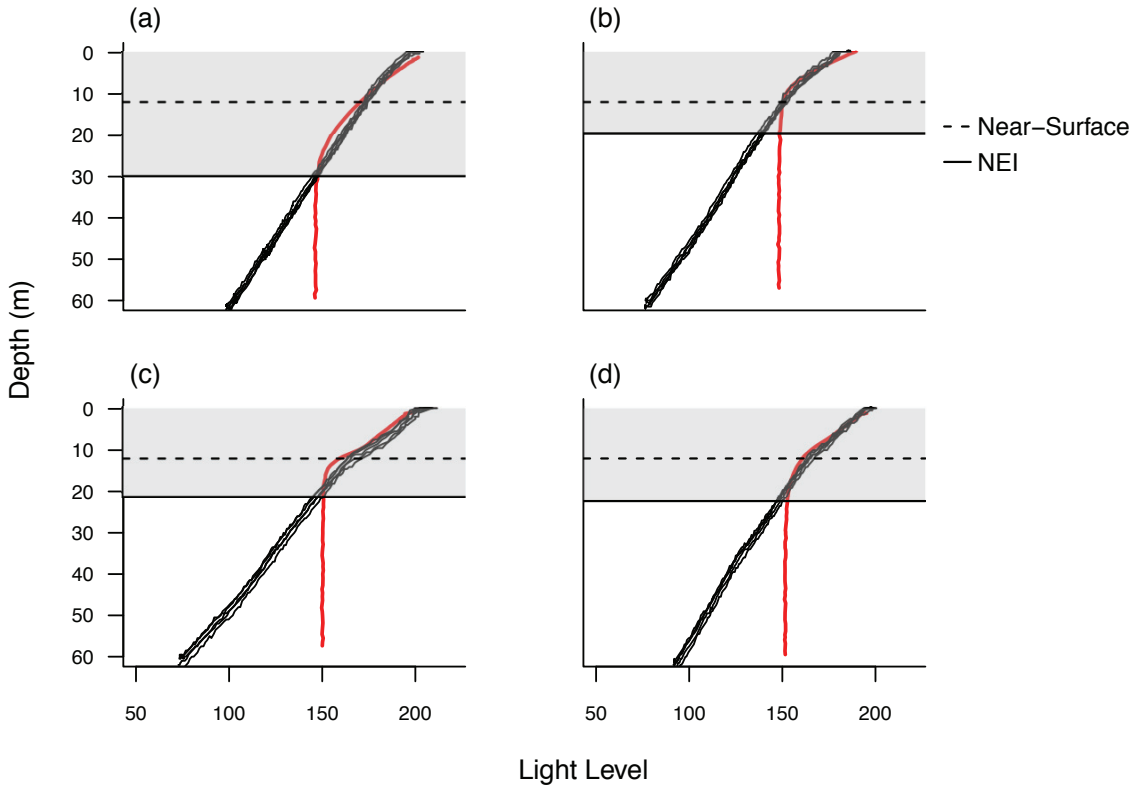

Figure 2.3 Light level profiles produced using time-depth-light recorders (black) and the HyperPro (red) on (a) March 7, 2012, (b) March 14, 2012, (c) April 2, 2012, and (d) May 5, 2012, highlighting the limitation of the HyperPro within the noise equivalence irradiance (NEI) depths (shaded) and the near-surface depth of 12 m (dashed line).

As the NEI depths were shallower than the MLD on several dates, the MLD could not be used for analysis of chl-*a* data. $F_{chl\text{-}a}$ data were not calibrated, providing only a relative measure of chl-*a* concentration, and commonly require correction of NPQ within surface waters. For these reasons, long-term chl-*a* measurements were instead taken using Niskin bottle data and analyses were restricted to near-surface waters where these data were available (i.e., 12 m depth). NEI depths exceeded the near-surface depth on all dates of the study. *LA* measurements made by TDLRs and the HyperPro within the near-surface depth were also compared using the *RMSE* and *MAPE*. To explore relationships

between optically active constituents and *LA* estimates within the near-surface depth, a correlation analysis was performed. $F_{chl\text{-}a}$ and F_{CDOM} were restricted to the near-surface depth and used as indicators of optically active constituents, despite the correction of NPQ. Chl-*a* and A_{CDOM} collected using Niskin bottles were also included. A_{CDOM} was restricted to a wavelength of 465 nm ($A_{CDOM(465)}$) corresponding to the peak sensitivity of TDLRs. A baseline correction was performed on these data by subtracting $A_{CDOM(685)}$ from that of $A_{CDOM(465)}$ (Helms et al. 2008; Xie et al. 2012). The spectral absorption coefficient ($a_{CDOM(465)}$; m^{-1}) was then calculated using the following equation:

$$a_{CDOM}(465) = 2.303 A_{CDOM}(465)/l \,, \quad \text{(Equation 6)}$$

where $A_{CDOM(465)}$ is the absorbance at 465 nm and *l* is the path length of 0.1 m (Xie et al. 2012). Data were numerically integrated using the midpoint Riemann sum. The widths of the rectangle bases were used as weights for the following equations:

$$\text{chl-}a = \frac{1}{6}\,\text{chl-}a_1 + = \frac{1}{2}\,\text{chl-}a_5 + \frac{1}{3}\,\text{chl-}a_{10} \,, \quad \text{(Equation 7)}$$

$$a_{CDOM}(465) = \frac{1}{6}\,a_{CDOM}(465)_1 + = \frac{1}{2}\,a_{CDOM}(465)_5 + \frac{1}{3}\,a_{CDOM}(465)_{10} \,, \quad \text{(Equation 8)}$$

using measurements at depths 1 m, 5 m, and 10 m. On dates where $a_{CDOM(465)}$ data were incomplete due to sampling errors, depths were re-weighted to reflect available data.

Chl-*a* data of this kind, along with near-surface *LA* estimates made by the HyperPro at 465 nm (LA_{HP}), were used to form a predictive bio-optical model suitable for application to TDLR data. Data were limited to dates on which both chl-*a* and LA_{HP} were available; as no measurements were made by the HyperPro in 2009, data spanned the years 2010 through 2015. Evidence of measurement error was present in some profiles and these dates were removed from the study; the standard procedure is visual validation

that profiles fall within what would be considered a reasonable range (personal communication, MEOPAR). LA_{HP} was measured using data from all three casts. The bio-optical model for the estimation of chl-*a* using LA_{HP} was constructed using a model II regression to account for the two random dependent variables. To predict one variable from the other, ordinary least squares (OLS) regression was used to minimize the squared residuals in the response variable (Legendre, 2018). Estimates of chl-*a* were consistent with findings of previous studies in this region (Li and Dickie 2001; Ji et al. 2007). Both chl-*a* and LA_{HP} were log-transformed to meet the assumptions of a linear regression. A lag of two was applied in order to remove the effects of serial correlation present in the dataset, due to the nature of weekly sampling replicates. Outliers were removed using the median absolute deviation to account for measurement error and anomalous observations likely to be highly influential on the overall fit of the model (i.e., unseasonably high chl-*a* concentrations for the respective light attenuation, cases where the influence of anomalous CDOM were obvious, or potentially erroneous measurements) (Leys et al. 2013).

To determine whether a bio-optical model formed in the BB is likely to be relevant to the optically complex conditions of the SS encountered by grey seals, the contribution of CDOM and non-algal particles to the light attenuation were further explored. Chl-*a* measurements were used to estimate $K_d(465)_{chl\text{-}a}$ using the global empirical algorithm:

$$K_d(465) = K_w(465) + \chi(465)(chl)^{e(465)} \quad \text{(Equation 9)}$$

using the empirical $K_w(465)$ value, the constants χ and e specific to the wavelength of 465 nm, and chl (chl-*a*; mg m^{-3}) measurements (Morel 1988; Morel and Maritorena

2001). This should result in calculated values of K_d attributable to chl-*a*, the amount of CDOM that covaries with it, and the contribution of water expected for a case 1 system:

$$K_d(\lambda) = K_w(\lambda) + K_{bio}(\lambda)$$

(Equation 10)

where K_w is the attenuation due to seawater and K_{bio} represents the attenuation of light by all biogenic constituents including phytoplankton, CDOM, and non-algal particles at a given wavelength (λ) (Smith and Baker 1978; Morel 1988; Morel and Maritorena 2001). $K_d(465)_{chl\text{-}a}$ were then compared to $K_d(465)_{HyperPro}$, calculated using the equation:

$$K_d(465, z_1 \leftrightarrow z_2) = -\frac{1}{z_2 - z_1} \ln\left(\frac{E_d(465, z_1)}{E_d(465, z_2)}\right),$$

(Equation 11)

by linearly regressing log-transformed $E_d(465)$ between the surface depth z_1 and near-surface depth z_2 (Gordon et al. 1980; Smith and Baker 1981; Darecki and Stramski 2004; Lee et al. 2005b). Under the premise of Eq. 10, differences between the calculated and observed values, $K_d(465)_{chl\text{-}a}$ and $K_d(465)_{HyperPro}$ respectively, should provide some indicator of contributions made to the biogenic attenuation of light in addition to those of chl-*a*; it is of note that some level of this influence may be attributable to differences in the community composition unique to the BB and SS (Jena 2017). As the empirical model used to calculate $K_d(465)_{chl\text{-}a}$ takes into account the influence of CDOM that should covary with a given chl-*a*, this analysis should reveal the effects of exogenous sources of CDOM. Observations were made in terms of K_d rather than *LL* for simplicity in using the standard empirical algorithm. Chl-*a* and Hyper Pro data were the same as those included in the formation of the bio-optical model. A linear model was produced and used for tests of significance against the expected relationship for a case 1 system, for which both the calculated and observed K_d would be the same. Although both variables

contained error, OLS was used as the error in $K_{d(465)_{chl\text{-}a}}$ was greater than that of $K_{d(465)_{HyperPro}}$ (Legendre 2018). Data were again lagged at an interval of two to remove the influence of serial correlation present in the residuals. Outliers removed using the median absolute deviation were all positive residuals, for which observed K_d values were lower than what would be expected for a case 1 system and thus expected to be due to measurement error by the HyperPro.

2.3 RESULTS

TDLRs performed consistently well against CTDs in estimating the MLD, providing further validation for use on temperature data collected by instrumented grey seals (Fig. 2.4). Although *RMSE* was somewhat large (3.65 m), differences of up to a few meters are relatively insignificant within the context of monitoring ecosystem-wide changes or determining a suitable MLD for chl-*a* estimation. MLDs estimated using TDLRs were closely correlated with those of the CTD (Table 2.1), such that spatial or temporal differences that may be of interest to oceanographic or biological research (e.g., shoaling of the mixed layer) should be revealed. MLDs estimated by TDLRs were more similar to each other and generally had low standard deviations (Table 2.2). The *RMSE* is therefore suspected to be a result of some inaccuracy in the measurement of depth inherent to TDLRs. This provides support for the use of TDLRs to monitor MLDs, as measurements made among grey seals should be consistent. *LA* measurements made by TDLRs were significantly correlated with $F_{chl\text{-}a}$ within these depths but showed low correlations with F_{CDOM} (Table 2.3), suggesting that a bio-optical model to estimate chl-*a* may be possible despite the presence of CDOM in the region. In agreement with the

classification of the BB as a case 2 water body, $F_{chl\text{-}a}$ and F_{CDOM} did not show a significant relationship (rho = -0.406, *p*-value = 0.25) within the mixed layer.

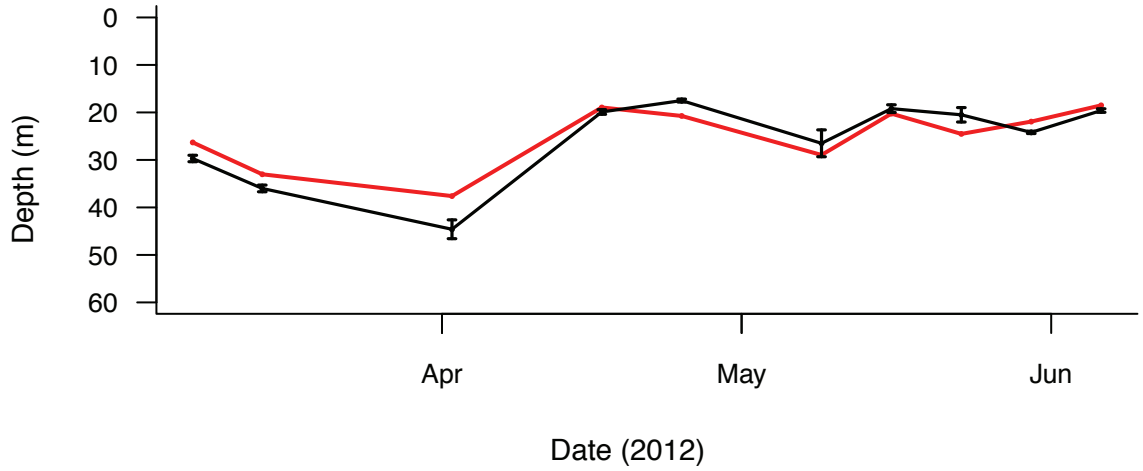

Figure 2.4 Mixed layer depth (m) estimates made using the CTD (red) and time-depth-light recorders (TDLRs; black) with 95% confidence intervals among TDLRs.

Table 2.1 Correlations among time-depth-light recorders and the CTD for calculated mixed layer depths (m).

	11A0091	**11A0214**	**11A0254**	**11A0256**	**11A0257**
rho	0.87	0.70	0.90	0.89	0.78
***p*-value**	0.003	0.024	< 0.001	< 0.001	0.007

Table 2.2 Mixed layer depths (m) determined using the CTD and time-depth-light recorder (TDLR) data with the standard deviation among TDLRs (σ_{TDLR}) on each date of the study.

Date	**CTD**	**11A0091**	**11A0214**	**11A0254**	**11A0256**	**11A0257**	$\boldsymbol{\sigma_{TDLR}}$
March 7	26.3	31.0	29.5	29.5	29.5	29.0	0.76
March 14	33.0	36.5	37.0	35.5	36.0	35.0	0.79
April 2	37.6	46.0	47.5	42.0	44.5	43.0	2.22
April 17	19.0	20.5	20.5	19.5	19.5	19.5	0.55
April 25	20.7	17.5	18.0	17.0	17.5	17.5	0.35
May 9	28.9	27.0	21.5	28.0	26.0	30.0	3.16
May 16	20.3	18.5	20.0	20.0	19.5	18.0	0.91
May 23	24.5	21.0	18.5	23.0	20.5	19.5	1.70
May 30	21.9	24.5	24.0	24.0	24.5	24.0	0.27
June 6	18.5	19.5	20.0	20.0	19.5	20.0	0.42

Table 2.3 Correlations of light attenuation (m^{-1}) measurements made using time-depth-light recorders with chlorophyll-*a* fluorescence ($F_{chl\text{-}a}$; V) and coloured dissolved organic matter fluorescence (F_{CDOM}; V) within the mixed layer depth estimated using CTD data on each date of the study.

	11A0091	**11A0214**	**11A0254**	**11A0256**	**11A0257**
rho ($\boldsymbol{F_{chl\text{-}a}}$)	0.73	0.77	0. 77	0.67	0.77
***p*-value ($\boldsymbol{F_{chl\text{-}a}}$)**	0.021	0.014	0.014	0.039	0.014
rho ($\boldsymbol{F_{CDOM}}$)	0.03	0.05	0.05	0.14	0.05
***p*-value ($\boldsymbol{F_{CDOM}}$)**	0.946	0.892	0.892	0.707	0.892

LA measurements made by the HyperPro were comparable to those of TDLRs above the NEI depths, supporting the use of these data for the formation of a bio-optical model and suitability for data collected by grey seals (Fig. 2.5). The overall *RMSE* for TDLRs was 0.250 with a *MAPE* of 8.68% and *LA* measurements were highly correlated

with the HyperPro (Table 2.4). When restricted to the near-surface waters, *LA* measurements made by the HyperPro were less representative of TDLRs, with a *RMSE* of 0.560 and *MAPE* of 17.39%. Correlations between TDLRs and the HyperPro made within these depths were also more variable but remained high (Table 2.5). Since estimation of *LA* by linear regression is increasingly accurate over greater depths (Lee et al. 2005b), this could also contribute to differences in the sensitivity range of TDLRs and the HyperPro and increased presence of attenuating substances at those wavelengths within the near-surface depth.

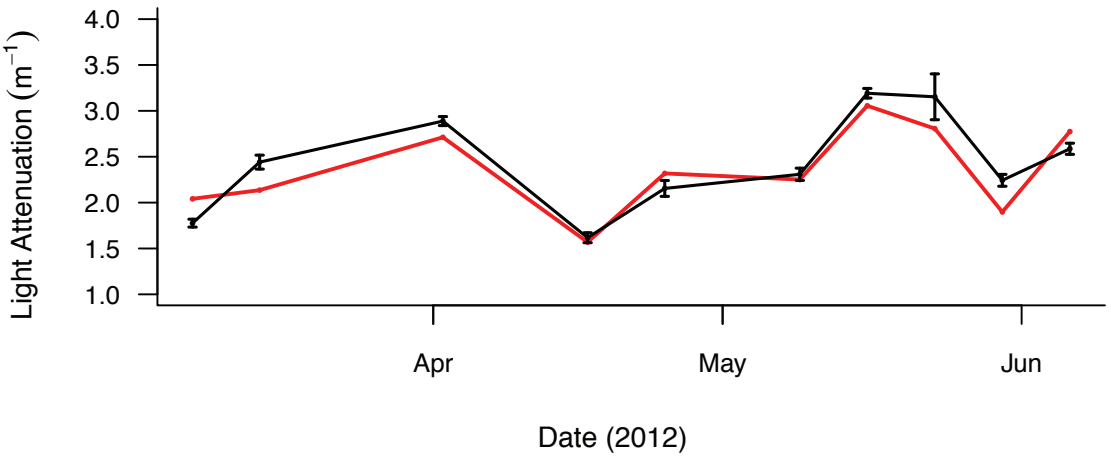

Figure 2.5 Light attenuation (m^{-1}) estimates made within the noise equivalence irradiance depths on each date of the study using the HyperPro (red) and time-depth-light recorders (TDLRs; black) with 95% confidence intervals among TDLRs.

Table 2.4 Correlations of light attenuation (m^{-1}) measurements made by time-depth-light recorders and the HyperPro within the noise equivalence irradiance depth determined on each date of the study.

	11A0091	**11A0214**	**11A0254**	**11A0256**	**11A0257**
rho	0.85	0.87	0.85	0.88	0.87
***p*-value**	0.004	0.003	0.004	0.002	0.003

Table 2.5 (a) Correlations among light attenuation (m^{-1}) measurements made by time-depth-light recorders and the HyperPro and indicators of optically active constituents including chlorophyll-*a* (chl-*a*) fluorescence ($F_{chl\text{-}a}$; V), coloured dissolved organic matter (CDOM) fluorescence (F_{CDOM}; V), chl-*a* concentration (mg m^{-3}), and CDOM absorption at 465 nm ($a_{CDOM}(465)$; m^{-1}) and (b) the respective *p*-values.

(a)

	11A0091	**11A0214**	**11A0254**	**11A0256**	**11A0257**	**HyperPro**	$F_{chl\text{-}a}$	F_{CDOM}	**chl-*a***
11A0091									
11A0214	0.95								
11A0254	0.90	0.95							
11A0256	0.95	0.87	0.95						
11A0257	0.90	0.85	0.90	0.99					
HyperPro	0.92	0.89	0.77	0.71	0.67				
$F_{chl\text{-}a}$	0.81	0.71	0.78	0.93	0.90	0.62			
F_{CDOM}	0.19	0.16	-0.018	0.15	0.18	0.20	0.067		
chl-*a*	0.52	0.37	0.45	0.66	0.62	0.43	0.84	0.15	
$a_{cdom}(465)$	0.32	0.35	0.21	0.18	0.12	0.42	-0.067	0.52	-0.11

(b)

	11A0091	**11A0214**	**11A0254**	**11A0256**	**11A0257**	**HyperPro**	$F_{chl\text{-}a}$	F_{CDOM}	**chl-*a***
HyperPro	0.00	0.00	0.01	0.02	0.03	0.00			
$F_{chl\text{-}a}$	0.00	0.02	0.01	0.00	0.00	0.05	0.00		
F_{CDOM}	0.60	0.65	0.96	0.68	0.63	0.58	0.85	0.00	
chl-*a*	0.13	0.29	0.19	0.04	0.05	0.21	0.00	0.68	0.00
a_{cdom}**(465)**	0.37	0.33	0.56	0.63	0.75	0.23	0.85	0.13	0.75

When compared to indicators of optically active constituents, *LA* estimates made by TDLRs and the HyperPro generally supported proceeding with the formation of a bio-optical model (Table 2.5; Fig. 2.6). $F_{chl\text{-}a}$ showed stronger correlations with *LA* than chl-*a*, and though it cannot be used in the bio-optical model, it provides assurance that phytoplankton are highly influential to the overall *LA* of the water column. Chl-*a* and $F_{chl\text{-}a}$ were highly correlated, confirming that weighted averages of chl-*a* provide good representation of vertically integrated chl-*a* measurements. F_{CDOM} and $a_{CDOM(465)}$ were only moderately correlated, indicating that $a_{\mathrm{CDOM}}(465)$ is not highly influential on the overall a_{CDOM} in the system. Correlations between $a_{CDOM(465)}$ and chl-*a* were comparable for LA_{HP}, which could be cause for concern that the bio-optical model may hold such high variability in attenuation due to the presence of CDOM that a discernable relationship with chl-*a* may be obscured. TDLRs showed reduced correlations with $a_{CDOM(465)}$, which may be attributable to TDLRs being sensitive to a wider range of wavelengths. TDLRs showed stronger correlations with chl-*a* and $F_{chl\text{-}a}$ than the HyperPro.

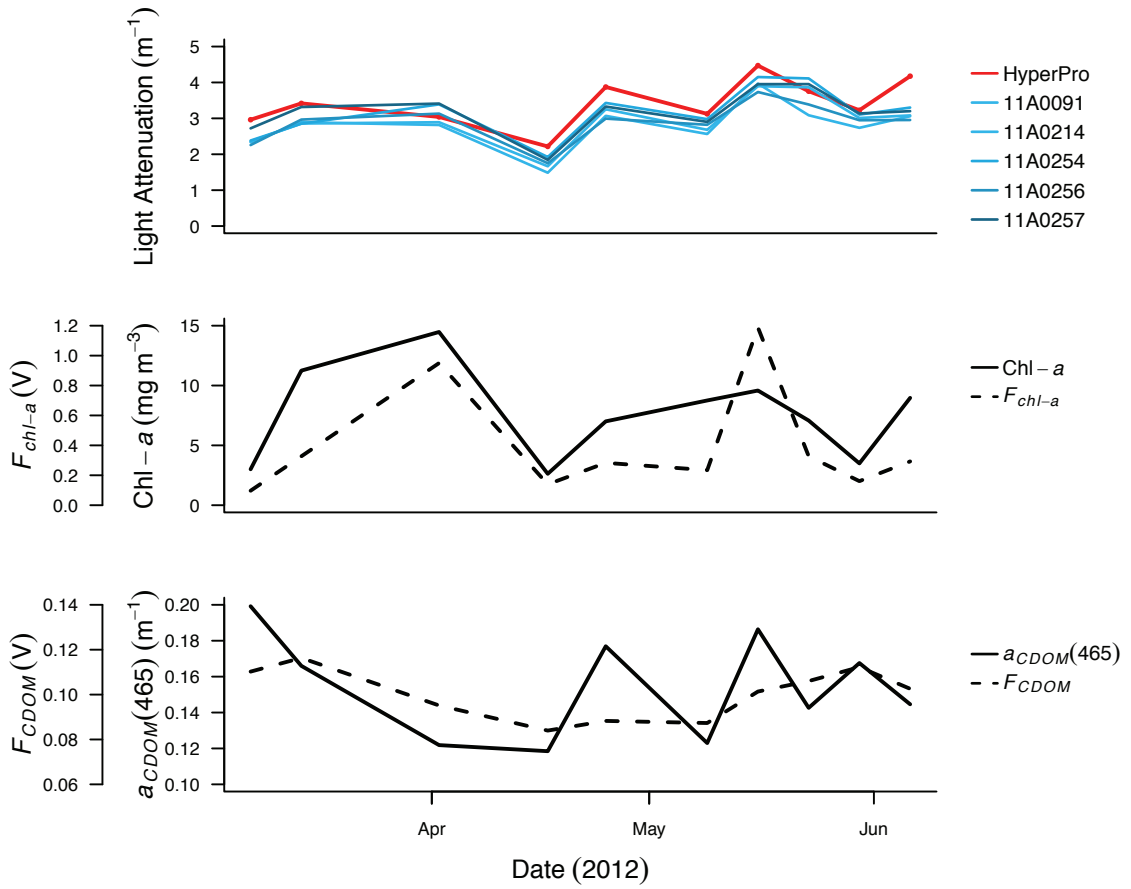

Figure 2.6 Light attenuation (m^{-1}) estimates made using the HyperPro and time-depth-light recorders within the near-surface depth (12 m) compared to the chlorophyll-*a* concentration (chl-*a*; mg m^{-3}), chlorophyll-*a* fluorescence ($F_{chl\text{-}a}$; V), absorption of coloured dissolved organic matter (CDOM) at 465 nm ($a_{CDOM}(465)$; m^{-1}), and CDOM fluorescence (F_{CDOM}; V).

The bio-optical model for the estimation of chl-*a* using *LA* measured by the HyperPro explained more than 70% of the variation in chl-*a* (Fig. 2.7). Model selection was performed using the Akaike Information Criterion with the most parsimonious model including season as an additive factor (Table 2.6). *LA* was positively related to chl-*a* (Table 2.7). Seasonality was significant only in winter, during which there was a trend of higher *LA* relative to the observed chl-*a* than in other seasons (Table 2.7).

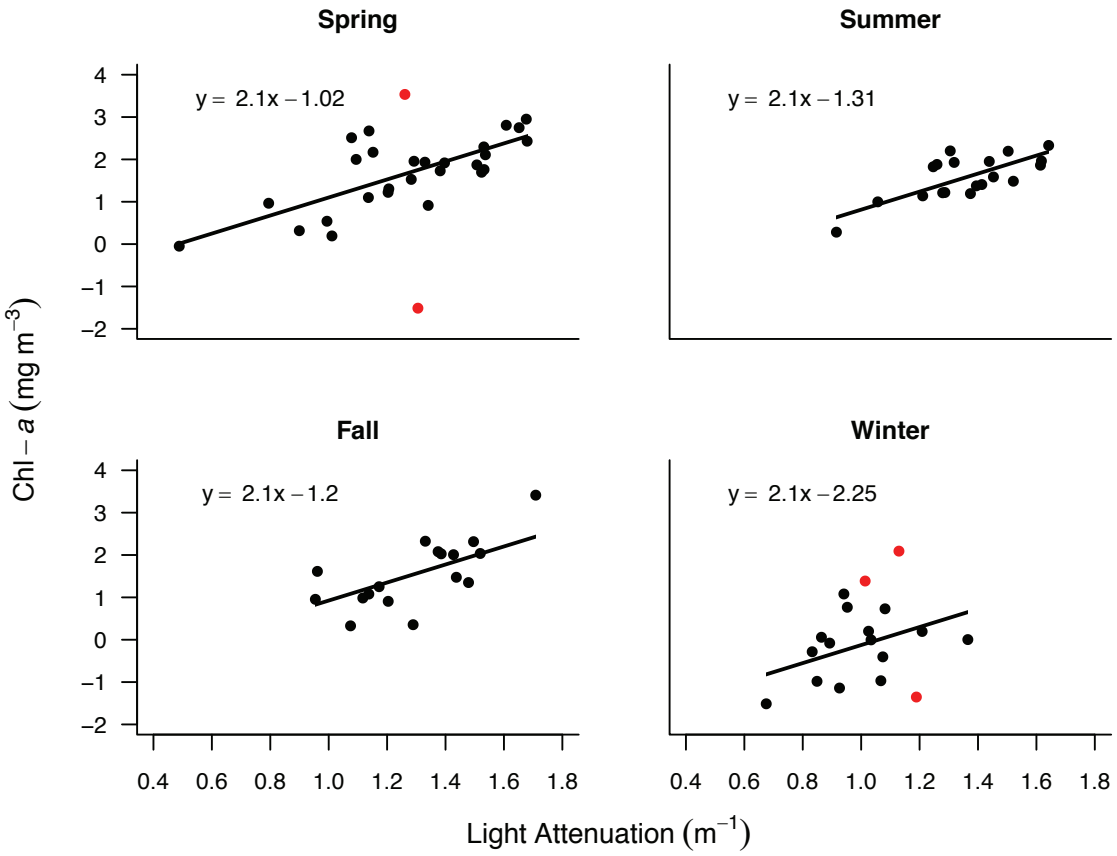

Figure 2.7 Ordinary least squares (OLS) regression ($R^2 = 0.72$, $R^2_{adj} = 0.70$, *p*-value < 0.001) of light attenuation (m^{-1}) against chlorophyll-*a* concentration (chl-*a*; mg m^{-3}) within the near-surface depth (12 m) between 2010 and 2015 (n = 78). Both axes have been log-transformed with a lag of two applied; outliers not included in the analysis are highlighted in red.

Table 2.6 Determination of the most parsimonious bio-optical model (bolded) by ordinary least squares (OLS) model II regression using the Akaike Information Criterion (AIC). Predictors include light attenuation (*LA*; m^{-1}) and season (S).

Candidate models	**AIC**	**ΔAIC**
***LA* + S**	**366.0**	**0**
LA + S + *LA*:S	370.66	4.62
LA	394.12	23.46
S	429.72	35.59
~ 1	490.28	60.57

Table 2.7 Coefficient results from the most parsimonious bio-optical model. Predictors include light attenuation (*LA*; m^{-1}) and season (S).

Variable	**Coefficient ± SE**	***p*-value**
Intercept	-1.20 ± 0.385	0.003
LA	2.13 ± 0.281	< 0.001
Season (Spring)	0.18 ± 0.171	0.31
Season (Summer)	-0.11 ± 0.185	0.55
Season (Winter)	-1.05 ± 0.214	< 0.001

To explore the contribution and variability in *LA* due to exogenous non-algal optically active constituents (i.e., CDOM), K_d(465) measured using the HyperPro was compared to the K_d(465) that would be expected for a case 1 system under observed chl-*a* conditions. The solid black line depicted in Fig. 2.8 is a regression through these data and the dashed line indicates the relationship that would be expected for a case 1 system. The difference between them indicates an additional source of *LA* present in the system that is not attributable to seawater or the amount of chl-*a* present and CDOM that covaries with it, and is therefore expected to be due to exogenous sources of biogenic material (i.e., CDOM). Despite the high proportion of variability explained by the bio-optical model, a wide range of CDOM was present in the system and conformed to a linear relationship (Fig. 2.8). This provides support for use of the bio-optical model under the influence of diverse conditions that grey seals may encounter, some with CDOM contributions so low as to resemble case 1 waters (Fig. 2.8). Student's t-Tests performed against the intercept (-0.18) and slope (1.06) revealed that while there was a consistent baseline level of CDOM for the system (t = -3.96, *p-value* = 0.0002), which has been previously described (Ciotti et al. 1999), the relationship between K_d expected from chl-*a* concentrations and

what was observed were otherwise equivalent (t = 0.55, *p-value* = 0.58). As the slope reveals a strong positive relationship between the observed and expected K_d for this system, the intercept is equivalent for all chl-*a* concentrations. This suggests a persistent source of exogenous CDOM was present over multiple years and seasons, which is incorporated in the bio-optical model.

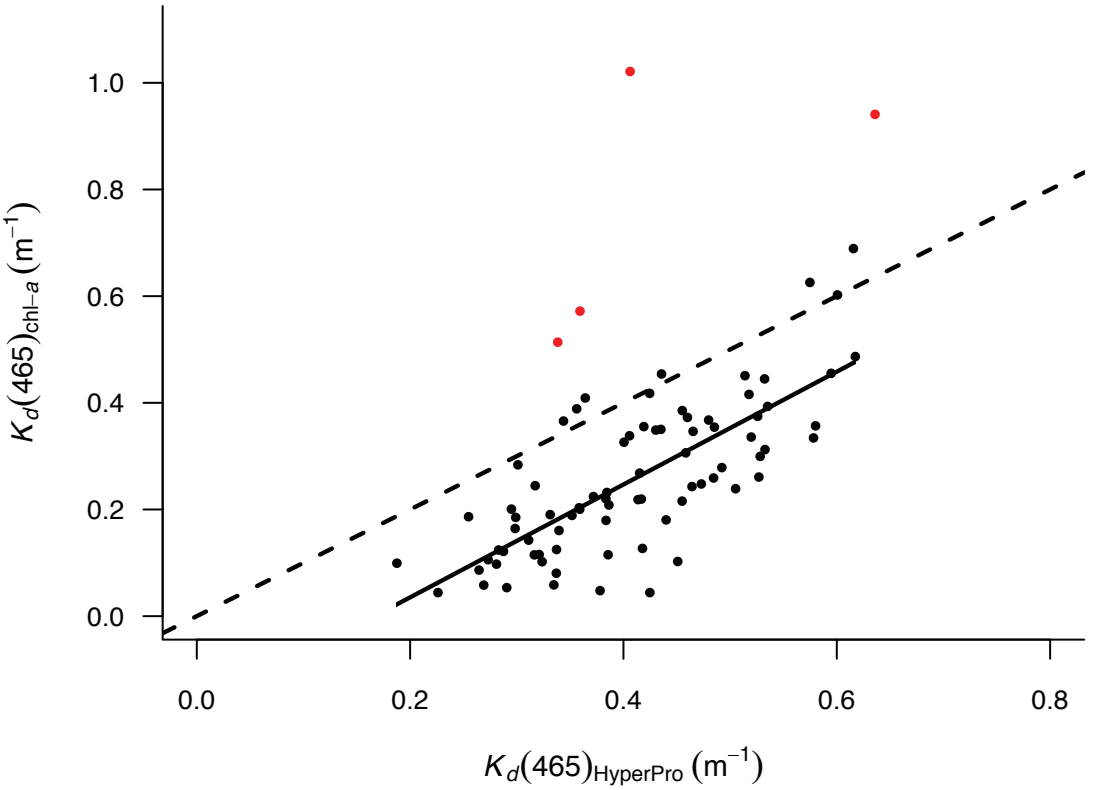

Figure 2.8 Ordinary least squares regression ($R^2 = 0.5671$, $R^2_{adj} = 0.5614$; *p*-value < 0.001) of observed diffuse attenuation coefficient of downwelling irradiance at 465 nm determined using the HyperPro ($K_d(465)_{HP}$; m^{-1}) data against that which would be expected for a case 1 system given measured chlorophyll-*a* concentrations ($K_d(465)_{chl\text{-}a}$; m^{-1}) (n = 79); outliers not included in the analysis are highlighted in red.

2.4 DISCUSSION

The results of the replicated experiment show that it is possible to use chl-*a* data and estimates of *LA* from standard oceanographic instruments to develop a predictive bio-

optical model for optically complex conditions on a continental shelf. These data also show that *LL* and temperature data collected by TDLRs are highly correlated with measurements made by oceanographic instruments. This study demonstrates that instrumented grey seals, and potentially other large-bodied diving species, can collect fine-scale chl-*a* data throughout the year on areas of continental shelves where sample coverage is consistently low or lacking. Despite the fact that MLD and chl-*a* data measured by TDLRs are relatively coarse, these data provide a useful tool for estimating *in situ* oceanographic conditions. The collection of chl-*a* data concurrently with animal locations allows for inferences to be made on the bottom-up forcing of primary productivity patterns on the movements of these species. The bio-optical model accounts for variability in the relationship between chl-*a* and *LA*, as well as regional specificity in phytoplankton community composition and the influence of exogenous sources of CDOM on *LA*.

2.4.1 Bio-Optical Model Formation

Monitoring the MLD is an important parameter in understanding the temporal and spatial dynamics of nutrient mixing and phytoplankton biomass in the water column (Sverdrup 1953). Chl-*a* algorithms have typically been applied within a single standardized depth that is considered to represent most of the primary productivity within the water column (i.e., euphotic zone depth (Jaud et al. 2012) or MLD (O'Toole et al. 2014)). Across the SS, the MLD has been found to be seasonally far deeper than the euphotic depth (Ross et al. 2017). The MLD was chosen to ensure that the deepest depth where chl-*a* may be present is included. By selecting a single MLD estimate that is representative of the majority of encountered MLDs, subsurface chl-*a* present below the

MLD during seasonal shoaling should not be missed (Ross et al. 2017). The use of TDLRs to estimate the MLD has been previously validated by Simmons et al. (2009), however this study also demonstrates the utility for estimating chl-*a* within the water column. In using grey seals to estimate location-specific MLDs, measurements of chl-*a* can be fine-tuned to the oceanographic conditions encountered by grey seals.

The validation that TDLR *LA* measurements were comparable to those of the HyperPro allowed for the inclusion of a much larger set of observations from which a long-term relationship between chl-*a* and *LA* for this system and the influence of CDOM was revealed. Preliminary comparisons of chl-*a* against *LA* in the near-surface depth included measurements made by TDLRs to better gauge how this bio-optical model will represent *in situ* collected data. As the HyperPro was limited to the peak sensitivity of TDLRs, this bio-optical model should be suitable for data collected by grey seals. TDLRs collect *LL* data at additional nearby wavelengths, which may explain differences observed between these instruments in the relationships with indicators of optically active constituents; as some amount of light is detected by TDLRs as low as 400 nm, the peak absorption of phytoplankton is better represented. While the overall trend between chl-*a* and *LA* should remain the same, the strength of the relationship should be improved for measurements of *LA* made by TDLRs. $a_{CDOM}(350)$ is commonly used as a proxy for CDOM concentrations, and because a_{CDOM} decreases exponentially with increasing wavelength (Fig. 2.9) (Twardowski et al. 2004), it is not surprising that $a_{\mathrm{CDOM}}(465)$ is not a suitable substitute (Kirk 1994). This is promising with respect to the limitations of this bio-optical model, as the contribution to *LA* at 465 nm should be reduced compared to what would be expected for the overall CDOM concentration. The fact that a_{CDOM} was

still large enough to be moderately influential to chl-*a* on the LA_{HP} supports the classification as a case 2 system.

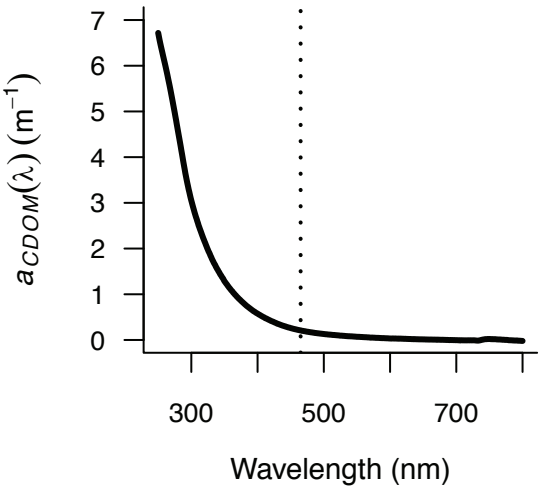

Figure 2.9 Spectral absorption of coloured dissolved organic matter ($a_{CDOM}(\lambda)$) with wavelength (nm) at 5 m depth on March 7, 2012; the peak wavelength of time-depth-light recorders of 465 nm is marked by the dotted line.

The success of this model is owed to the spectral sensitivity of TDLRs, for which the attenuation by chl-*a* is near a maximum and the influence of CDOM present is largely reduced. Evidence for seasonality in phytoplankton community composition and abundances supported the inclusion of season as an explanatory variable (Li et al. 2006; Craig et al. 2015). Phytoplankton biomass is lowest in winter, as the water column is completely mixed, and both temperatures and *LL*s are reduced (Longhurst 1995; Li et al. 2006). Remote-sensing methods estimate that chl-*a* is at a minimum in summer (Fuentes-Yaco et al. 2015), suggesting that pigment packaging and other physiological differences among species may be seasonally specific. Changes in phytoplankton community composition to species better adapted to reduced temperatures and *LL* may be influential for this model (Li et al. 2006). On the SS, the chl-*a* typically range from 0.5 to 3.0 mg m^{-3} with seasonally-dependent ranges (Fuentes-Yaco et al. 2015). While BB data are said to

be representative of the SS, observed phytoplankton concentrations included in this model span a much wider range from 0.22 to 30.36 mg m^{-3} (Li et al. 2006). The existence of a baseline CDOM present in the system at all chl-*a* concentrations over multiple years suggests the influence of exogenous sources of CDOM is somewhat stable for these waters. The persistence over time is thus irrespective of lag in the transport of GSL waters to the inner-shelf region and flushing time of the BB (Shan and Sheng 2012; Dever et al. 2016).

2.4.2 Application to the Scotian Shelf

A previous analysis by Lagman (2013) attempted to develop a bio-optical model using satellite-derived estimates of chl-*a* aligned with K_d measured by instrumented grey seals for the SS, however no relationship could be resolved. This was partially attributed to inaccuracies in the chl-*a* data retrieved. Shallow components of the SS (i.e., inner-shelf and banks) are commonly omitted from remote-sensing chl-*a* estimates due to poor performance of regional algorithms in these areas (Devred et al. 2005; Fuentes-Yaco et al. 2005; Song et al. 2010; Fuentes-Yaco et al. 2015). The reliance of grey seals upon these topographical features (i.e., shallow banks; Breed et al. 2006; Breed et al. 2009) is problematic for these kinds of comparisons. The synoptic (both spatial and temporal) nature of chl-*a* and K_d data available for comparison may have further contributed to these inaccuracies (Moses et al. 2009; Dragon et al. 2010).

An assumption of this model is that the optical conditions of the BB are reasonably representative of those that grey seals would encounter in other case 2 components of the SS. Waters over the SS can be traced to two main sources: the cooler, fresher water of the GSL and the warmer, more saline water from the shelf-break (Smith

and Schwing 1991; Loder et al. 1997; Loder et al. 1998; Han et al. 1999). Water originating from the GSL becomes trapped along the coast of Nova Scotia to become the NSC (Dever et al. 2016). Near-surface waters of the BB included in the formation of this model consist largely of seawater stemming from the SS, along with freshwater inputs at the surface as a result of precipitation and outflow from the Sackville River (Shan and Sheng 2012; Kerrigan et al. 2017). As estimates of *LA* are linearly regressed within these depths, *LA* should be representative of inner-shelf NSC waters. The outflow of the GSL also extends southwestward across the ESS forming the upper layer, reaching between 30 to 40 m in summer and up to 100 m deep in winter (Han et al. 1999). The upper layer of the SS is predominantly made up of water originating from the GSL (Dever et al. 2016). As such, these waters are rich in CDOM, which can be visualised through remote sensing data (Laliberté et al. 2018). While the bottom layer is comprised of incoming slope waters, due to density differences, the presence of shallow banks in this subregion limits the flow of these waters northwards (Loder et al. 1998). Telemetry research has shown that grey seals predominantly inhabit the ESS and lower GSL, particularly during summer and fall pre-breeding season when most data are available (Breed et al. 2006; Lidgard et al. 2014). Individuals spend most of their time at sea foraging, during which movements are concentrated over shallow banks characteristic of this region (Breed et al. 2006; Breed et al. 2009). Although grey seals are benthic foragers, their dive depths average only around 50 m (Beck et al. 2003a). For these reasons, it is believed that grey seals should largely encounter waters stemming from the GSL during movements across the SS.

Grey seals have been equipped with telemetry instruments on the SS for several decades. The bio-optical model provides an opportunity to analyse *LL* data that have been collected by grey seals and contribute to long-term observations of chl-*a*. Grey seals forage on shallow banks (Breed et al. 2006), some of which (e.g., Middle Bank) have shown high levels of biological productivity and importance, yet have not been well-studied (King et al. 2016). The instrumentation of grey seals to estimate chl-*a* using this bio-optical model allows for the *in situ* monitoring of primary productivity patterns throughout the year in what may be considered the most productive and ecologically valuable regions of the SS. The collection of chl-*a* data using animal-borne instruments is particularly useful for the application to broader ecological questions. The role of chl-*a* on the distribution and foraging patterns of large marine predators has received considerable attention (Polovina et al. 2004; Miller et al. 2015). These studies have typically relied upon satellite-derived chl-*a*, providing only a synoptic representation of chl-*a* conditions (Moses et al. 2009). It is particularly challenging to gain sufficient useful information concurrent with animal movements along an entire track to make conclusions about observed behaviour (O'Toole et al. 2014). By using chl-*a* data collected by grey seals, we can improve our understanding of the influence of bottom-up forcing by primary productivity on their movement patterns.

CHAPTER 3: GREY SEALS (*HALICHOERUS GRYPUS*) AS BIOPROBES: FINE-SCALE MEASUREMENTS OF OCEANOGRAPHIC PROPERTIES USING AN INSTRUMENTED LARGE MARINE PREDATOR

3.1 INTRODUCTION

The impacts of ocean warming (e.g., changes in vertical stratification, primary productivity patterns, biodiversity, species distributions, trophic interactions, physiological mechanisms, incidence of disease, etc.) have been well-documented on a global scale (Walther et al. 2002; Sarmiento et al. 2004; Hoegh-Guldberg et al. 2010; Doney et al. 2012). These impacts are further complicated by other anthropogenic influences, such as fishing pressures, pollution, and habitat destruction (Harley et al. 2006).

Measurement of oceanographic properties is required to better understand ecosystem changes and forecast future conditions, however the collection of such data can be logistically challenging and costly to undertake. Measurements have traditionally been taken aboard research vessels, which are expensive and limited in both spatial coverage and frequency of observations. The use of drifters and floats are significantly less labour-intensive, allowing for numerous simultaneous deployments and improved spatial coverage at broader scales (e.g., Argo float array; Riser et al. 2016). Moorings and buoys provide an alternative with repeated sampling at specific locations, but generally lack spatial coverage. The use of marine autonomous systems (i.e., autonomous underwater vehicles (AUVs) or gliders) largely overcome these limitations, however these are again costly to deploy and can be limited by certain conditions (e.g., currents; Wynn et al. 2017; Ross et al. 2017). Remote sensing has been pivotal in overcoming

many challenges, as it offers estimation of several oceanographic variables over large spatial scales and at far more frequent timescales. However, this too comes with limitations, including being restricted to the first optical depth, the requirements for atmospheric correction, inaccuracies associated with making synoptic observations, and gaps in data due to cloud or ice cover (Cullen 1982; Saunders and Kriebel 1988; Gao et al. 2000; Moses et al. 2009). Thus, these various methods are often combined to provide a more complete representation of oceanographic conditions (Montes-Hugo et al. 2009).

The instrumentation of marine animals as autonomous samplers is an additional source for acquiring oceanographic data. For example, pinnipeds (namely seals, sea lions, and fur seals) are generally large-bodied making them able to safely carry instruments capable of accurate geolocation and sampling of oceanographic properties throughout the water column. Some species can be easily live-captured and recaptured, allowing for the deployment of instruments and recovery of archival data (Boehlert et al. 2001); in other cases, this data can be transmitted via satellite (Roquet et al. 2014). Instrumented pinnipeds ("bioprobes") have collected data on ocean temperature (Campagna et al. 2000; Boyd et al. 2001; Lydersen et al. 2004; Simmons et al. 2009), bathymetry (Padman et al. 2010), salinity (Hooker and Boyd 2003; Boehme et al. 2009), and chlorophyll-*a* (chl-*a*) concentrations (Teo et al. 2009; Jaud et al. 2012; O'Toole et al. 2014). Although these data have been available for some time (Costa 1993; Boehlert et al. 2001; Fedak 2004; Costa et al. 2010; Fedak 2013; Roquet et al. 2014; Treasure et al. 2017), uptake by the oceanographic community has been largely system-specific and remain overlooked in many regions.

Pinnipeds generally inhabit higher latitudes and thus provide an opportunity to collect oceanographic data in areas where other methods are difficult to use (e.g., due to increased cloud cover, sea ice, low solar elevation, remoteness) or extremely costly (Sumner et al. 2003; Kovacs et al. 2012; Lowther et al. 2016). These more polar regions also have improved satellite coverage, resulting in more numerous at-sea locations of pinniped bioprobes (Patterson et al. 2010; Dujon et al. 2014). Operating analogously to AUVs, diving animals sample properties of the water column along a transect line, although in this case, of their choosing. Many individuals exhibit repeated use of some habitats (e.g., foraging patches), which has the advantage of providing persistent observations for those areas (or ocean "hotspots"; Breed et al. 2006). In addition, some individuals may range widely, offering an opportunity to sample remote areas that cannot be routinely sampled otherwise.

The Scotian Shelf (SS) is a Large Marine Ecosystem (LME) with a series of banks and basins largely concentrated on the eastern Scotian Shelf (ESS). These topographical features and the resulting hydrographic complexity contribute to a heterogeneous structuring of bio-physical processes (Han and Loder 2003). Over the past several decades, the SS has undergone dramatic changes, particularly with respect to populations of groundfish species as a result of changing temperatures and substantial pressure from commercial fisheries (Frank et al. 2005; Worcester and Parker 2010; Shackell et al. 2012; Brennan et al. 2016). These changes include water freshening (Belkin 2004; Greene et al. 2008; Hebert et al. 2018), warming temperatures (Brickman et al. 2018; Hebert et al. 2018), and changes in vertical stratification (Worcester and Parker 2010); reductions in body size, biomass, and physiological condition of fish

species (Choi et al. 2004; Shackell and Frank 2007; Shackell et al. 2010); and shifts in species ranges (Frank et al. 1996; Lucey and Nye 2010), community composition (Bundy 2005; Choi et al. 2005; Frank et al. 2005), and trophic dynamics (Frank et al. 2005; Shackell and Frank 2005; Shackell and Frank 2007; Shackell et al. 2010; Worcester and Parker 2010). How further climate change may influence the already altered SS ecosystem is an area of ongoing interest (Shackell et al. 2014).

The SS is inhabited by approximately 424,300 grey seals (*Halichoerus grypus*) (Hammill et al. 2017a). As central place foragers, grey seals show high site fidelity in haulout locations making the retrieval of biologging devices considerably more successful than in other systems (Bowen et al. 2015). This species is known to forage benthically (Thompson et al. 1991) and to perform frequent, deep dives (Beck et al. 2003a; Beck et al. 2003b; Austin et al. 2006), allowing for collection of oceanographic data throughout the water column along an animal's path. This study aims to demonstrate how instrumented grey seals can be used to collect high-resolution oceanographic data at fine spatial and temporal scales across the SS.

3.2 METHODS

3.2.1 Study Site

Grey seals were instrumented and subsequently recaptured on Sable Island, Nova Scotia (43º55'N, 60º00'W) between October 15, 2009 and January 21, 2016. Sable Island is a narrow, partially-vegetated sandbar located approximately 300 km off the coast of Halifax, NS, Canada. Located on the central, outer edge of the continental shelf, Sable Island supports the largest breeding colony of grey seals in the world (Bowen et al. 2007)

and has been used for the deployment of instruments on individuals for nearly two decades (Beck et al. 2000; Beck et al. 2003a; Beck et al. 2003b; Austin et al. 2004; Austin et al. 2006; Breed et al. 2006; Breed et al. 2009; Lidgard et al. 2014).

3.2.2 Animal Handling and Tag Deployment

One-hundred-seventeen individuals (34 males, 83 females) were selected for instrumentation with telemetry and biologging devices (Table 3.1). Grey seals were captured onshore in summer following the spring moult (June) or fall (late September or early October) using handheld nets (Bowen et al. 1992). They were then weighed using a 300 kg (±1 kg) Salter spring balance and immobilized with an intramuscular injection of Telazol (male dose 0.45 mg kg^{-1}, female dose 0.90 mg kg^{-1}) (Bowen et al. 1999); standard body length was also taken at this time. Each seal was equipped with a VHF transmitter (164 to 165 MHz; www.astrack.com) and a Mk10-AF Fastloc^{TM} GPS bio-logging transmitter (time-depth-light recorder or TDLR; Wildlife Computers, www.wildlifecomputers.com). The VHF transmitter was attached to the TDLR using a stainless-steel hose clamp and both were glued to the fur on the top of the seal's head using 5 min epoxy (Boness et al. 1994). The tag mass burden (total mass of tag/average body mass) was 0.26% for males (tag mass = 0.53 kg; average body mass = 204.91 kg) and 0.32% for females (tag mass = 0.53 kg; average body mass = 164.93 kg). TDLRs were programmed to record depth (m), temperature (ºC), and light level (*LL*) every 10 s during dives. Depth was measured between 0 and 1000 m with a resolution of 0.5 m and an accuracy of 1% of the depth reading. Temperature was measured using a fast-response external thermistor within a range of -40 to 60 ºC at a resolution of 0.05 ± 0.1 ºC. Light sensors were comprised of a photodiode with a blue-window transmittance filter resulting

in a peak sensitivity of 465 nm and parabolic range between 400 and 490 nm (Vacquié-Garcia et al. 2017). Light intensity is detected between 5 x 10^{-12} W cm^{-2} and 5 x 10^{-2} W cm^{-2}. Light intensity (W cm^{-2}) was log-transformed onboard tags to a three-digit *LL* value to increase resolution at depth where light intensity is reduced, resulting in a range of 25 to 225 units. TDLRs recorded accurate GPS locations every 15 minutes after tags were considered to be wet for 45 s out of every 1 min; in 2009 tags recorded GPS locations every 5 minutes. Both environmental and location data were stored onboard the tag which were downloaded upon retrieval.

Table 3.1 Deployment and recovery record of Mk10-AF Fastloc™ GPS time-depth-light recorders on grey seals during the study period.

Year	Deployment Month	Instruments Deployed	Instruments Recovered	Data Recovered		
				Total	Males	Females
2009	October	15	13	13	5	8
2010	September	20	20	20	6	14
2011	June	20	16	13	0	13
2012	June	17	16	15	5	10
2013	June	15	12	12	4	8
2014	June	15	12	12	5	7
2015	June	15	11	9	0	9
Total		117	100	94	25	69

During the subsequent breeding season, the VHF transmitters were used to locate individuals returning to Sable Island (late December through January). Males were captured at the first available opportunity, whereas females were captured three days following parturition to assure the development of a strong mother-pup bond (Beck et al.

2000). Data were recovered from 94 (80% of) individuals (25 males, 69 females) (Table 3.1): 17 seals (8 males, 9 females) did not return to Sable Island to breed and the tags recovered from 6 seals (1 male, 5 females) contained too many erroneous readings (i.e., GPS location, temperature, depth) to properly reconstruct oceanographic datasets. Saltwater switches of tags deployed in 2012 intermittently malfunctioned, resulting in a reduced number of GPS locations for that year.

3.2.3 Dive Data Processing

Dive data were analyzed using Wildlife Computers Dive Analysis Program (WC-DAP) provided by the tag manufacturers. All dive depth records were zero-offset corrected for drift in the pressure transducers over time. A surface error of 1.0 m was used in all WC-DAP analyses. Dives < 5 m (referred to as the surface interval) were removed from the dataset to eliminate the influence of sea-surface conditions and near-surface rolling. This depth was selected for consistency with previous studies (Beck et al. 2003a; Beck et al. 2003b; Austin et al. 2006), considering the resolution of depth measurement and body length of animals (maximum 2.32 m) (Heerah et al. 2014). Dives > 30 min were not included as they were likely a result of two or more consecutive dives erroneously merged together by the dive analysis software (Beck et al. 2003a; Beck et al. 2003b); those ≤ 20 s were also removed. Summary statistics were calculated for each dive including the time and duration of the dive, time spent at the bottom of the dive, maximum depth, and average ascent and descent rates. Dives were separated into three phases (i.e., descent, bottom, ascent). Bottom time was defined as any depth reading made at or below 80% of the maximum for each dive. The remainder of dive data analyses were performed using R statistical software (R Core Team, 2018). Dives were

filtered by removing those with ascent and descent rates ≥ 6 m s^{-1} or equal to 0 m s^{-1} (Burns et al. 2004, Kuhn et al. 2006, Krause et al. 2016). Dives with maximum depth readings > 2000 m were removed from the record as they exceeded the feasible range in the study area. GPS locations with < 5 satellites and/or residual error values > 30 (Dujon et al. 2014; Lidgard et al. 2014) were removed from the data. A speed filter of 10 m s^{-1} between neighbouring locations was also applied. The remaining locations were considered to have negligible error and accuracies of 10s of meters (Bryant 2007).

Environmental data were assigned a dive phase based upon the summary statistics of each dive using a purpose-built algorithm. These data were used to calculate environmental summary statistics for each dive. Although a lag in temperature measurement is inherent to tags (Jaud et al. 2012; O'Toole et al. 2014), a correction could not be applied, as calibrations were not performed prior to or following deployment (Simmons et al. 2009). To improve the overall accuracy of these measurements, temperatures were corrected by subtracting 0.05 ºC from each reading (Simmons et al. 2009). Environmental data collected during the ascent phase of dives were used to calculate water column properties including mixed layer depth (MLD), mean upper-water column temperature (T_{50}), and mean light attenuation (LA) for the estimation of chl-*a*. The ascent phase of dives was used so that dive summary data corresponded most closely with GPS locations recorded following dives and to ensure that tags, which are equipped with cosine *LL* sensors, were facing upwards during *LL* measurements (Boehme et al. 2009; Teo et al. 2009; Roquet et al. 2011). MLD was estimated using the finite depth criterion method using temperature profiles (de Boyer Montegut et al. 2004). A criterion value of 0.5 ºC was chosen and a near-surface reference depth of 15 m was used to

remove the influence of diurnal surface heating (Xing et al. 2012). A single MLD was selected to represent the depth at which most primary productivity occurs within the water column and standardize measurements throughout the duration of the study. For this, a MLD of 50 m was used, as the majority of MLD encountered by grey seals were above this depth (89.3 % of dives where the MLD was detected) (Fig. 3.1). Dives were then restricted to those that included measurements over the entire MLD, reaching at least 50 m and with a minimum of one measurement taken within the surface interval (i.e., between 0 and 5 m depth) (Jaud et al. 2012). The mean temperature above 50 m was taken to be the upper-water column temperature (T_{50}). *LA* (m^{-1}) was calculated over this depth by linearly regressing *LL* data using the following equation (O'Toole et al. 2014):

$$LA = -\frac{LL_1 - LL_2}{z_2 - z_1}, \quad \text{(Equation 12)}$$

where LL_1 represents the *LL* within the surface interval (z_1) and LL_2 represents the *LL* at 50 m (z_2). These values were used to estimate chl-*a* concentration by season using the coefficient estimates of the bio-optical model (see Chapter 2). Only *LL* profiles within a 4 hour period surrounding local noon (10:00 to 14:00 AST) were used (see discussion in Teo et al. 2009). An extended time period was used, as this study was performed at a relatively low latitude with respect to the solar elevation; LL measurements made below the surface further reduce solar zenith angles. To filter *LL* profiles for erroneous readings, several thresholds were used based upon the range limits of *LL* sensors and blue light intensity calibrations. Only profiles with $LL \leq 170$ and ≥ 225 within the surface interval were used, corresponding to the maximum light level possible and the minimum value expected for a daytime reading (i.e., very dark day), respectively. A light level of 170 corresponded well with outlier assessment (IQR minimum of 166.25). Profiles with a

minimum light level < 25 were also removed. The presence of passing clouds can result in intermittent *LL* lower than what would be expected for a given profile (Beck 2016). These incidences are particularly influential when measurements are near-surface and the rate of change in *LL* is highest; since *LL* data are linearly regressed to produce *LA*, this can result in incorrect estimates of *LA*. To filter *LL* profiles for this effect, profiles were removed where the surface interval *LL* did not correspond to the maximum *LL*. Sea surface temperature (SST) was also taken from the ascent phase of dives. Data collected within the top 1 m of the water column were considered to be at the surface. Although the definition of surface interval within the context of this study and others (Richaud et al. 2016) has been considered < 5 m depth, almost all surface locations (i.e., the minimum depth during the ascent phase) fell within the top meter and it was therefore confined to this depth for consistency among observations.

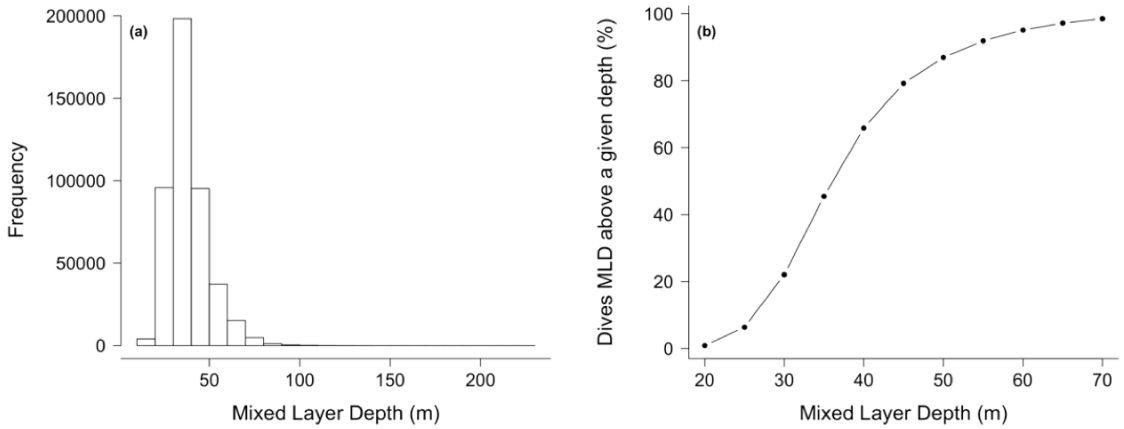

Figure 3.1 (a) Frequency of mixed layer depths (MLD) encountered by grey seals over the Scotian Shelf and (b) the percentage of dives within which the MLD was above a given depth.

3.2.4 Mapping Oceanographic Data

Each dive was assigned a Fastloc GPS location. As multiple dives commonly occurred between each location, summary statistics of the last dive where data were available prior to each location were used. The minimum convex polygon (MCP) surrounding all grey seal relocations was used to determine the range of sampling locations for oceanographic properties and regional suitability of the bio-optical model. This was performed using the R package *adehabitatHR* (Calenge 2006). The MCP is a widely used and standard home range estimation technique. While this method has been criticized (Burgman and Fox 2003), my aim was to simply demonstrate the general correspondence of grey seal habitat to climatological sub-regions of the SS. The sampling extent of grey seals was compared to the boundaries of the SS LME (Lonneville et al. 2019). Based on previous research describing foraging hotspots of grey seals in this area (Breed et al. 2006; Breed et al. 2009), custom polygons overlaid on the bathymetry of Middle Bank and Canso Bank were used to illustrate monitoring of oceanographic conditions of these regions. Bathymetry data were acquired from the NOAA ETOPO1 database (Amante and Eakins 2009) and the isobath at 100 m was used to highlight topographical features (King et al. 2016).

3.3 RESULTS

A large number of observations were collected by the instruments fitted to grey seals in all years and across all seasons prior to the breeding season (Table 3.2, Table A.1). There were fewer observations in January, as animals had already returned to the breeding colony or did so partway through the month; for this reason, these data were not

included in figures or reported totals. Compared to other methods employed on the SS (e.g., fixed stations, ecosystem trawl surveys, etc.), sampling of oceanographic properties (595,866 total) were far more numerous (e.g., compared to 572 hydrographic station occupations in a single year, see Table 1 in Johnson et al. 2018) and also continuous throughout the deployment period (Table 3.2) with high spatial coverage (Fig. 3.2) (Johnson et al. 2018). The number of available profiles were comparable to those of other databases, relative to the duration of the study and method of data recovery (Boehlert et al. 2001; Roquet et al. 2014).

Grey seals were distributed broadly across the SS during summer and fall, with movements extending over the central Scotian Shelf (CSS) and high into the Gulf of St. Lawrence (GSL) (Fig. 3.2). The MCP surrounding 95% of all relocations indicated that sampling coverage by grey seals extended over 72.90% of the LME (Fig. 3.3), on average sampling 26.3% of the area each month (Table 3.3). The area sampled by seals each month reflected both seasonal movement patterns and the number and sex ratio of individuals sampled. Seal locations were heavily concentrated over the eastern Scotian Shelf (ESS) and lower GSL (Fig. 3.4) with up to 90% of relocations occurring within these regions; notably, up to 70% of locations occurred over the ESS alone (Fig. 3.4).

Table 3.2 Total number of locations where oceanographic properties were measured by month and by year of deployment; totals do not include observations made in January.

Year	Jun	Jul	Aug	Sep	Oct	Nov	Dec	Total
2009	0	0	0	0	12756	31080	27776	71612
2010	0	0	0	11752	31899	35569	26890	106110
2011	7952	12449	9305	9687	16004	16297	13182	84876
2012	809	4737	4516	4303	4087	4084	3981	26517
2013	1444	15715	14757	14691	17075	19134	15554	98370
2014	9872	19047	15720	16230	21485	24801	18431	125586
2015	7236	14459	8391	9284	12721	16112	14592	82795

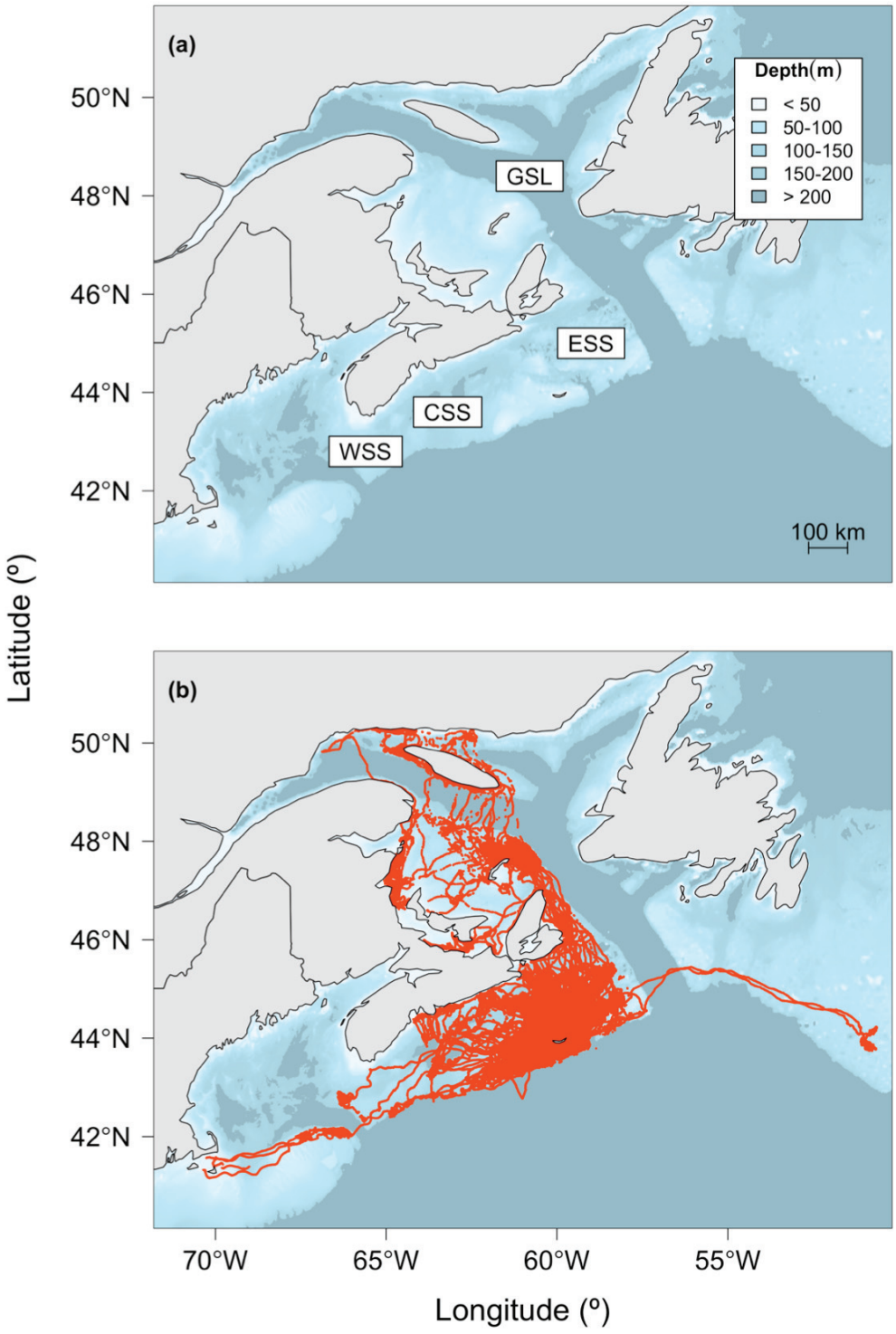

Figure 3.2 (a) Scotian Shelf ecosystem with the eastern Scotian Shelf (ESS), central Scotian Shelf (CSS), western Scotian Shelf (WSS), and Gulf of St. Lawrence (GSL) sub-regions identified and (b) distribution of grey seal (n = 79) locations obtained over the study period; data collected in January are not included in this figure.

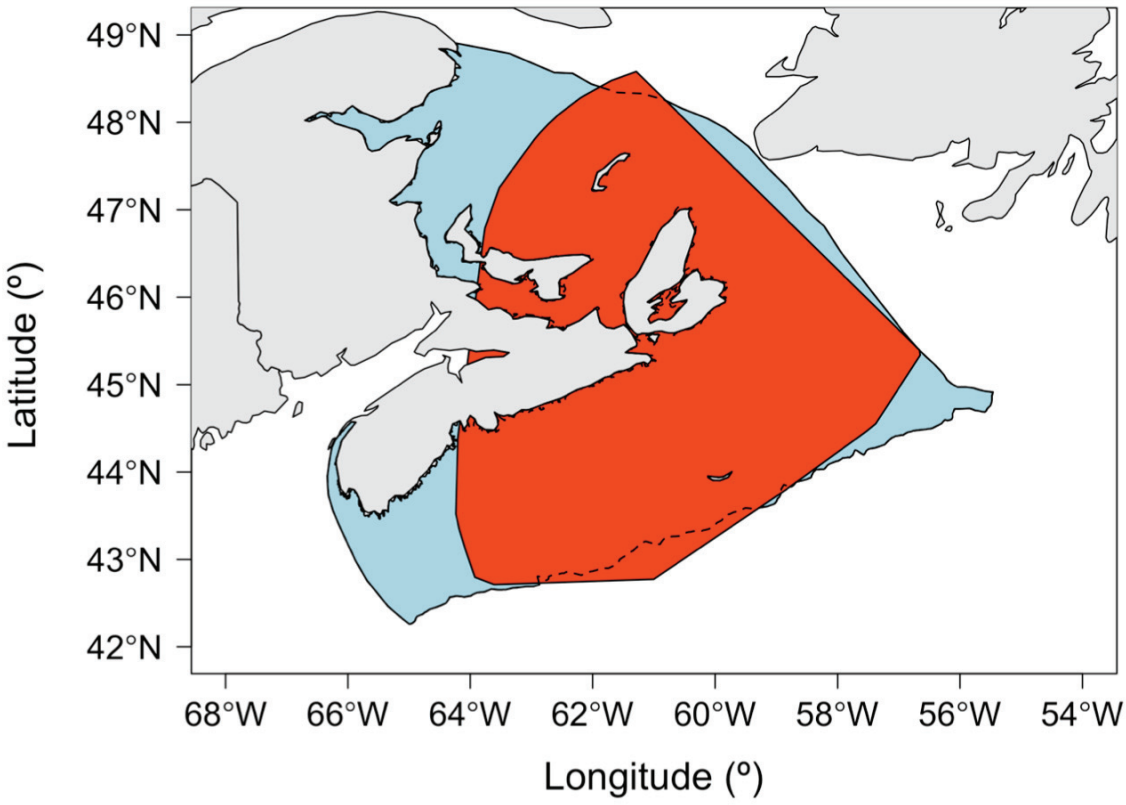

Figure 3.3 The Scotian Shelf Large Marine Ecosystem (Lonneville et al. 2019) boundary (blue) overlain with the minimum convex polygon (convex hull) including 95% of grey seal (n = 79) locations over the study period (red).

Table 3.3 Percentage of sampling coverage within the Scotian Shelf Large Marine Ecosystem using the 95% minimum convex polygon surrounding grey seal locations in each month of each year of the study period.

Year	Jun	Jul	Aug	Sep	Oct	Nov	Dec
2009	0	0	0	0	6.1	16.4	18.3
2010	0	0	0	14.8	25.2	27.8	24.7
2011	6.0	39.7	18.1	20.9	27.0	7.6	9.5
2012	2.4	32.5	29.9	24.2	21.3	16.4	24.1
2013	4.2	33.8	59.9	50.3	33.1	51.9	56.3
2014	13.3	44.2	47.0	42.3	44.0	40.5	22.6
2015	9.5	21.6	21.3	32.1	23.0	27.8	26.3

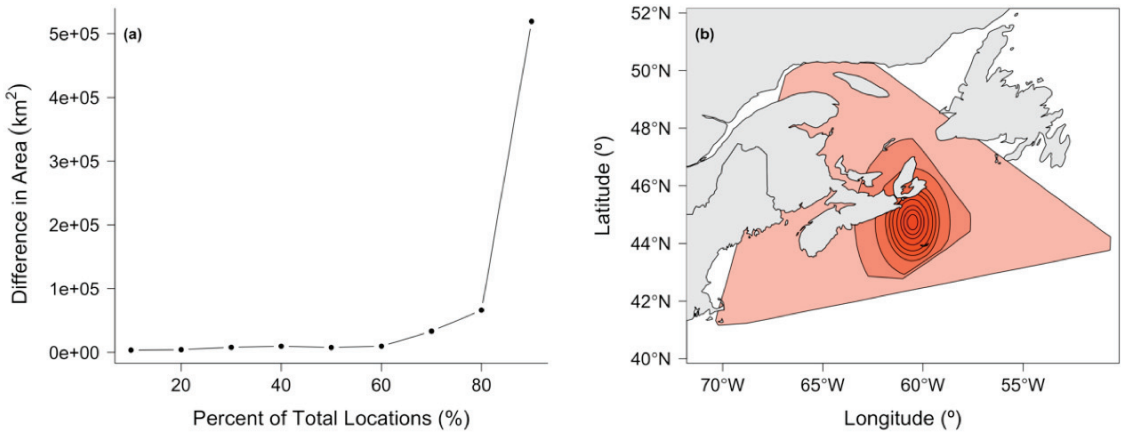

Figure 3.4 (a) Relationship between the differences in area (km^2) covered by minimum convex polygons at incremental changes (Δ 10%) in the percent of total grey seal (n = 79) locations included and (b) distributions across the Scotian Shelf.

Grey seal relocations were centered around Middle Bank and Canso Bank (Fig. 3.5), which are notably biologically productive areas. These polygons alone contain 82,031 observations (i.e., 13.77% of all grey seal locations), not including the full extent of either bank. The bio-optical chl-*a* algorithm used permitted the estimation over shallow banks that may otherwise be omitted from chl-*a* analyses (Song et al. 2010).

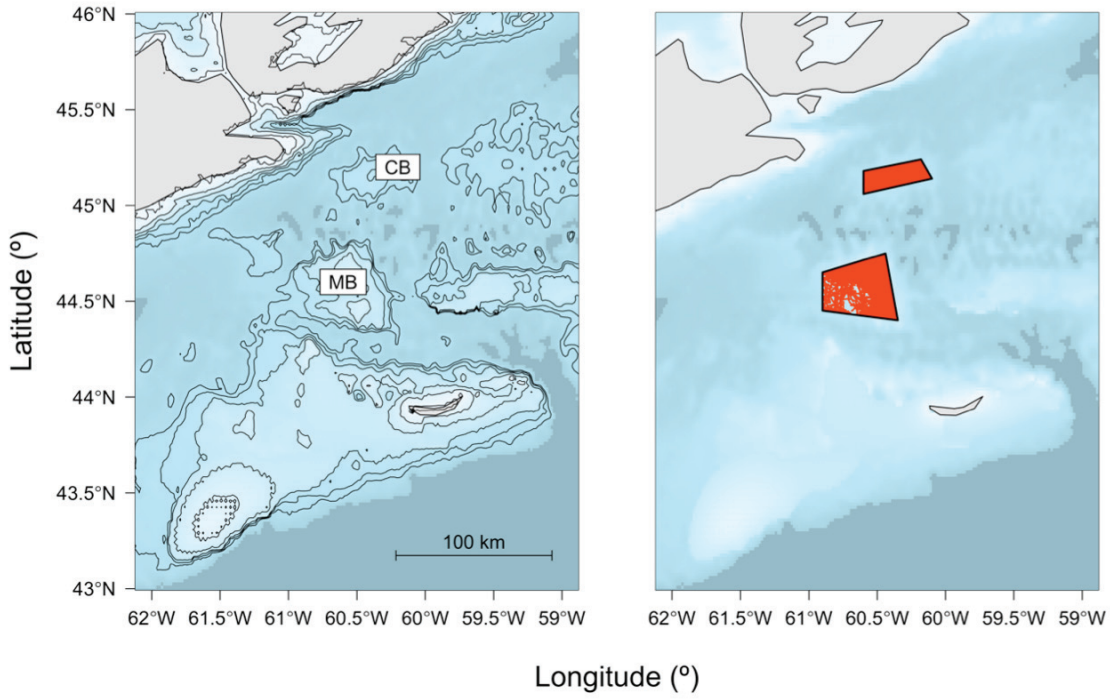

Figure 3.5 Middle Bank (MB) and Canso Bank (CB) with isobaths marked between 0 m and 100 m depth at 20 m intervals and polygons used to subset grey seal locations for monitoring of oceanographic conditions within these areas.

The fine-scale geolocation data paired with *in situ* measurements revealed highly detailed spatial and temporal variation in oceanographic properties (Fig. 3.6). Despite this heterogeneity over longer time scales, persistent patterns were still evident. For example, the presence of cooler waters stemming from the GSL (Fig. 3.6b). In visualising the oceanographic conditions encountered by individual grey seals throughout a deployment (Fig. 3.7), temporal patterns in oceanographic properties, such as deepening of the mixed layer and cooling of SST, become clear. Inter-annual and monthly variation in these properties are evident and, with high frequency of observations, provide insight into the range of values present across the ecosystem and general trends (Figs. 3.8 and 3.9, respectively). Sampling gaps in the dataset (e.g., late October in Fig. 3.7a and

intermittently in Fig. 3.7b) are owed to the seal hauling out or diving to insufficient depths for some measurements (i.e., 50 m). These discrepancies in sampling are generally nonsynchronous among individuals (Fig. 3.7). For example, topographical features with frequent visitation by grey seals allowed for high temporal coverage and localized monitoring of these areas over time (Fig. 3.10).Through the instrumentation of many individuals each year, the spatio-temporal coverage of data collection was improved, providing a fuller picture of the oceanographic conditions across the SS.

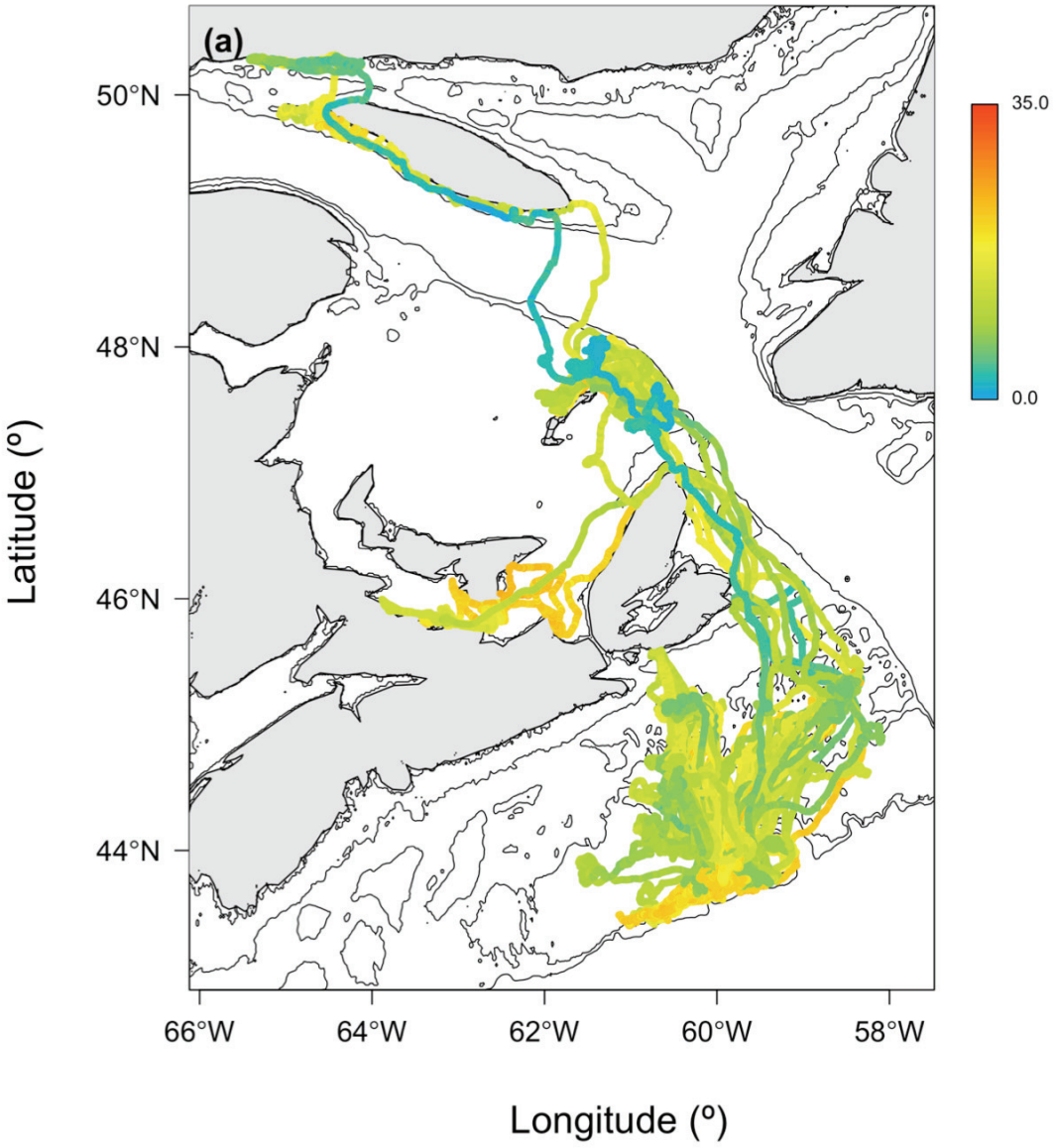

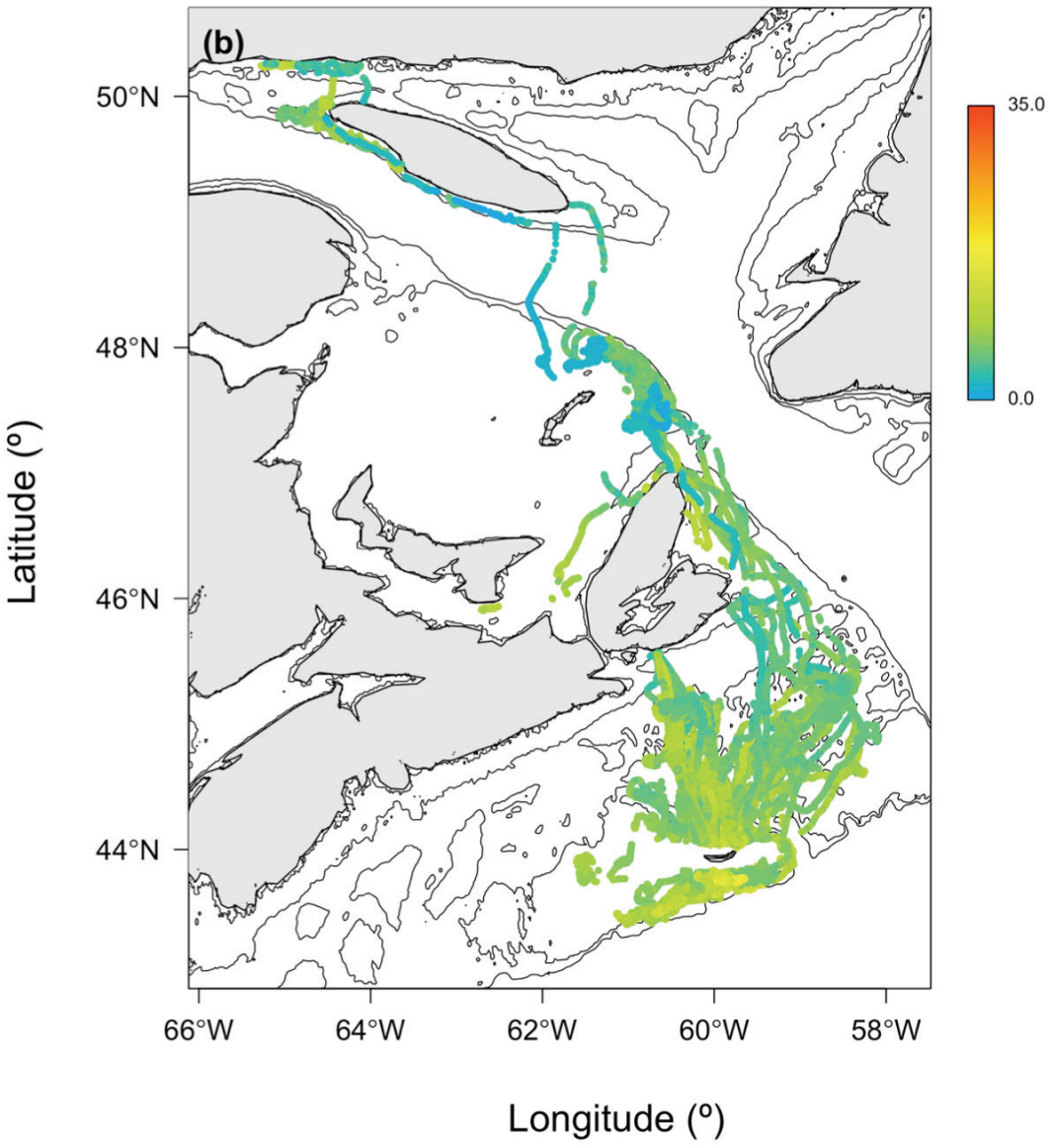
(b)
50°N
48°N
46°N
44°N
Latitude (°)
66°W
64°W
62°W
60°W
58°W
Longitude (°)
35.0
0.0

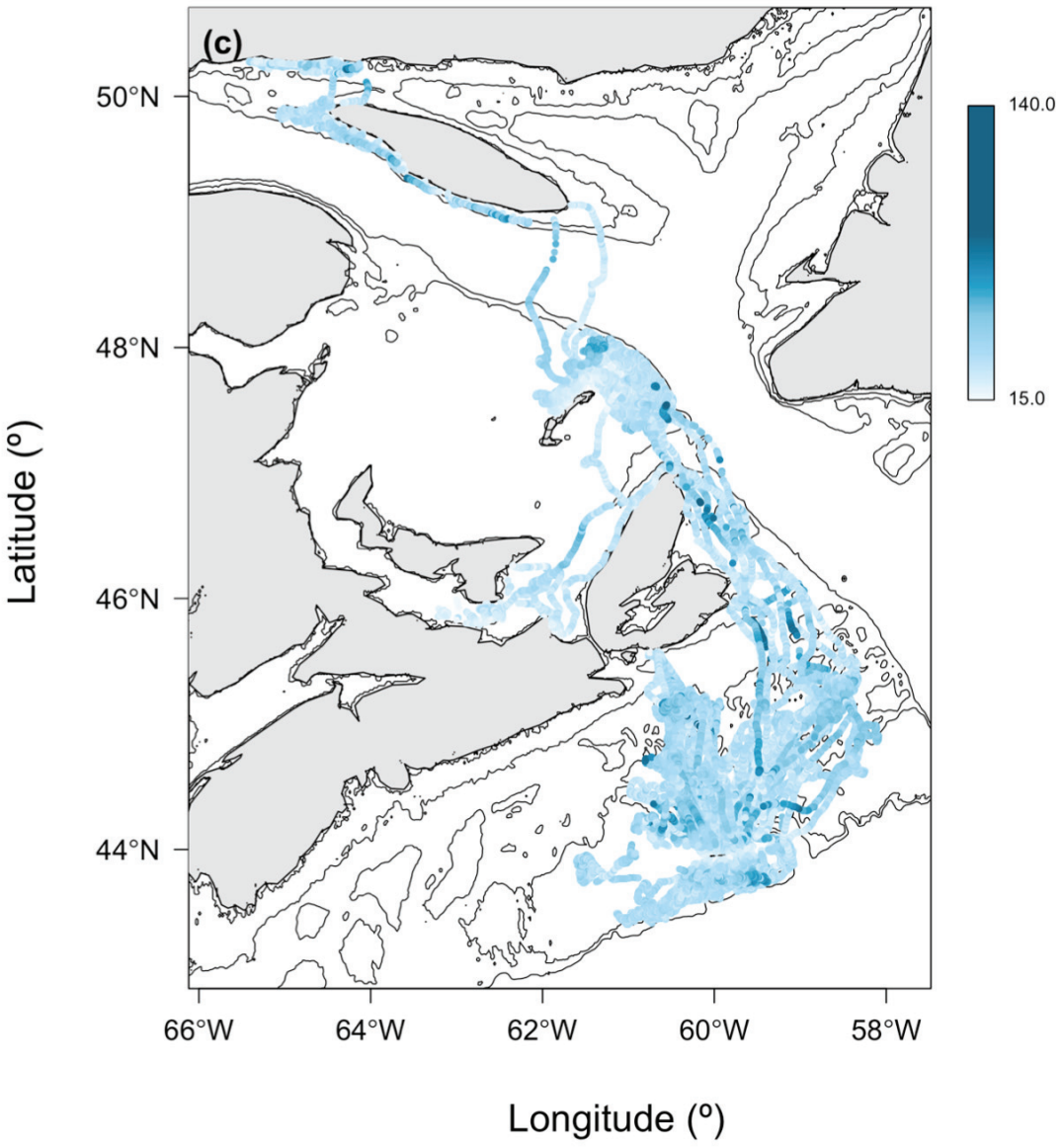
(c)
50°N
48°N
46°N
44°N
66°W
64°W
62°W
60°W
58°W
Latitude (°)
Longitude (°)
140.0
15.0

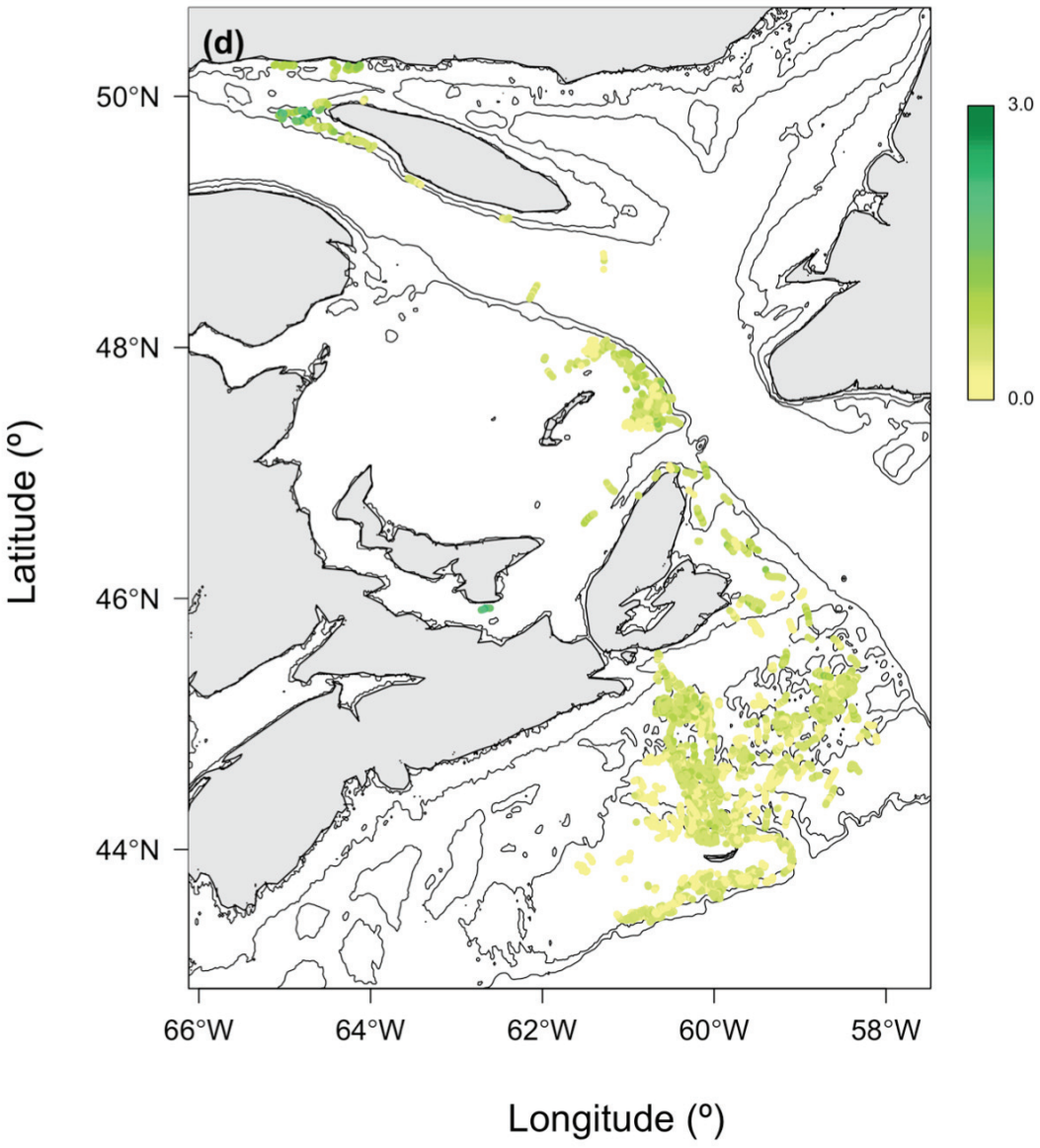

Figure 3.6 Gradient maps of (a) sea surface temperature (SST; ºC), (b) upper-water column temperature (T_{50}; ºC), (c) mixed layer depth (MLD; m), and (d) chlorophyll-*a* concentration (chl-*a*; mg m^{-3}) measured using instrumented grey seals between June and December of 2014.

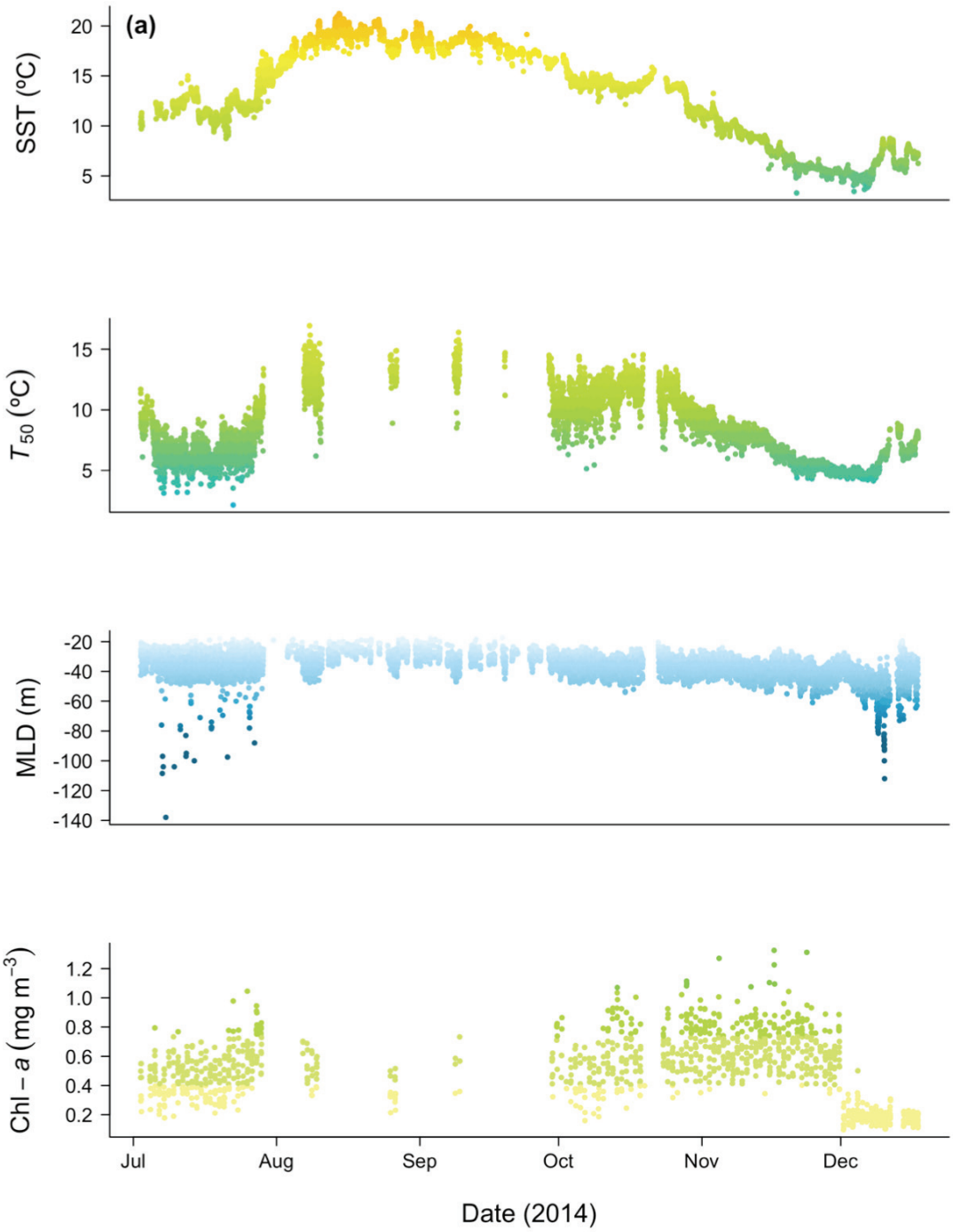
(a)
SST (°C)
20
15
10
5
T_{50} (°C)
15
10
5
MLD (m)
-20
-40
-60
-80
-100
-120
-140
Chl – a (mg m^{-3})
1.2
1.0
0.8
0.6
0.4
0.2
Jul
Aug
Sep
Oct
Nov
Dec
Date (2014)

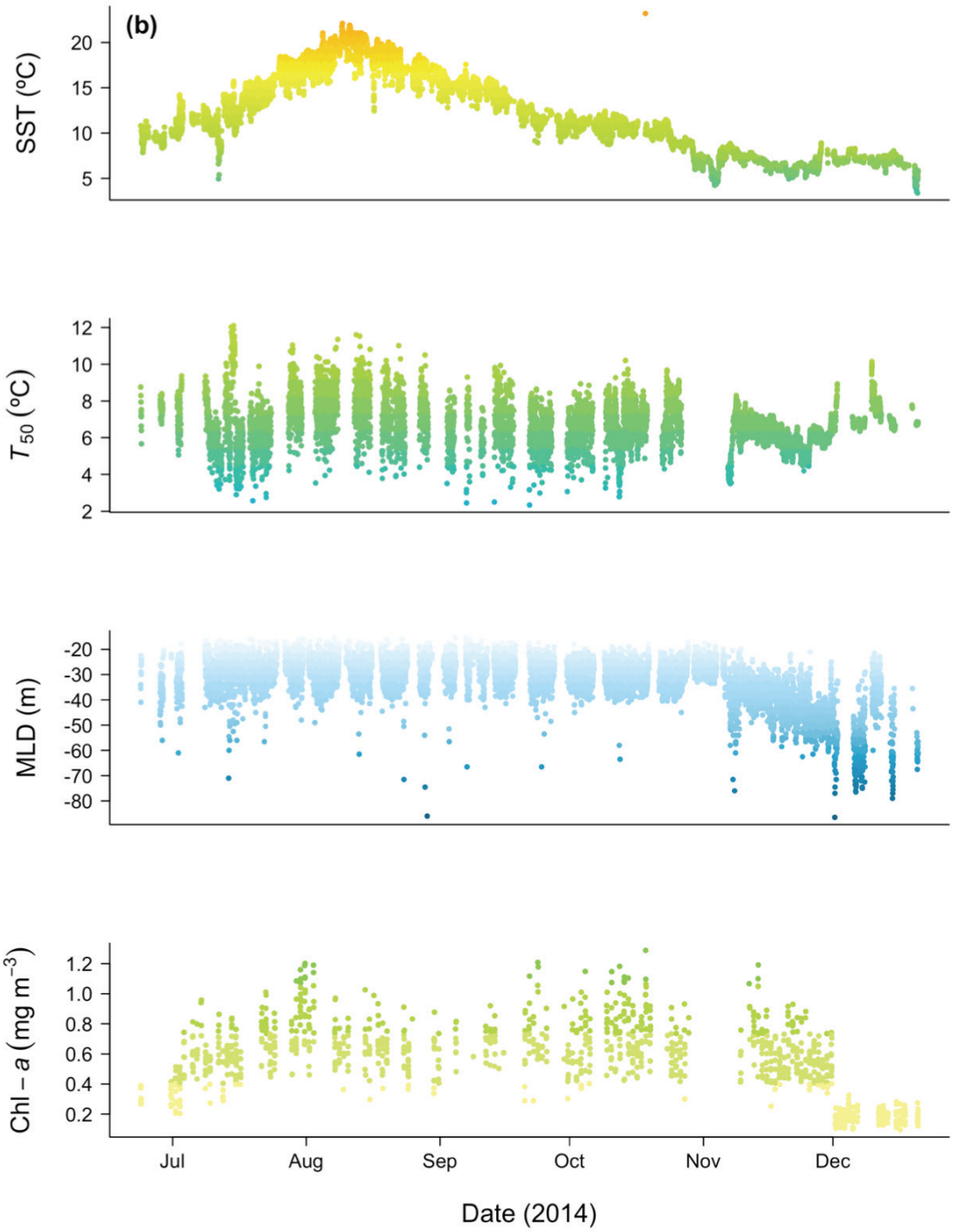

Figure 3.7 Oceanographic properties including sea surface temperature (SST; ºC), upper-water column temperature (T_{50}; ºC), mixed layer depth (MLD; m), and chlorophyll-*a* concentration (chl-*a*; mg m^{-3}) measured by an individual (a) female and (b) male grey seal throughout their respective deployments in 2014.

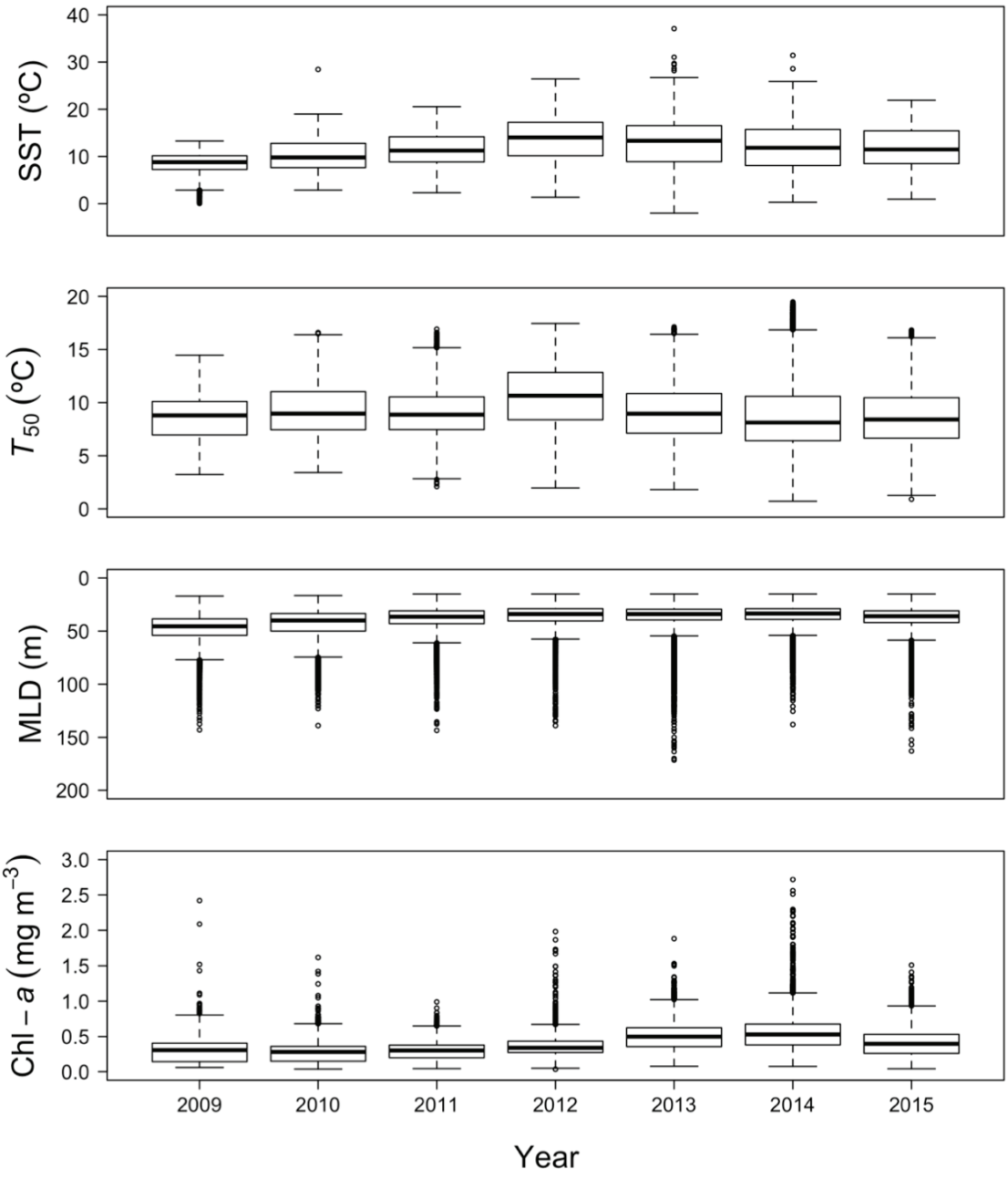

Figure 3.8 Inter-annual variation of oceanographic properties including sea surface temperature (SST; ºC), upper-water column temperature (T_{50}; ºC), mixed layer depth (MLD; m), and chlorophyll-*a* concentration (chl-*a*; mg m^{-3}) across the Scotian Shelf measured by grey seals over the duration of the study period (n = 79).

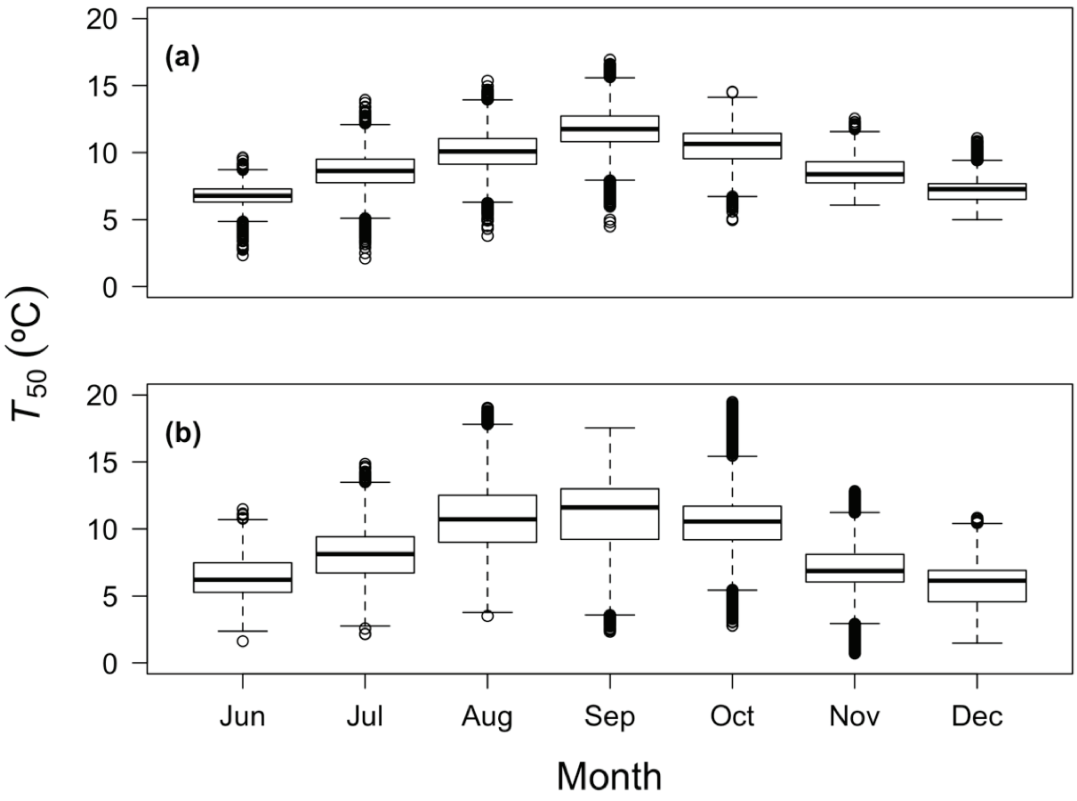

Figure 3.9 Monthly variation in upper-water column temperature (T_{50}; ºC) across the Scotian Shelf measured by instrumented grey seals deployed in (a) 2011 (n = 13) and (b) 2014 (n = 12).

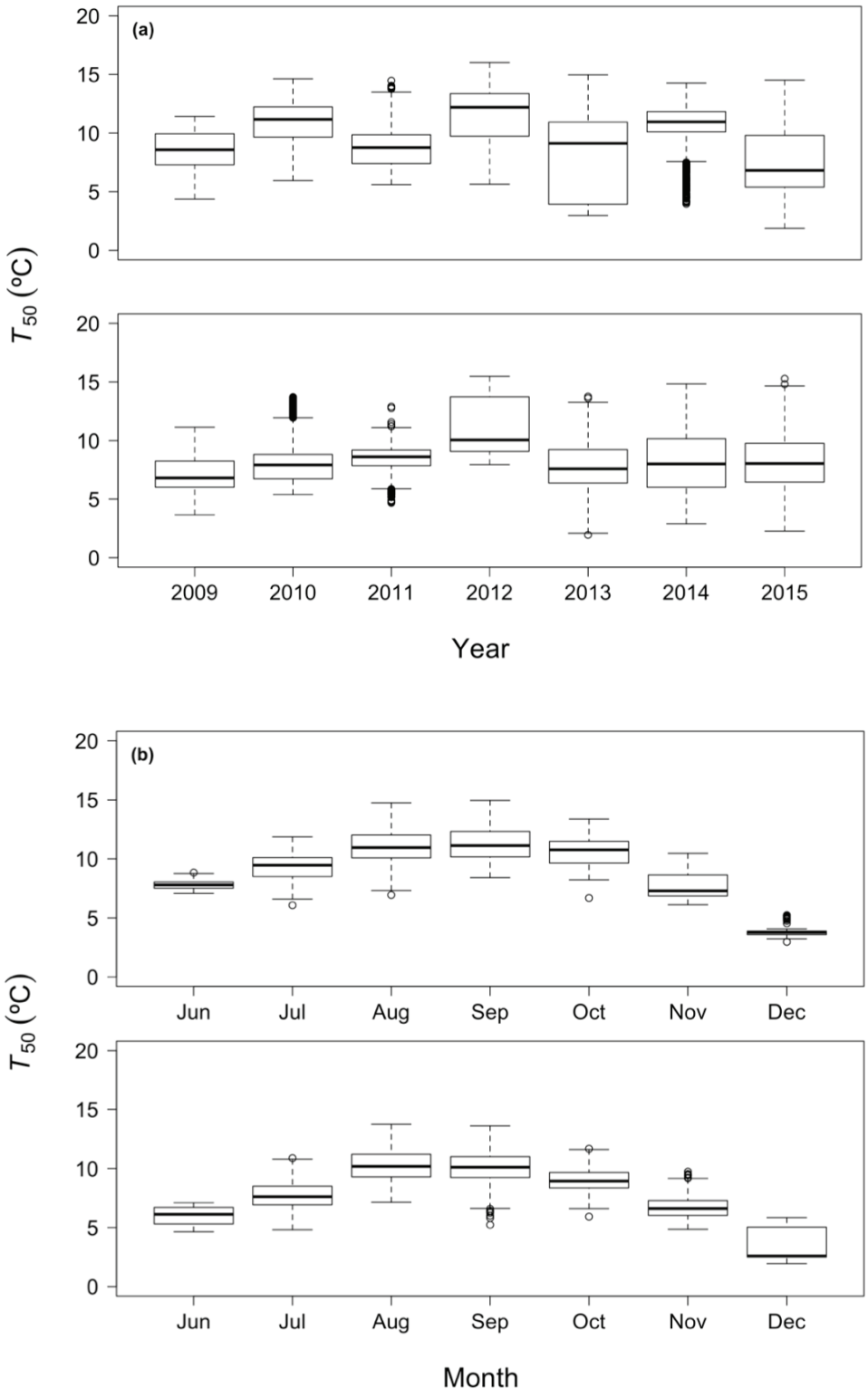

Figure 3.10 (a) Inter-annual and (b) monthly variation in upper-water column temperature (T_{50}; ºC) measured by grey seals over Middle Bank (top) and Canso Bank (bottom); monthly data were collected in 2013 (n = 12).

3.4 DISCUSSION

Monitoring of meso-and fine-scale oceanographic conditions is needed to better understand species' responses to environmental variability. Grey seals fitted with electronic bio-loggers can provide high resolution oceanographic information across the SS and into the GSL with a total of 595,866 profiles and sampling coverage of 72.90% of the LME (Fig. 3.2). These data serve to complement the suite of oceanographic data currently collected on the SS (Grist et al. 2011; Nordstrom et al. 2013b; Roquet et al. 2014; Johnson et al. 2018) and could be useful in the verification of circulation models for this continental shelf ecosystem (Roquet et al. 2013). The concentration of grey seal sampling over Middle Bank and Canso Bank (Fig. 3.5) permits consistent monitoring of these, and other, ecologically important areas over time (King et al. 2016).

While some studies using pinnipeds as autonomous samplers of *LA* and chl-*a* have used the euphotic zone depth (e.g., Jaud et al. 2012), the use of the MLD (e.g., O'Toole et al. 2014) is particularly important in the context of the SS. The waters of the SS originate from two sources: the fresher, cooler outflow of the GLS and more saline, warmer waters stemming from the slope (Smith & Schwing 1991; Loder et al. 1997; Loder et al. 1998, Han et al. 1999; Hannah et al. 2001). Water originating from the GSL flows westward over the ESS and becomes trapped along the coast to form the Nova Scotia Current (NSC) (Han et al. 1999; Sheng 2001; Ohashi and Sheng 2013; Dever et al. 2016; see Figure 1 in Hebert et al. 2018). Incoming water from beyond the shelf slope remains near-bottom due to density gradients and flows northward within deeper basins (Loder et al. 1997; Han et al. 1999; Panteleev et al. 2004). This results in a two-layer system in winter where the cooler, fresher waters of the GLS overlay the warmer, more

saline slope waters. In summer, heating of the upper fresher layer forms a three-layer system with a warmer, fresher layer, a cold intermediate layer, and a warmer, more saline bottom layer (Smith & Schwing 1991; Loder et al. 1997, Han et al. 1999; Hannah et al. 2001; Ohashi and Sheng 2013). As a result, stratification over the SS is driven by salinity and temperature gradients (Li et al. 2015; Hebert et al. 2018). The MLD in this system exceeds the euphotic zone depth at all times of the year (Ross et al. 2017). The optical conditions where the bio-optical model was formed are expected to be most representative of those of the NSC, and ultimately waters originating from the GSL (Shan and Sheng 2012; Dever et al. 2016). As most grey seal locations occurred over the ESS, the use of a bio-optical algorithm developed for waters stemming from the GSL is supported.

Oceanographic conditions and trends observed in this dataset were consistent with previous research and support the incorporation of these data into future assessments. Although some SST values were more variable, observations fell within the expected range (Ohashi et al. 2009; Galbraith and Larouche 2013). Estimates of MLD and the resulting selection of 50 m were consistent with previous observations across the SS (Craig et al. 2015; Dever et al. 2016; Hebert et al. 2018). Seasonal variability in upper layer stratification as well as the spring phytoplankton bloom are known to occur above this depth (Li et al. 2015; Johnson et al. 2018). Temporal trends in MLD were revealed, deepening in winter as the warm upper layer cools and becomes uniform with the cold intermediate layer (Galbraith and Larouche 2013). Observed upper-water column temperatures were also consistent with expected trends, cooling progressively throughout the year (Galbraith et al. 2012). These data were able to capture anomalous warming

events previously detected by other methods of oceanographic sampling, particularly the largest in 2012 (Fig. 3.8; Dever et al. 2016; Brickman et al. 2018). Chl-*a* estimates were normal for this subregion, particularly given the time of year that sampling occurred (Platt et al. 2008; Fuentes-Yaco et al. 2015).

3.4.1 Ocean Circulation Models

Although the instrumentation of grey seals provides a marked increase in the data available for this region at fine spatio-temporal scales, it is limited by the distribution of grey seals across the SS. However, these data can serve as a valuable resource for monitoring ecosystem-wide environmental change by providing verification of oceanographic conditions for three-dimensional ocean circulation models (Khan et al. 2013; Li et al. 2015; Richaud et al. 2016). Monitoring the persistence of large climatic regimes (i.e., North Atlantic Oscillation and Atlantic Multidecadal Oscillation) is increasingly important, as they often result in widespread environmental changes within this ecosystem (Petrie 2007; Loder et al. 2013). Another important example is the warming events that occurred in 2012, 2014, and 2015 resulting from anomalous eddies across the continental shelf. Circulation models were used to investigate these events and highlighted the limitation of space-time coverage for the region (Brickman et al. 2018). In regions where other oceanographic data are not readily available (e.g., Southern Ocean), large datasets collected by instrumented pinnipeds have been the primary source of oceanographic data and utilised to improve circulation models (Roquet et al. 2013; Fedak 2013; Roquet et al. 2014).

3.4.2 Monitoring Meso-Scale Environmental Change

The patchy distribution of habitat (i.e., temperature, salinity, depth) and resources results in an equally patchy distribution of fish species, both within the water column and across the SS (Horsman and Shackell 2009; Ricard and Shackell 2013). Understanding the preferred conditions for species inhabiting this area is of great interest in light of climate change, as many oceanographic conditions (e.g. timing and depth of stratification, water temperatures, etc.) have undergone changes and are expected to continue to do so (Khan et al. 2013; Loder et al. 2013; Ricard and Shackell 2013; Shackell et al. 2014; Stortini et al. 2015). In order to persist, species are forced to either adapt or shift their distributions (Perry and Smith 1994; Brennan et al. 2016). In an adjacent region of the Northwest Atlantic continental shelf, commercial fish species have mostly retained their preferred temperature ranges, and instead modified their distributions in response to changing water temperatures (Nye et al. 2009; Nye et al. 2010). The responses of species to changing environmental conditions is complicated by anthropogenic pressures (i.e., fisheries; Zwanenburg 2000) and resulting changes in trophic dynamics (e.g., natural mortality; Frank et al. 2005). The challenges in mitigating these issues are highlighted by the collapse of groundfish populations on the ESS, which has resulted in dramatic ecosystem restructuring and shown little evidence for recovery, despite severe reductions in fishing pressures (Bundy and Fanning 2005; Frank et al. 2005; Shackell et al. 2010; Frank et al. 2011). Whether changes in the distributions and abundances of species are due to a gradually changing environment, anomalous climatic events, or trophic interactions is of significant interest ecologically and economically, but often remains to be seen (Sinclair et al. 2015). Oceanographic data collected by

instrumented grey seals provides a mechanism for routine sampling below the surface at fine spatio-temporal scales which can be used together with data collected on present and shifting species distributions.

3.4.3 Monitoring High-Use Areas

The distribution of grey seals occurs predominantly over the ESS and lower GSL (Fig. 3.2). Unlike many other pinniped species that travel long distances to foraging patches (e.g., Hindell et al. 1991; Burton and Koch 1999; Le Boeuf et al. 2000), grey seals are confined to the continental shelf within a relatively small area (between 125 and 300 km offshore). This allows for persistent sampling of high-use areas; Middle Bank and Canso Bank are biologically-productive areas that are also heavily used by grey seals. The ecologically valuable features of both Middle Bank and Canso Bank have previously been summarised (see Tables 23 and 25 in King et al. 2016). In short, Middle Bank is an important area for adult Atlantic cod (*Gadus morhua*) and spawning and nursery habitat, has high larval and small fish richness, contains an abundance of several demersal fish species with possibly spawning and nursery habitat, and is historically an area of high fish biomass and high primary productivity (King et al. 2016). Canso Bank together with Canso Basin have high larval and small fish species richness, as well as adult fish species richness and evenness, and persistent high chl-*a* (King et al. 2016). They are also important habitats for sand lance (*Ammodytes dubius*), a major prey species of grey seals (Beck et al. 2007) and American plaice (*Hippoglossoides platessoides*), which is currently listed as Threatened by COSEWIC (King et al. 2016). Research in this region has included Canso Basin due to high larval and adult fish and invertebrate diversity (King et al. 2016). The importance of oceanographic data collected by

instrumented grey seals is two-fold: first, they provide an opportunity for nearly continuous monitoring of biologically productive regions of the SS and second, these areas receive disproportionate use by one of the most abundant, large marine predators in this ecosystem. Despite their relatively close proximity (Fig. 3.5), even small differences in the timing, magnitude, and variability of change in oceanographic conditions are evident using animal-borne data (Fig. 3.10). These data are particularly useful for monitoring temporal changes in oceanographic properties among areas at fine spatial scales, such as cooling of the upper mixed layer (Fig. 3.10b).

CHAPTER 4: OCEANOGRAPHIC CONDITIONS PREDICT AT-SEA BEHAVIOURAL STATES IN A SIZE-DIMORPHIC MARINE PREDATOR: THE GREY SEAL (*HALICHOERUS GRYPUS*)

4.1 INTRODUCTION

Physical and biological oceanographic features of continental shelf ecosystems are dynamic over a range of spatio-temporal scales (Simpson and Sharples 2012). This results in some areas having disproportionately high levels of primary productivity (Sathyendranath et al. 1995; Antoine et al. 1996; Muller-Karger et al. 2005) that support assemblages of species at higher trophic levels (Richardson et al. 2000; Platt et al. 2003; Stevick et al. 2008; Benoit-Bird et al. 2013; Davoren et al. 2013). In addition to the availability of resources, the distributions of fish species are also constrained by a suite of preferred environmental conditions (e.g., temperature, depth, salinity), which in temperate ecosystems may change in time (Scott 1982; Ricard and Shackell 2013; Brennan et al. 2016). The heterogeneous nature of oceanographic conditions results in a three-dimensionally patchy distribution of prey species available to upper-trophic level predators (Cox et al. 2018).

Foraging animals should make search decisions (Sims et al. 2018) to maximize fitness with respect to their immediate energetic costs and the risk of predation (MacArthur and Pianca 1966; Charnov 1976; Orians and Pearson 1979; Abrams 1991; Heithaus and Frid 2003). Bio-physical features may influence the availability of prey within a habitat landscape and thus foraging decisions of predators. Within prey patches, foraging success should be improved as less energy will be expended searching for prey and the quantity that can be consumed may be higher (Gende et al. 2006; Boyd et al. 2016). This patchiness can persist throughout the food web, exerting bottom-up control

on local species abundances, and result in multi-trophic level hotspots (Springer et al. 1984; Sydeman et al. 2006; Benoit-Bird et al. 2013; Cox et al. 2018).

Oceanographic conditions and features have been linked to the movements and foraging patterns in diverse marine taxa (Cox et al. 2018), including sea turtles (Dodge et al. 2014), large bony fishes (Thys et al. 2015), elasmobranchs (Miller et al. 2015), seabirds (Holm and Burger 2002; Yen et al. 2004), cetaceans (Bailey and Thompson 2010), and pinnipeds (Guinet et al. 2001; Dragon et al. 2010; O'Toole et al. 2015). To date, many of these studies have used oceanographic data derived from remote sensing (Johnston et al. 2005; Bailey et al. 2012) and/or a previous knowledge of persistent, predictable meso-scale (10s – 100s km) bio-physical features (i.e., topography, fronts, or current systems) to make inferences (Field et al. 2001; Baylis et al. 2008; Breed et al. 2009; Scales et al. 2014; Cotté et al. 2015). To infer foraging patterns, broad associations with these features (Campagna et al. 2006) or diving behaviour (Field et al. 2001; Kuhn 2011; Blanchet et al. 2015) have often been used; yet how these relate to foraging behaviours at finer scales remains unclear (Robinson et al. 2010; Dragon et al. 2012; Carter et al. 2016). An alternative approach is to directly relate oceanographic conditions to inferred behavioural states using either prey encounter events (Guinet et al. 2014; Vacquié-Garcia et al. 2015) or state-space models (Bestley et al. 2013; O'Toole et al. 2015; Jonsen et al. 2018). For central place foragers (e.g., some seabirds and pinnipeds) whose time at sea should reflect foraging decisions, associations with bio-physical features may be more obvious. While these methods have proven useful for pelagic species, which dive during foraging but otherwise remain near-surface and whose foraging behaviours are driven by surface conditions (Guinet et al. 2001; Ream et al.

2005; Nordstrom et al. 2013a; Sterling et al. 2014), they are less useful for species that forage near the ocean floor. Obtaining sub-surface oceanographic data that are concurrent with animal movements and relevant to the resolution at which decisions are made is challenging, as these data are often broad-scale or patchy and may contain spatio-temporal bias (Ream et al. 2005; Scales et al. 2017). The use of marine species as autonomous samplers has become increasingly prevalent as a means of collecting oceanographic data in ecosystems where sampling is limited (Boehlert et al. 2001; Nordstrom et al. 2013b; Roquet et al. 2014; Nakanowatari et al. 2017). These data can be used together with movement characteristics to improve our understanding of how oceanographic conditions influence how animals make decisions in time (Biuw et al. 2007; Jaud et al. 2012).

The ability to infer at-sea behaviour, typically reported as "transiting" or "foraging", defined as interpatch movements and area-restricted search (ARS), respectively, promotes a better understanding of the internal and external drivers of movement patterns (Barraquand and Benhamou 2008; Breed et al. 2009). While animals may have some prior spatial memory of where relevant bio-physical features exist, our understanding of this is somewhat limited (Fagan et al. 2013; Carroll et al. 2018). The suite of environmental conditions encountered by individuals while searching for and consuming prey may be used as cues which may ultimately drive foraging decisions. This is especially valuable in regions where bio-physical features are highly dynamic or exist at finer scales, such that apparent foraging locations may not always be easily discernable from inter-patch movements (Carroll et al. 2017).

The grey seal is a relatively large-bodied phocid species inhabiting continental shelves on both sides of the North Atlantic Ocean. The western North Atlantic population is large and increasing in size (Bowen et al. 2003; Hammill et al. 2017a). Sable Island is the largest breeding colony of grey seals in the world (Bowen et al. 2007). Seals from this colony forage throughout the Scotian Shelf (SS) ecosystem (Stobo et al. 1990; Breed et al. 2006; Breed et al. 2009). Although movement patterns of this population have been studied extensively, those studies have primarily focused on the internal drivers of foraging behaviours, such as sex differences and seasonal influences (Beck et al. 2003a; Beck et al. 2003b; Austin et al. 2004; Austin et al. 2006; Breed et al. 2006). Research has shown that prey patches are not randomly distributed across their environment (Austin et al. 2004). As a result, grey seals tend to exhibit foraging trips with clear outbound, foraging, and inbound segments (Breed et al. 2009), although evidence suggests some level of opportunistic feeding along these trips (Austin et al. 2006). To date, the only oceanographic feature that has been considered concurrently with foraging behaviours has been bathymetry, whereby grey seals preferentially forage over shallow banks (Breed et al. 2009). While the bio-physical processes that surround these features may change (e.g., circulation, temperature, etc.), the presence of topographical features are permanent in both space and time. By contrast, exothermic prey species on the Scotian Shelf have been classified as either depth-keepers or temperature-keepers (Perry and Smith 1994) and have shown seasonal variations in spatial distributions (e.g., Sinclair and Iles 1985; Mahon and Smith 1989; Swain et al. 1998). Despite the permanence and importance of topographical features to the foraging distributions of grey seals, this population has shown marked differences in distributions with respect to sex and season, suggesting

some other or combination of drivers influencing these patterns (Breed et al. 2006; Breed et al. 2009).

The SS is topographically complex with a series of banks and basins largely concentrated over the eastern Scotian Shelf (ESS). These features influence the hydrodynamic properties of the region, as cooler, fresher water from the Gulf of St. Lawrence (GSL) becomes coastally-trapped as the Nova Scotia Current (NSC) and permeates across the ESS to form the top layer of this stratified shelf sea (Han et al. 1999; Ohashi and Sheng 2013; Dever et al. 2016). Inflow of warmer, more saline waters from the slope occurs through deeper channels such as the Gully, but due to density gradients are largely unable to flow above the shallow banks (Loder et al. 1997; Han et al. 1999; Panteleev et al. 2004). This results in distinct bottom climatologies that have been used to differentiate from the central Scotian Shelf (CSS) and western Scotian Shelf (WSS) subregions (Fuentes-Yaco et al. 2015). Together, these result in fine-scale circulation patterns that vary three-dimensionally across the continental shelf (Petrie et al. 1996; Hannah et al. 2001; Han and Loder 2003; Hebert et al. 2018).

In this study, I examined the influence of oceanographic drivers on foraging patterns using *in situ* environmental data collected by grey seals. As noted above, previous studies have shown strong sex-specific and seasonal differences in ranging, foraging behaviour, and diet of grey seals in the study population. Therefore, I also tested the hypothesis that the influence of oceanographic drivers on behaviours may differ between females and males and by season.

4.2 METHODS

4.2.1 Tag Deployment and Dive Data Processing

The study was conducted on Sable Island (43º55'N, 60º00'W), a crescent-shaped sandbar located on the ESS approximately 300 km east of Halifax, Nova Scotia, Canada. Sable Island supports a large breeding colony of grey seals (Bowen et al. 2007; Hammill et al. 2017a) that has been the subject of long-term studies of foraging ecology and demography (e.g., Breed et al. 2006; Lidgard et al. 2012).

Between October 2009 and January 2016, 117 grey seals were live-captured onshore in summer following the spring moult (June) or in fall (late September or early October) (Table 4.1). Seals were weighed using a 300 kg (±1 kg) Salter spring balance and then immobilised using the chemical anaesthetic Telazol (males 0.45 mg kg^{-1}; females 0.90 mg kg^{-1}; Bowen et al. 1999) to equip each seal with telemetry and data-logging devices. Seals were equipped with a VHF transmitter (164 to 165 MHz, astrack.com) to allow us to locate the animal upon its return to the breeding colony and a Mk10-AF Fastloc™ GPS data-logger (referred to as a time-depth-light recorder or TDLR, www.wildlifecomputers.com). Tags recorded temperature (ºC), depth (m), light level, and condition (wet/dry) every 10 sec during dives and Fastloc GPS locations were taken after every 15 min when the animal surfaced; in 2009 locations were taken after 5 min. GPS locations were suspended during haul out periods once a location was taken and the tag recorded dry conditions for 45 s out of every 1 min for 20 min. Location attempts resumed when the seal returned to sea and the tag recorded wet conditions for 45 s out of 1 min.

Table 4.1 Deployment and recovery record of Mk10-AF Fastloc^{TM} GPS time-depth-light recorders on grey seals during the study period.

Year	Deployment Month	Instruments Deployed	Instruments Recovered	Data Recovered		
				Total	Males	Females
2009	October	15	13	13	5	8
2010	September	20	20	20	6	14
2011	June	20	16	13	0	13
2012	June	17	16	15	5	10
2013	June	15	12	12	4	8
2014	June	15	12	12	5	7
2015	June	15	11	9	0	9
Total		117	100	94	25	69

Data stored onboard tags were downloaded after tags had been recovered from re-captured seals on Sable Island during the following breeding season. Data were successfully recovered from 94 individuals (69 females and 25 males). 17 seals failed to return to Sable Island to breed and the tags on 6 seals had too many erroneous readings (i.e., GPS location, temperature, depth) to properly reconstruct movements or oceanographic datasets. In 2012, wet/dry sensors of tags intermittently malfunctioned on all tags, resulting in a reduced number of GPS locations for this year. For this reason (further explained in section 4.2.2) data collected in this year were omitted from behavioural state analyses, leaving 79 individuals (59 females and 20 males). GPS locations with <5 satellites and/or residual error values >30 (Dujon et al. 2014; Lidgard et al. 2014) were removed from the data; a speed filter of 10 m s^{-1} was also applied. The remaining locations were considered to have negligible error and accuracies of 10s of meters (Bryant 2007).

Dive data were analysed using WC-DAP, freely available software provided by the tag manufacturer. Dives < 5 m and > 30 min were removed from the dataset to avoid the influence of surface noise and misidentification of single dives. Data were automatically zero-offset corrected to account for pressure transducer shift onboard tags. Summary statistics calculated for each dive including the timing and duration of dives and dive phases, maximum depth, and average ascent and descent rates. Dives were separated into three phases (i.e., descent, bottom, ascent); the bottom phase was defined as any depth made at or below 80% of the maximum depth for each dive. Additional dive data analyses were performed using R statistical software (R Core Team 2018).

Environmental data were assigned to a dive using a purpose-built algorithm. Between the hours of 10:00 and 14:00 (AST), the ascent phase of dives was used to calculate the mixed layer depth (MLD; m), mean upper-water column temperature (T_{50}; ºC), light attenuation (LA; m^{-1}), and estimated chlorophyll-*a* concentration (chl-*a*; mg m^{-3}) within the upper-water column (50 m) (see Chapter 3 for details). Mean depth (m) and temperature (ºC) were calculated for the bottom phase of each dive to gain information on the environmental conditions under which grey seals are likely to be foraging (Thompson et al. 1991; Beck et al. 2003b; Breed et al. 2009). Dive data were then filtered to remove erroneous observations based on the ranges of values possible for tags. Season was included as a categorial variable and assigned as summer (June-August) and fall (September-December) (Breed et al. 2006; Beck et al. 2007; Breed et al. 2009).

4.2.2 Hidden Markov Movement Model (HMMM)

To model the behavioural states along individual grey seal tracks, the hidden Markov movement model (HMMM) in the R package *swim* was used (Whoriskey 2017;

Whoriskey et al. 2017). The model provides a relatively new, frequentist approach for identifying behavioural states using a widely-implemented first-difference correlated random walk switching (DCRWS) model process equation (Jonsen et al. 2005) with maximum likelihood estimation to decrease computation time. Parameters estimated by this model operationally define two behavioural states: directed movement ($\theta \approx 0$ and $\gamma > 0.5$) or tortuous movement ($\theta \approx \pi$ and $\gamma < 0.5$), which his often inferred as "transiting" and "foraging" (i.e., ARS), respectively. As the HMMM is a discrete model, the time step to be used must be established *a priori*. The discretization of time is not unique to this model (e.g., Morales et al. 2004; McClintock et al. 2014), however, the selection of an appropriate time step is discretionary and little advice is available for those employing these methods. In choosing a suitable time step, I took into consideration previous knowledge of grey seal foraging patterns, the scale at which inferences would be biologically meaningful, and temporal resolution of observations. I determined the most suitable time step for these tracks was three hours. Given foraging patch sizes and residence times, swim speeds when foraging, and distances to foraging patches (Breed et al. 2009), this coarser resolution was required to reliably estimate parameters and resolve behavioural states. As a result of discretization of time steps, locations were linearly interpolated along grey seal tracks. This posed a substantial issue for deployments in 2012, where there were numerous gaps where no locations were recorded. As a result, the 2012 data could not be reliably fit to the HMMM.

4.2.3 Statistical Analysis

To examine the influence of environmental conditions encountered during foraging trips on behavioural states exhibited by grey seals, I fit generalized linear mixed-

effects models (GLMMs) to account for the serial correlation of measurements within individual tracks. Using point biserial correlation tests, individual body length (cm) (r_{pb} = 0.80, p-value < 0.001, n = 79) and recovery mass (kg) (r_{pb} = 0.78, p-value < 0.001, n = 51) were highly correlated with sex and were not considered as predictors in these models. As estimated chl-*a* concentrations were restricted by both time of day (i.e., 10:00 to 14:00 AST) and dive depth (i.e., 50 m), I formulated two models: the first representing conditions of the water column likely to influence productivity and potentially pelagic prey species, and the second including environmental conditions encountered by grey seals when searching for demersal prey. Models were fit using penalized quasilikelihood (PQL) estimation with the function *glmmPQL* in the R package *MASS* (Breslow and Clayton 1993; Venables and Ripley 2002; Bolker et al. 2009). This software allows for a binomial response to accommodate behavioural states 0 (transiting) and 1 (ARS), inclusion of random effects, and specification of an appropriate autocorrelation structure. The full models, including main effects and two-way interaction terms were:

Water Column Model (Model 1):

$$b_t = \beta_0 + \beta_1 chl_t + \beta_2 T_{50,t} + \beta_3 sex + \beta_4 season_t + \beta_5 chl_t * sex + \beta_6 chl_t * season_t + \beta_7 T_{50,t} * sex + \beta_8 T_{50,t} * season_t + \beta_9 sex * season_t + \nu_{seal} + \epsilon_t \,, \quad \text{(Equation 13)}$$

Bottom Conditions Model (Model 2):

$$b_t = \beta_0 + \beta_1 dur_t + \beta_2 T_t + \beta_3 depth_t + \beta_4 sex + \beta_5 season_t + \beta_6 dur_t * sex + \beta_7 dur_t * season_t + \beta_8 T_t * sex + \beta_9 T_t * season_t + \beta_{10} depth_t * sex + \beta_{11} depth_t * season_t + \beta_{12} sex * season_t + \nu_{seal} + \epsilon_t \,, \quad \text{(Equation 14)}$$

where b_t corresponds to behavioural state at time t, chl_t to chl-*a* concentration, $T_{50,t}$ the mean temperature of the upper-water column, ν_{seal} the random effect of individual seals with autocorrelated structure in the covariance matrix, ϵ_t the random deviation in the

model independent of v_{seal}, dur_t the bottom duration, T_t the mean bottom temperature, and $depth_t$ the mean dive depth. A continuous first-order autoregressive structure or "CAR(1)" was used as gaps in the data were present when dive data were not available (e.g., animals were hauled out). Depth was log-transformed to meet the assumptions of the GLMM. To assess whether individual predictors affected the behavioural states of individuals, a single set of hypotheses were tested for the full models using the *t*-values and resulting *p*-values of individual parameters to avoid bias in parameter estimation (Whittingham et al. 2006).

4.3 RESULTS

A total of 1,668,086 dives and 569,349 locations were recorded from 79 individuals over the study period (Table 4.2). The combined-sex spatial distribution of at-sea locations is illustrated in Figure 4.1. Data collected in January were sparse, as animals had either already returned to the breeding colony or did so partway through the month, and as in previous studies, were not included in these analyses (Breed et al. 2006; Breed et al. 2009). The spatial distributions of males and females differed by season and by sex (Fig. 4.2). Fine-scale location data collected by grey seals revealed precise habitat use common among individuals (Fig. 4.3). Average number of days that individuals were tracked was about 180 days, excepting the fall deployments in 2009 and 2010 (Table 4.2). As expected, the adult males sampled were both heavier ($t_{(21.94)} = 8.44$, $p < 0.001$) and longer ($t_{(27.20)} = 10.34$, $p < 0.001$) than females (Table 4.2). The males sampled were on average, younger than females ($t_{(17.65)} = -4.65$, $p < 0.001$).

4.3.1 HMMM Fitting

Oceanographic data were assigned to 73,144 interpolated locations with corresponding behavioural state estimates produced by HMMMs (Table 4.2); the Water Column Model included 13,129 observations, while the Bottom Conditions Model included 73,036. Although grey seal movements were concentrated over the ESS and lower GSL (Fig. 4.1), foraging ranges and behavioural patterns were variable among individuals, as illustrated in Figure 4.4. HMMMs fit the data well (Fig. 4.5). Estimates of theta for the transiting behavioural state were closely centered around zero, corresponding well with persistent directional movements to foraging patches, evident in mapped behavioural states (Fig. 4.4). Theta estimates for the inferred foraging behavioural state were transformed to center around zero for interpretation, as many of the output estimates were near multiples of π (i.e., a complete circle). Aside from a single outlier, gamma estimates were divergent at the expected 0.5, indicative of distinct similar, faster movements and then dissimilar, slower movements. Estimates of gamma for transiting were very high, nearing one; those corresponding to the area-restricted search behaviour were low, but showed higher variability, which may be owed to differences in foraging behaviour among individuals.

4.3.2 Effects of Covariates on Behaviour

Oceanographic conditions encountered by grey seals significantly influenced behavioural states and, as might be expected, varied along the course of individual tracks (Fig. 4.6).

4.3.2.1 Water Column Model (Model 1)

Season had no effect on the odds of foraging and there was no evidence for a sex-specific interaction; however, data used in this model were only collected at mid-day (Table 4.3). Females were almost 310% more likely than males to be foraging at any given time. While upper-water column temperature had no effect on foraging for males, for every increase in 1.0 ºC, females were 6.6% more likely to be transiting. There were no seasonal effects of upper-water column temperature on the chances of performing area-restricted search. For every increase in chl-*a* by 1.0 mg m^{-3}, the chances of foraging increased by almost 100%. The variation in chl-*a* was relatively low (Table A.2), such that increases in odds for encountered concentrations would be less dramatic. The effect of chl-*a* on conditioning foraging was significantly reduced by about 70% in summer months. The effect of estimated chl-*a* concentration on foraging behaviour did not differ by sex.

Table 4.2 Sample means and standard deviations of the age (years), mass (kg), length (cm), duration of deployment (days), number of dives, duration of time spent diving (days), proportion of time spent diving, number of locations, number of hidden Markov movement model (HMMM) locations, and proportion of HMMM locations spent foraging (n = 79).

	2009		**2010**		**2011**	**2013**		**2014**		**2015**
	M	**F**	**M**	**F**	**F**	**M**	**F**	**M**	**F**	**F**
Age	21.00	22.50	16.67	23.86	24.29		24.71	14.20	25.71	28.11
σ	5.61	1.60	8.12	1.41	1.70		5.22	1.48	4.92	1.69
Mass	258.10	176.63		170.00	208.67	282.25	193.36	292.00	199.03	215.44
σ	28.70	23.95		1.41	6.51	31.35	30.32	29.11	27.25	28.71
Length	214.40	188.50	208.00	186.36	184.85	211.00	188.75	206.20	181.29	186.78
σ	5.77	5.21	14.20	7.83	7.16	6.78	4.13	6.61	5.62	10.23
Duration	73.19	66.12	100.08	102.44	183.28	180.62	182.83	193.98	194.59	192.56
σ	1.05	3.96	7.83	6.21	20.99	6.75	6.00	6.98	7.80	7.50
Dives	11925.00	10909.63	13707.50	15900.64	24137.92	31052.25	25136.63	28972.40	27305.00	26804.22
σ	1206.85	1223.22	1212.17	2772.25	4314.94	5088.26	4756.96	3502.61	4468.37	3315.80
Dive Time	42.99	44.09	59.75	67.21	111.15	109.59	114.12	110.46	118.95	111.69
σ	4.62	4.18	3.56	6.44	16.40	7.02	8.53	8.72	8.83	12.66
Dive Proportion	0.59	0.67	0.60	0.66	0.61	0.61	0.62	0.57	0.61	0.58
σ	0.07	0.04	0.06	0.04	0.05	0.05	0.04	0.04	0.04	0.06

	2009		2010		2011	2013		2014		2015
	M	**F**	**M**	**F**	**F**	**M**	**F**	**M**	**F**	**M**
Locations	7681.60	4150.50	4776.67	5532.14	6528.92	8683.25	7954.63	10412.20	10503.57	9199.44
σ	3271.06	352.02	1583.48	1484.88	2622.60	3804.74	2086.70	1012.52	1178.81	981.29
HMMM Locations	494.20	462.75	641.50	684.14	1119.69	1199.25	1144.75	1197.20	1225.43	1163.22
σ	19.04	33.04	71.15	48.28	153.65	86.09	78.03	82.67	81.34	106.26
Foraging Proportion	0.47	0.58	0.60	0.77	0.74	0.49	0.72	0.72	0.83	0.78
σ	0.17	0.33	0.18	0.07	0.12	0.21	0.23	0.12	0.07	0.04

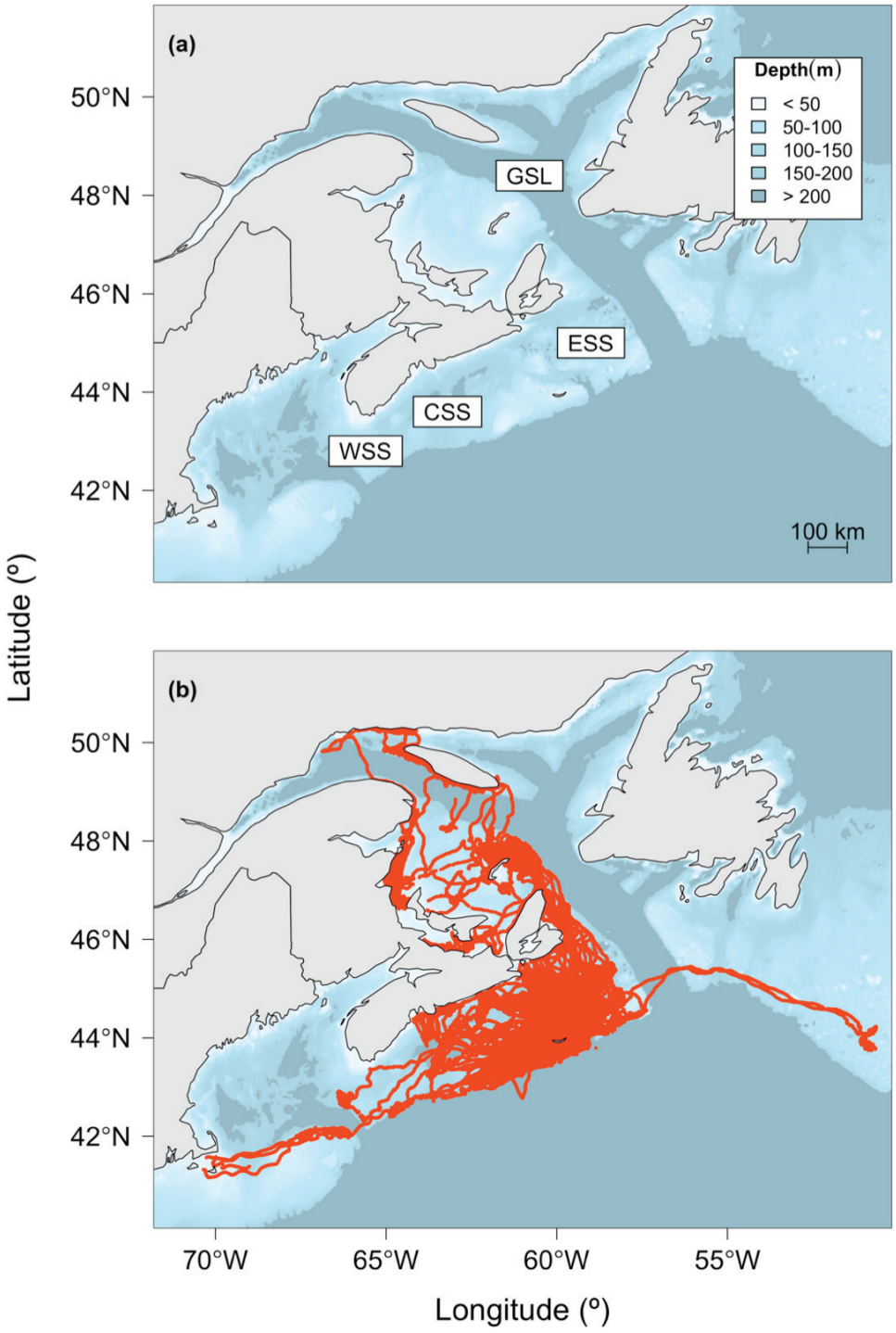

Figure 4.1 (a) Scotian Shelf ecosystem with the eastern Scotian Shelf (ESS), central Scotian Shelf (CSS), western Scotian Shelf (WSS), and Gulf of St. Lawrence (GSL) sub-regions identified and (b) distribution of grey seal (n = 79) locations obtained over the study period; data collected in January are not included in this figure.

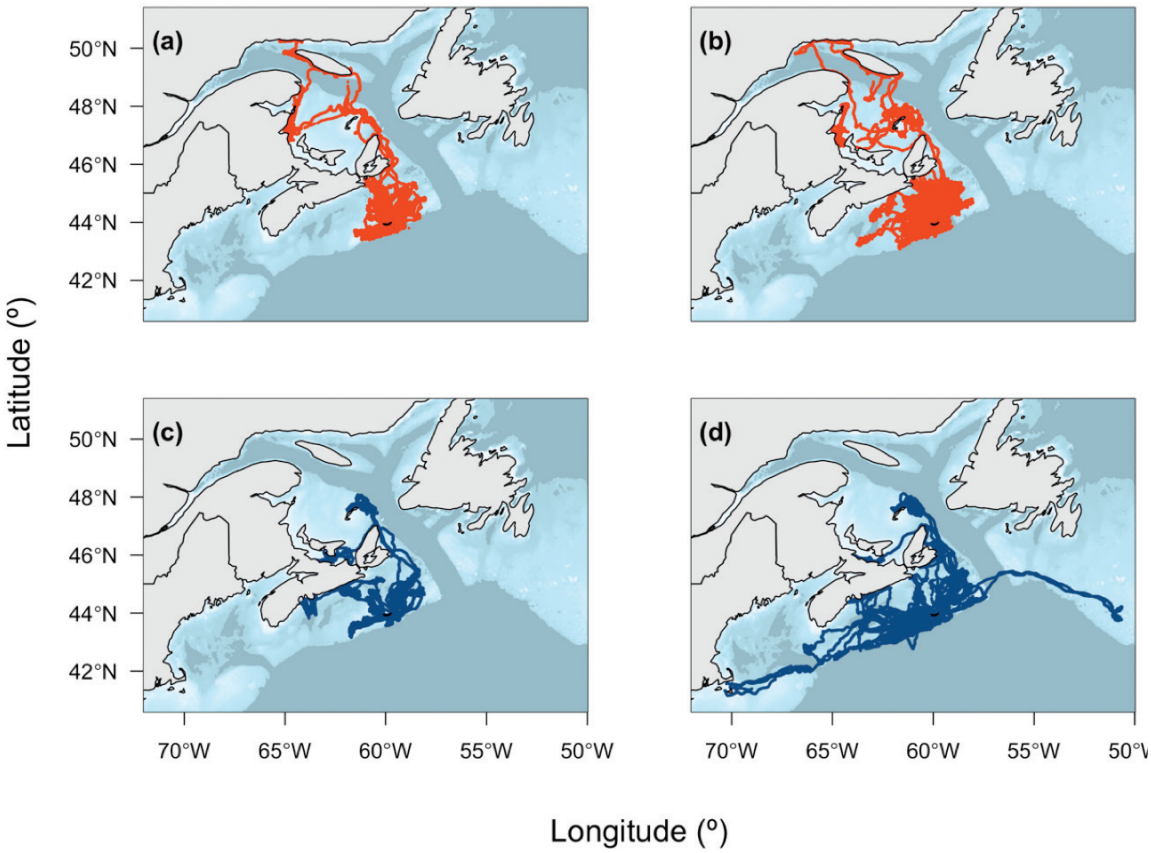

Figure 4.2 Locations of grey seals deployed between the years 2009 and 2015 (n = 79) separated by season and by sex: (a) females in summer (n = 37), (b) females in fall (n =59), (c) males in summer (n = 9), and (d) males in fall (n = 20); data collected in January are not included in these figures.

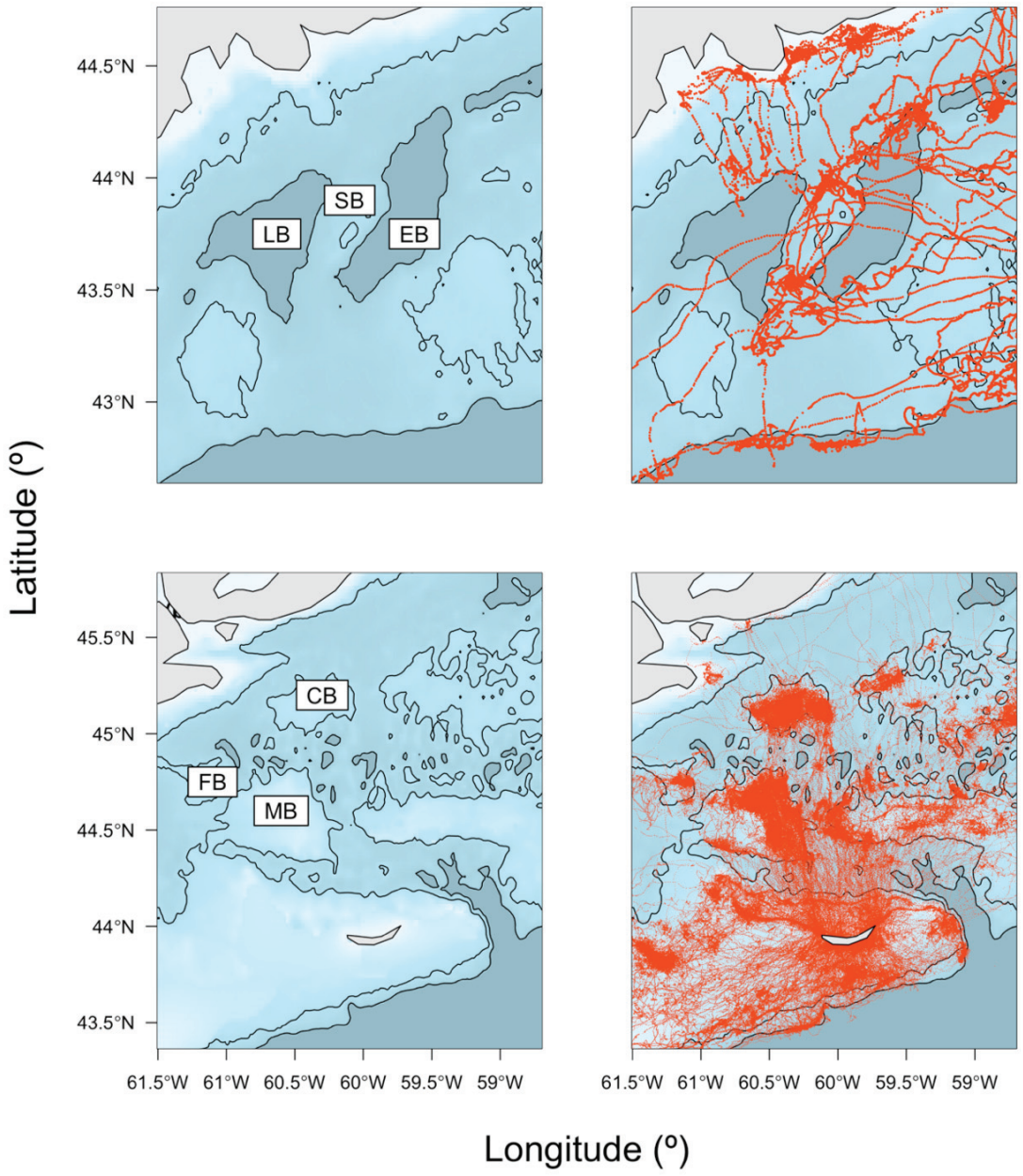

Figure 4.3 Locations of instrumented grey seals throughout the study period (n = 79) to highlight habitat selectivity over topographical features (a) LaHave Basin (LB), Sambro Bank (SB), and Emerald Basin (EB) and (b) Middle Bank (MB), Canso Bank (CB), and French Bank (FB); data collected in January are not included in these figures. Isobaths at 100 m and 200 m depths are included as black lines.

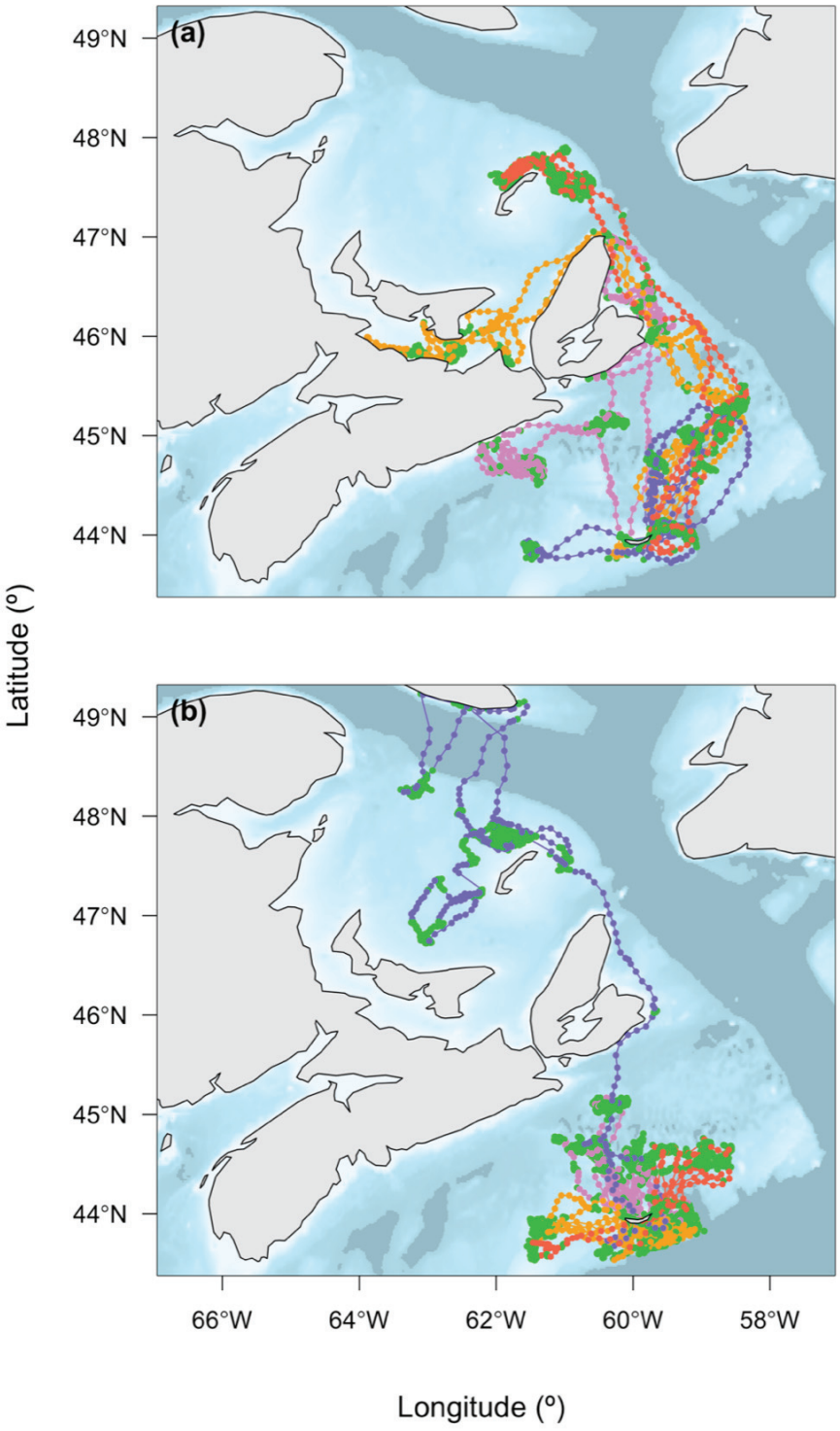

Figure 4.4 Interpolated locations and corresponding behavioural states (green = apparent foraging) estimated by the hidden Markov movement models for (a) four males and (b) four females selected from deployments between 2011 and 2015.

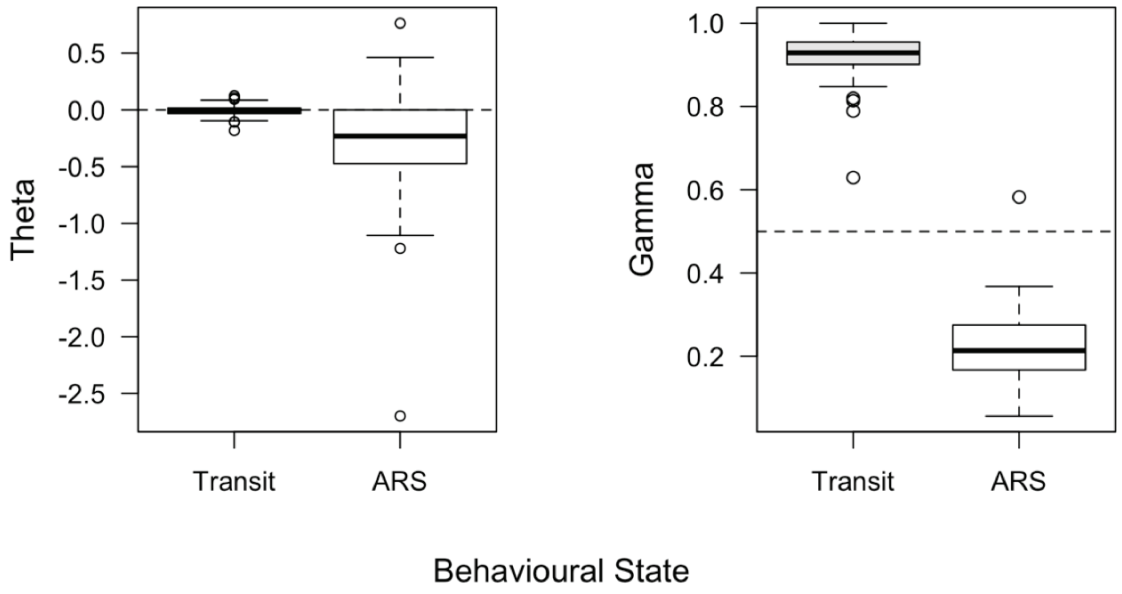

Figure 4.5 Parameter estimates of theta (i.e., turning angle) and gamma (i.e., autocorrelation in both direction and speed) for each behavioural state estimated using hidden Markov movement models fit with the R package *swim* (Whoriskey 2017).

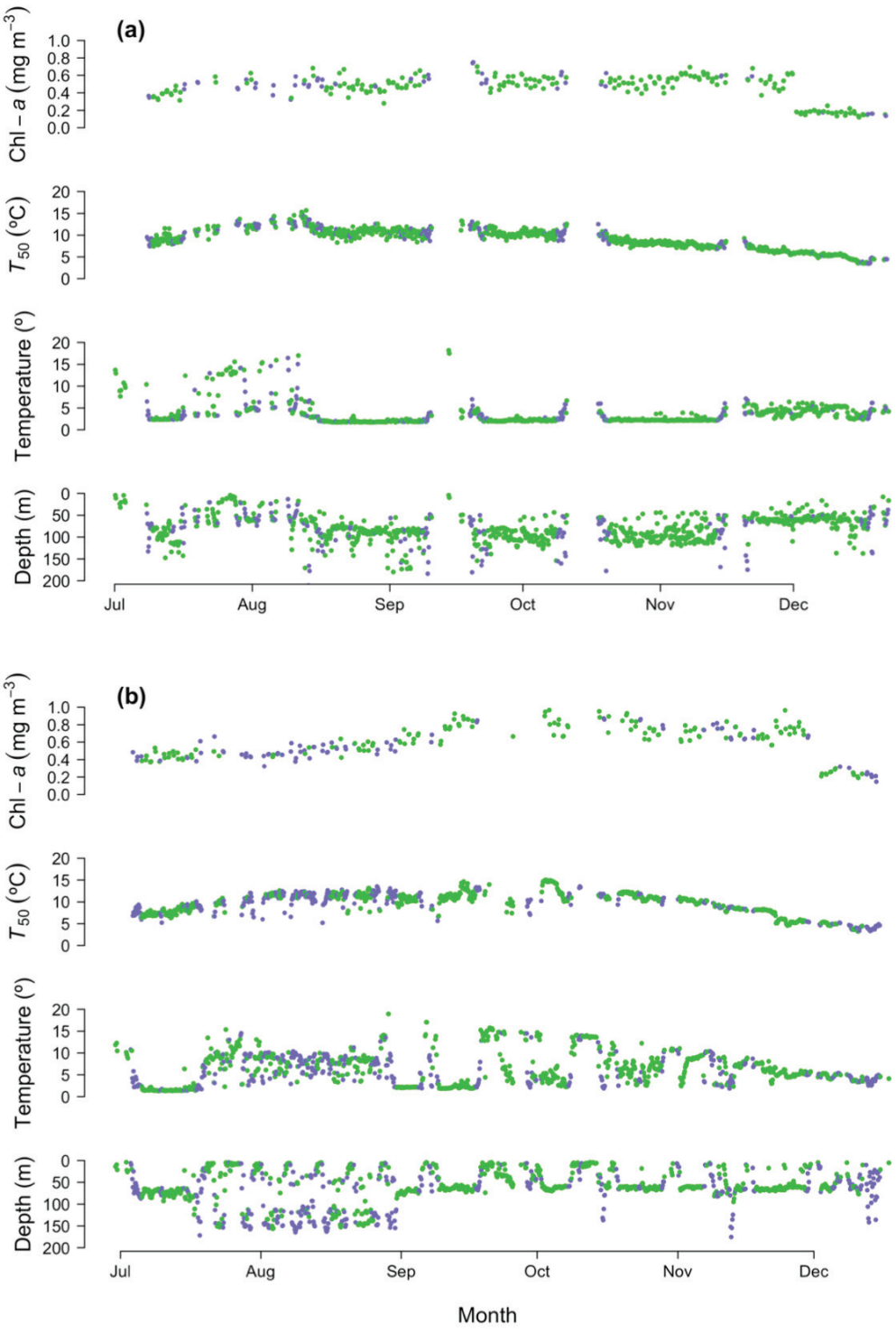

Figure 4.6 Behavioural states estimated using hidden Markov movement models for each location and corresponding measurements of chlorophyll-*a* concentration (chl-*a*; mg m^{-3}), upper-water column temperature (T_{50}; ºC), bottom temperature (ºC), and bottom depth (m) for an individual (a) female and (b) male deployed in 2013.

Table 4.3 Results of the Water Column Model (Model 1) predicting the probability of being in the foraging behavioural state with the intercept representing males in fall. Coefficients are exponentiated to odds ratios (odds and ratios of odds ratios) with upper and lower 95% confidence limits. Levels of significance are noted as *0.05, **0.01, and ***0.001.

	Coefficient (SE)	**Lower**	**Odds Ratio**	**Upper**	***p*-value**
Intercept	-0.088 (0.30)	0.50	0.916	1.66	0.77
Season (Summer)	0.323 (0.36)	0.68	1.382	2.79	0.37
Sex (Female)	1.403 (0.36)	2.02	4.066	8.17	< 0.001***
T_{50}	0.015 (0.03)	0.96	1.015	1.07	0.59
Chl-*a*	0.683 (0.29)	1.12	1.979	3.48	0.02*
Season (Summer): T_{50}	-0.010 (0.03)	0.93	0.990	1.05	0.75
Season (Summer): Chl-*a*	-1.075 (0.33)	0.18	0.341	0.66	< 0.01**
Sex (Female): T_{50}	-0.068 (0.03)	0.88	0.934	1.00	0.04*
Sex (Female): Chl-*a*	-0.298 (0.34)	0.38	0.742	1.44	0.38
Season (Summer): Sex (Female)	0.163 (0.20)	0.79	1.177	1.75	0.42

4.3.2.2 Bottom Conditions Model (Model 2)

Season was not a significant predictor of behavioural state and there were no significant seasonal relationships with any properties associated with the bottom of dives (Table 4.4). In agreement with the Water Column Model, there were sex-specific differences in the odds of foraging, where females were 230% more likely than males to be foraging at any given time. There were significant sex-by-season interactions, whereby females in summer had further increased odds of foraging by almost 50%. An increase in bottom duration by 1 s significantly reduced the chances of foraging by about 0.13% for males. For every 1 s increase in bottom duration, females were 0.05% less

likely than males to be transiting, exhibiting significantly smaller differences in bottom duration between behavioural states. An increase in bottom temperature by 1 ºC resulted in increased odds of foraging by about 2.1 %. There was no significant difference for the effect of bottom temperature among sexes. Dive depth did not significantly influence the behavioural states of males, however for females, every doubling of dive depth increased the chances of being in the transiting state by about 8.4%.

Table 4.4 Results of the Bottom Conditions Model (Model 2) predicting the probability of being in the foraging behavioural state with the intercept representing males in fall. Bottom depth was log-transformed prior to model fitting. Coefficients are exponentiated to odds ratios (odds and ratios of odds ratios) with upper and lower 95% confidence limits. Levels of significance are noted as *0.05, **0.01, and ***0.001.

	Coefficient (SE)	**Lower**	**Odds Ratio**	**Upper**	***p*-value**
Intercept	0.447 (0.24)	0.98	1.564	2.49	0.06
Season (Summer)	-0.097 (0.22)	0.59	0.908	1.39	0.65
Sex (Female)	1.205 (0.29)	1.90	3.335	5.86	< 0.001***
Bottom Duration	-0.001 (0.00)	1.00	0.999	1.00	< 0.001***
Bottom Temperature	0.021 (0.01)	1.01	1.021	1.04	< 0.01**
Bottom Depth	0.017 (0.02)	0.98	1.017	1.05	0.34
Season (Summer): Duration	0.000 (0.00)	1.00	1.000	1.00	0.76
Season (Summer): Temperature	-0.004 (0.01)	0.98	0.996	1.01	0.63
Season (Summer): Depth	-0.058 (0.03)	0.89	0.944	1.00	0.05
Sex (Female): Duration	0.001 (0.00)	1.00	1.001	1.00	< 0.01**
Sex (Female): Temperature	-0.005 (0.01)	0.98	0.995	1.01	0.59
Sex (Female): Depth	-0.087 (0.03)	0.87	0.916	0.96	< 0.001***
Season (Summer): Sex (Female)	0.380 (0.11)	1.18	1.463	1.82	< 0.001***

4.4 DISCUSSION

The results of this study highlight the value of *in situ* measurements of oceanographic properties that can be collected at high temporal resolution by animal-borne data loggers. These data provide insight into the conditions encountered which directly or indirectly influence behavioural decisions made by large marine predators, such as the grey seal. Sex-by-season interactions were present, and well-aligned with our current understanding of foraging effort in this population. Sex was significant in a number of properties in both oceanographic models. Among oceanographic properties, season was only significantly influential for chl-*a* concentration. Chl-*a* concentration was positively associated with ARS behaviours, particularly during fall, coincident with the phytoplankton bloom in the region. These findings are supported by those of other pinniped species, which have demonstrated that areas of increased chl-*a* may cause bottom-up forcing on the structuring of foraging patterns (Guinet et al. 2001; Dragon et al. 2010; O'Toole et al. 2015). In females, foraging preferentially occurred in areas with cooler upper-water column temperatures, which may be indicative of preferences for increased stratification. The importance of water mass properties and structuring relevant to preferred prey species has also been observed in other pinnipeds (Vacquié-Garcia et al. 2015). Bottom temperature, dive depth, and bottom duration were all significantly related to foraging probabilities when considering both sexes, but showed no seasonal differences in patterns. This study demonstrates that grey seals exhibit preferences for the temperature and depth conditions expected to be important to preferred prey species, as reported in other species (McIntyre et al. 2011; Nordstrom et al. 2013a; Sterling et al. 2014; Malpress et al. 2017).

4.4.1 Generalized Linear Mixed-Effects Modelling

In using a switching model with two discrete behavioural states, locations that were inferred as apparent foraging where the animal may have been sleeping could not be accounted for. For some pelagic species, which sleep near-surface, dives are easily able to be filtered from analyses (e.g., Northern fur seal (*Callorinus ursinus*), Lyamin et al. 2017). Grey seals do not show evidence of near-surface sleeping for prolonged periods of time and based upon the duration of foraging trips are expected to do so at depth (Breed et al. 2009). Animal-borne imagery and accelerometry data from this population both indicate that grey seals do sleep at depth (Bowen, Broell, and Lidgard, unpublished data); however, this behaviour has not been quantified.

Although PQL estimation is known to be less accurate for binary data (Breslow 2004), such as behavioural states used in this study, it remains widely implemented (Bolker et al. 2009). Furthermore, limitations of software available for alternative methods (i.e., Laplace approximation, Gauss-Hermite quadrature), notable the inability to specify temporal correlation structures and challenges of implementation (i.e., INLA) made these alternatives unsuitable (Bolker et al. 2009). PQL models risk biased estimates for small effect sizes or large variances of the random effects (Bolker et al. 2009). This should not pose a problem in this study given the large number of behavioural state observations for each individual (Table 4.2).

4.4.2 Oceanographic Conditions Predict Behavioural States

Oceanographic conditions within the SS ecosystem have undergone dramatic changes as a result of a globally changing climate (Loder et al. 2013). Due to added pressures from commercial fisheries, several groundfish stocks have markedly declined

or collapsed (Frank et al. 2005; Worcester and Parker 2010; Shackell et al. 2012; Loder et al. 2013; Brennan et al. 2016). The grey seal has been the subject of controversy over its role in the depression of groundfish stocks (Mohn and Bowen 1996; Trzcinski et al. 2006; Bundy et al. 2009; Benoit et al. 2011; O'Boyle and Sinclair 2012; Sinclair et al. 2015; Neuenhoff et al. 2018), yet minimal research on the bottom-up forcing of oceanographic conditions has been performed to date. Large marine predators of diverse taxa have shown associations with mesoscale oceanographic features which promote primary productivity (Ream et al. 2005; Biuw et al. 2007; Dragon et al. 2010; Miller et al. 2015; Cox et al. 2018). However, in this ecosystem, dominant features (i.e., shelf-slope front and eddies) exist at or past the boundary of the continental shelf and largely outside of grey seal habitat (Herman and Denman 1979; Bisagni and Smith 1998) and less prominent features are easily traversed (i.e., Gully Front and Cape North Front; Belkin et al. 2009) (Fig. 4.1). The results of this study provide evidence that grey seal behaviours and habitat use are sensitive to the fine-scale environmental conditions they encounter that presumably structure the prey field across the oceanographically heterogeneous SS.

The lack of any seasonal variation in apparent foraging in the Water Column Model could be a result of restrictions imposed in the dataset, such that only dives 50 m and deeper and those between the hours of 10:00 and 14:00 AST were included. Previous studies of this population have shown sex-specific, seasonal patterns in diurnal dive behaviours (Beck et al. 2003a; Beck et al. 2003b). By contrast, in the Bottom Conditions Model, seasonal and sex-specific differences in apparent foraging behaviour over the 7-month pre-breeding period are thought to be reflective of differences in energetic requirements throughout the year, and consistent with the timing of mass gain and diet

composition (Beck et al. 2003a; Beck et al. 2003b; Beck 2003c; Breed et al. 2006; Beck et al. 2007; Tucker et al. 2007; Breed et al. 2009). Thus, the results of this study support previous research, demonstrating that females exhibit a prolonged preparation for the breeding period, while males lay down lipid stores in the 3-month period immediately prior (Beck et al. 2003c). The consequences of insufficient mass gain prior to the breeding season are higher for females than for males (Beck et al. 2003c; Lidgard et al. 2003; Lidgard et al. 2005), as heavier females produce larger pups at weaning which have improved chances of survival (Mellish et al. 1999; Bowen et al. 2015). It may be for these reasons that females were more likely to perform ARS than males at any given time. Females generally consume a higher quality, more specialized diet of smaller sized prey than males (e.g., sand lance), and thus may have to forage more often to satisfy their energy requirements (Beck et al. 2007). Females were more likely to be in the foraging state during summer, consistent with exploiting foraging patches closer to Sable Island, spending proportionally less time in the transiting state (Breed et al. 2009).

Although grey seals are prey generalists, there is considerable inter-annual and between-individual variation in diets (Beck et al. 2007; Bowen and Harrison 2007). Chl-*a* is a useful predictor of behavioural states in both seasons and sexes, indicating that grey seals generally exploit predictably productive areas. The influence of chl-*a* on behavioural on behavioural patterns and foraging decisions is greater in the fall, when the bloom is known to occur and the spatial variation in chl-*a* concentrations may be more heterogeneous (Fuentes-Yaco et al. 2015). Primary productivity levels over the SS decline following the spring bloom, and as a result, the relative differences in chl-*a* between suitable and unsuitable foraging areas should be less pronounced in summer

(Fuentes-Yaco et al. 2015). This is supported by the reduction in odds of predicting behavioural state during this time. Together with observed variation in movement patterns among sexes and seasons (Fig. 4.2) and among individuals (Fig. 4.4) (Austin et al. 2006), these results suggest oceanographic conditions may play a role in generating individual variability in diets that has been previously observed (Beck et al. 2007; Bowen and Harrison 2007). Southern elephant seals (*Mirounga leonina*) have also shown increased probabilities of foraging in areas of high phytoplankton biomass (O'Toole et al. 2015). While the shelf-slope front is largely outside of the grey seal habitat, at least one male exhibited movement patterns corresponding to the position of the shelf-break and shelf-slope front (Fig. 4.2), an area which is known to be highly productive (Breeze et al. 2002). In previous deployments during these periods, males showed a higher association with this area than seen here (Breed et al. 2006).

The association of ARS behaviour by females with both upper-water column and bottom temperature are particularly interesting given the thermal structuring of water masses over the SS. Selection of cooler waters within the upper-water column and warmer bottom temperatures may correspond to preference for more strongly stratified waters. Stratification over the ESS due to cooler water stemming from the GSL also corresponds well with their overall distribution (Fig. 4.2). Northern fur seals (*Callorhinus ursinus*) have been shown to preferentially forage in areas with strong thermoclines (Kuhn et al. 2011). This supports previous research suggesting females may be more reliant on pelagic prey species than males. Females have shown both diel variability in dive depths associated with movement of prey within the water column (Scott and Scott 1988; Gauthier and Rose 2002; Beck et al. 2003a) as well as a dietary niche indicating

that they consume a higher proportion of prey species that forage pelagically (Tucker et al. 2007). Increased stratification results in more concentrated resources within the upper layer available to species that move vertically throughout the water column, such as sand lance or redfish (*Sebastes sp.*). The Southern elephant seal also performs vertical migrations within the water column, corresponding to diel movements of their preferred prey. Foraging patterns exhibited by this species are also conditioned by water mass structuring and community composition of prey within distinct environments (Vacquié-Garcia et al. 2015). The influence of water mass conditions on movement patterns has been demonstrated in several pinniped species (Dragon et al. 2010; Heerah et al. 2013). Males tend to forage more broadly across the CSS and WSS where waters are less influenced by the GSL, as the Gully separating these regions allows off-shelf warm slope waters into these parts of the shelf (Fig. 4.2). Bottom temperature has been shown to influence both dive properties (McIntyre et al. 2011) and habitat use (Malpress et al. 2017) corresponding to foraging in other pinniped species. Warmer bottom temperatures associated with ARS highlight the reliance on warm slope waters over banks by both sexes over both seasons. Although only a small effect of bottom temperature was present, conditions encountered by individuals in both states were quite variable (Table A.2). This may explain the intense use of Middle Bank by both sexes, as this area is immediately adjascent to the Gully (Strain and Yeats 2005; Breed et al. 2009). As exothermic species in this region have been found to migrate to warmer, shallower banks during summer and fall (Perry and Smith 1994; Helser et al. 1995; Swain et al. 1998; Methratta and Link 2006; Siemann et al. 2018), it is likely that grey seals are following these temperature-keeping species. Although bottom temperature has been previously considered (Austin et

al. 2006), the lack of perceived effect may have been due the discrepancy in sampling period or potential for differences in dive depth from the substrate. This highlights the value of collecting *in situ* oceanographic measurements that are relevant to the conditions that grey seals encounter. Grey seals may perhaps be altering their foraging patterns to follow both the temperature and depth preferences of their prey species as distributions shift throughout the seasons (Methratta and Link 2006; Breed et al. 2009). This provides an explanation for the seasonal variability in the distributions of grey seals (Breed et al. 2006) and lack of seasonal interaction for oceanographic properties that otherwise influenced behavioural state.

To increase the net energy gained during foraging trips, animals should only dive as deep as necessary to encounter available prey species (Houston and McNamara, 1985). Females were more likely to perform shallower dives during ARS, which may allow them to maximize the aerobic budget as they expend less energy during descent and ascent. This is also consistent with foraging in areas of shallower bathymetry (Breed et al. 2009). Females also spend slightly shorter amounts of time at the bottom of dives during ARS, possibly owed to the energetic requirements of search behaviours and foraging. Variability in bottom time was large across states, sexes, and seasons (Table A.2). As bottom duration increased, males were also more likely to be in the transiting state. This is not entirely unsurprising as dive depth did not differ between ARS and transiting states and is likely a consequence of slightly higher energy expenditure of searching for and attempting to capture prey during foraging dives. Validation of foraging tactics must therefore be performed (e.g., accelerometery or animal-borne imagery). Given the mean duration and variation in bottom times (Table A.2), the number of dives made per day

(Table 4.2), and the proportion of time at sea spent foraging (Table 4.2; Breed et al. 2009), these relatively small differences could become biologically important. Grey seals of both sexes dive to depth during both foraging and transiting dives. Whether this is solely an evolutionary adaptation for predator avoidance during transit (Brodie and Beck 1983; LeBoeuf et al. 1988; Heithaus and Frid 2003), to increase opportunistic prey encounters (Austin et al. 2006), or a mechanism for encountering suitable conditions for foraging habitat is beyond the scope of this study. These results do not provide evidence for active feeding, but rather generalize behaviours and conditions during inter- and intra-patch movements. As almost all grey seal dives occur in bouts (Beck et al. 2003b; Austin et al. 2006), variation in dive depth and duration exhibited by grey seals may have been smeared within perceived states. The results of this study support previous findings that environmental variables become important at some scales and not others (Guinet et al. 2001; Austin et al. 2006).

4.4.3 Fine-Scale Habitat Selection

The high-resolution GPS locations obtained during this study revealed the fine-scale nature of habitat use by grey seals (Fig. 4.3). Although it has been previously demonstrated that habitat boundaries of grey seals appear to be sharp and that locations are focused over shallow banks (Breed et al. 2009), the way in which these topographical features are used was much more precise than anticipated. The coarse resolution of previously used Argos location data goes some way to explaining the differences in habitat use. With the development of Fastloc GPS technology, highly accurate relocations to 10s of meters could be retrieved. For example, movements surrounding LaHave Basin (43º65’N, 63º75’W) and Emerald Basin (43º80’N, 62º90’W), both with depths > 200 m,

were largely confined to a shallow bridge occurring between them, Sambro Bank (43º90'N, 63º30'W) (Fig. 4.3a). Middle Bank (44º50'N, 60º50'W) has been long regarded as a foraging hotspot for this population (Breed et al. 2006; Breed et al. 2009) and provides a compelling example of the fine-scale nature of grey seal movements (Fig. 4.3b). It is evident that while Middle Bank is an important habitat, almost exclusively the eastern side is used aside from a single area at the western boundary; this is particularly interesting result, as this pattern of space-use is consistent across all individuals of the population. Whether this is attributable to prey preferences for bottom temperature or depth, seabed morphology (i.e., the western side is a continuation of the Country Harbour Moraine; Davis and Browne 1996), circulation patterns (Strain and Yeats 2005), or some combination remains to be seen. French Bank, located nearby to Middle Bank, also shows a similar pattern of only partial use by grey seals (Fig. 4.3b). In contrast, Canso Bank (45º20'N, 60º30'W) is covered entirely with remarkably clear distinction at the boundaries of the bank edge (Fig. 4.3b). Due to high invertebrate and both larval and adult fish diversity, Canso Basin has been regarded as a continuation of this Ecologically and Biologically Significant Area (King et al. 2016). Despite its productivity, little exploration of this area by grey seals occurs. Reliance upon Canso Bank by males and females in both seasons sampled during the study period corresponds well with the high abundance of sand lance (King et al. 2016) and prevalence of this species in the grey seal diet (Beck et al. 2005; Beck et al. 2007; Bowen and Harrison 2007). This provides further evidence that while bathymetric features may provide suitable habitat for grey seal prey species, the complexity of oceanographic processes are clearly influential on the movements of grey seals across the continental shelf.

CHAPTER 5: CONCLUSIONS

Obtaining detailed spatial and temporal data on physical and biological oceanography is of great importance given the impacts of climate change, among other factors, on global ecosystems. The instrumentation of deep-diving, large marine predators has proven useful in sampling these conditions below the surface at fine spatio-temporal scales that would otherwise be extremely challenging. These data allow for monitoring of areas that are ecologically important to upper-trophic level species, and potential hotspots of biological productivity. By measuring oceanographic conditions concurrently with animal movements, we can make inferences using data that are both spatially and temporally relevant to the decisions made by animals along the course of foraging trips.

This thesis resulted in several key findings, improving our understanding of how oceanographic conditions structure the movements of a highly abundant, large marine predator, the grey seal. In Chapter 2, I demonstrated that a bio-optical model for the estimation of chl-*a* using light attenuation measured by biologging devices could be formed for the optically complex conditions of the Scotian Shelf. The presence of exogenous sources of CDOM proved influential on light attenuation measurements, but was able to be incorporated by this model. In Chapter 3, this bio-optical model was applied to light attenuation data collected by instrumented grey seals for the estimation of chl-*a* within the mixed layer depth. Along with other oceanographic properties (i.e., sea surface temperature, upper-water column temperature, and mixed layer depth), chl-*a* was mapped across the Scotian Shelf, demonstrating the spatio-temporal scales at which these data were collected. Grey seals sampled conditions broadly across this region, with consistently high coverage over the eastern Scotian Shelf and biologically productive

areas. These data provide a valuable resource that can serve to complement current methods of oceanographic data collection, providing a means of validating subsurface conditions for circulation models. In Chapter 4, I examined the extent to which these oceanographic processes influence the movement patterns of grey seals across the Scotian Shelf. By fitting hidden Markov movement models to grey seal location data, I was able to obtain estimated behavioural states along the course of foraging trips. Sex-by-season interactions were present and well-aligned with our current understanding of foraging effort in this population, as females exhibit early preparation for the breeding season. Increased levels of chl-*a* in the water column were positively associated with performing area-restricted search, showing seasonal variation consistent with known primary productivity patterns (i.e., bloom period). In females, cooler upper-water column temperatures were associated with area-restricted search, but showed no effect in males. Together with preferences for warmer bottom temperatures during foraging, it is possible that females are seeking out areas of increased stratification that may be important for preferred prey species. Males also showed increased odds of area-restricted search with warmer bottom temperatures, highlighting the importance of warm slope waters for both sexes and seasons. Shorter bottom duration was associated with foraging in both sexes, but showed a stronger effect in males. Females also performed shallower dives during area-restricted search. Given the large number of dives and proportion of time at sea spent foraging exhibited by adult grey seals, even small differences may become biologically important. This study highlights the value of *in situ* measurements of oceanographic properties and demonstrates the influence of these conditions on the movement patterns of grey seals across the Scotian Shelf.

REFERENCES

Abrams, P. A. 1991. Strengths of indirect effects generated by optimal foraging. Oikos 62:167-176.

Ackerman, S. A., K. I. Strabala, W. P. Menzel, R. A. Frey, C. C. Moeller, and L. E. Gumley. 1998. Discriminating clear sky from clouds with MODIS. Journal of Geophysical Research: Atmospheres 103:32141-32157.

Amante, C. and B. W. Eakins. 2009. ETOPO1 1 arc-minute global relief model: procedures, data sources, and analysis. NOAA Technical Memorandum NESDIS NGDC-24: 19 pp.

Antoine, D., J. André, and A. Morel. 1996. Oceanic primary production: 2. Estimation at global scale from satellite (coastal zone color scanner) chlorophyll. Global Biogeochemical Cycles 10:57-69.

Austin, D., W. Bowen, and J. McMillan. 2004. Intraspecific variation in movement patterns: modeling individual behaviour in a large marine predator. Oikos 105:15-30.

Austin, D., W. D. Bowen, J. I. McMillan, and S. J. Iverson. 2006. Linking movement, diving, and habitat to foraging success in a large marine predator. Ecology 87:3095-3108.

Babin, M., D. Stramski, G. Ferrari, H. Claustre, A. Bricaud, G. Obolensky, and N. Hoepffner. 2003. Variations in the light absorption coefficients of phytoplankton, nonalgal particles, and dissolved organic matter in coastal waters around Europe. Journal of Geophysical Research-Oceans 108:3211.

Bailey, H., and P. Thompson. 2010. Effect of oceanographic features on fine-scale foraging movements of bottlenose dolphins. Marine Ecology Progress Series 418:223-233.

Bailey, H., S. R. Benson, G. L. Shillinger, S. J. Bograd, P. H. Dutton, S. A. Eckert, S. J. Morreale, F. V. Paladino, T. Eguchi, D. G. Foley, B. A. Block, R. Piedra, C. Hitipeuw, R. F. Tapilatu, and J. R. Spotila. 2012. Identification of distinct movement patterns in Pacific leatherback turtle populations influenced by ocean conditions. Ecological Applications 22:735-747.

Bailleul, F., J. Charrassin, P. Monestiez, F. Roquet, M. Biuw, and C. Guinet. 2007. Successful foraging zones of southern elephant seals from the Kerguelen Islands in relation to oceanographic conditions. Philosophical Transactions of the Royal Society B-Biological Sciences 362:2169-2181.

Bailleul, F., M. Authier, S. Ducatez, F. Roquet, J. Charrassin, Y. Cherel, and C. Guinet. 2010. Looking at the unseen: combining animal bio-logging and stable isotopes to reveal a shift in the ecological niche of a deep diving predator. Ecography 33:709-719.

Baker, K., and R. Smith. 1982. Bio-Optical Classification and Model of Natural-Waters .2. Limnology and Oceanography 27:500-509.

Banse, K. 1977. Determining Carbon to Chlorophyll Ratio of Natural Phytoplankton. Marine Biology 41:199-212.

Barraquand, F., and S. Benhamou. 2008. Animal Movements in Heterogeneous Landscapes: Identifying Profitable Places and Homogeneous Movement Bouts. Ecology 89:3336-3348.

Bayle, S., P. Monestiez, C. Guinet, and D. Nerini. 2015. Moving toward finer scales in oceanography: Predictive linear functional model of chlorophyll a profile from light data. Progress in Oceanography 134:221-231.

Baylis, A. M. M., B. Page, and S. D. Goldsworthy. 2008. Effect of seasonal changes in upwelling activity on the foraging locations of a wide-ranging central-place forager, the New Zealand fur seal. Canadian Journal of Zoology-Revue Canadienne De Zoologie 86:774-789.

Beck, C.A. 2002. Sex differences in the foraging ecology of a size-dimorphic marine carnivore. PhD Thesis, Dalhousie University, Halifax, NS, Canada.

Beck, M. 2016. Defining a multi-parameter optics-based approach for estimating chlorophyll *a* concentration using ocean gliders. MSc Thesis, Dalhousie University, Halifax, NS, Canada.

Beck, C. A., S. J. Iverson, W. D. Bowen, and W. Blanchard. 2007. Sex differences in grey seal diet reflect seasonal variation in foraging behaviour and reproductive expenditure: evidence from quantitative fatty acid signature analysis. Journal of Animal Ecology 76:490-502.

Beck, C. A., W. D. Bowen, J. I. McMillan, and S. J. Iverson. 2003a. Sex differences in the diving behaviour of a size-dimorphic capital breeder: the grey seal. Animal Behaviour 66:777-789.

Beck, C. A., W. D. Bowen, J. I. McMillan, and S. J. Iverson. 2003b. Sex differences in diving at multiple temporal scales in a size-dimorphic capital breeder. Journal of Animal Ecology 72:979-993.

Beck, C. A., S. J. Iverson, and W. D. Bowen. 2005. Blubber fatty acids of gray seals reveal sex differences in the diet of a size-dimorphic marine carnivore. Canadian Journal of Zoology-Revue Canadienne De Zoologie 83:377-388.

Beck, C. A., W. D. Bowen, and S. J. Iverson. 2003c. Sex differences in the seasonal patterns of energy storage and expenditure in a phocid seal. Journal of Animal Ecology 72:280-291.

Beck, C., W. Bowen, and S. Iverson. 2000. Seasonal changes in buoyancy and diving behaviour of adult grey seals. Journal of Experimental Biology 203:2323-2330.

Behrenfeld, M. J., R. T. O'Malley, E. S. Boss, T. K. Westberry, J. R. Graff, K. H. Halsey, A. J. Milligan, D. A. Siegel, and M. B. Brown. 2016. Revaluating ocean warming impacts on global phytoplankton. Nature Climate Change 6:323-330.

Behrenfeld, M. J., T. K. Westberry, E. S. Boss, R. T. O'Malley, D. A. Siegel, J. D. Wiggert, B. A. Franz, C. McLain, G. Feldman, and S. C. Doney. 2009. Satellite-detected fluorescence reveals global physiology of ocean phytoplankton. Biogeosciences 6:779-794.

Behrenfeld, M. J., J. T. Randerson, C. R. McClain, G. C. Feldman, S. O. Los, C. J. Tucker, P. G. Falkowski, C. B. Field, R. Frouin, W. E. Esaias, D. D. Kolber, and N. H. Pollack. 2001. Biospheric primary production during an ENSO transition. Science 291:2594-2597.

Behrenfeld, M. J., R. T. O'Malley, D. A. Siegel, C. R. McClain, J. L. Sarmiento, G. C. Feldman, A. J. Milligan, P. G. Falkowski, R. M. Letelier, and E. S. Boss. 2006. Climate-driven trends in contemporary ocean productivity. Nature 444:752-755.

Behrenfeld, M., and P. Falkowski. 1997. Photosynthetic rates derived from satellite-based chlorophyll concentration. Limnology and Oceanography 42:1-20.

Belkin, I. M. 2004. Propagation of the "Great Salinity Anomaly" of the 1990s around the northern North Atlantic. Geophysical Research Letters 31:L08306.

Belkin, I. M., P. C. Cornillon, and K. Sherman. 2009. Fronts in large marine ecosystems. Progress in Oceanography 81:223-236.

Benoit, H. P., D. P. Swain, W. D. Bowen, G. A. Breed, M. O. Hammill, and V. Harvey. 2011. Evaluating the potential for grey seal predation to explain elevated natural mortality in three fish species in the southern Gulf of St. Lawrence. Marine Ecology Progress Series 442:149-167.

Benoit-Bird, K. J., B. C. Battaile, S. A. Heppell, B. Hoover, D. Irons, N. Jones, K. J. Kuletz, C. A. Nordstrom, R. Paredes, R. M. Suryan, C. M. Waluk, and A. W. Trites. 2013. Prey Patch Patterns Predict Habitat Use by Top Marine Predators with Diverse Foraging Strategies. Plos One 8:e53348.

Bestley, S., I. D. Jonsen, M. A. Hindell, C. Guinet, and J. Charrassin. 2013. Integrative modelling of animal movement: incorporating in situ habitat and behavioural information for a migratory marine predator. Proceedings of the Royal Society B-Biological Sciences 280:20122262.

Biermann, L., C. Guinet, M. Bester, A. Brierley, and L. Boehme. 2015. An alternative method for correcting fluorescence quenching. Ocean Science 11:83-91.

Bisagni, J. J., and P. C. Smith. 1998. Eddy-induced flow of Scotian Shelf water across Northeast Channel, Gulf of Maine. Continental Shelf Research 18:515-539.

Biuw, M., L. Boehme, C. Guinet, M. Hindell, D. Costa, J. -. Charrassin, F. Roquet, F. Bailleul, M. Meredith, S. Thorpe, Y. Tremblay, B. McDonald, Y. -. Park, S. R. Rintoul, N. Bindoff, M. Goebel, D. Crocker, P. Lovell, J. Nicholson, F. Monks, and M. A. Fedak. 2007. Variations in behavior and condition of a Southern Ocean top predator in relation to in situ oceanographic conditions. Proceedings of the National Academy of Sciences of the United States of America 104:13705-13710.

Blain, S., S. Renaut, X. Xing, H. Claustre, and C. Guinet. 2013. Instrumented elephant seals reveal the seasonality in chlorophyll and light-mixing regime in the iron-fertilized Southern Ocean. Geophysical Research Letters 40:6368-6372.

Blanchet, M., C. Lydersen, R. A. Ims, and K. M. Kovacs. 2015. Seasonal, Oceanographic and Atmospheric Drivers of Diving Behaviour in a Temperate Seal Species Living in the High Arctic. Plos One 10:e0132686.

Block, B., H. Dewar, S. Blackwell, T. Williams, E. Prince, C. Farwell, A. Boustany, S. Teo, A. Seitz, A. Walli, and D. Fudge. 2001. Migratory movements, depth preferences, and thermal biology of Atlantic bluefin tuna. Science 293:1310-1314.

Blondeau-Patissier, D., J. F. R. Gower, A. G. Dekker, S. R. Phinn, and V. E. Brando. 2014. A review of ocean color remote sensing methods and statistical techniques for the detection, mapping and analysis of phytoplankton blooms in coastal and open oceans. Progress in Oceanography 123:123-144.

Boehlert, G. W., D. P. Costa, D. E. Crocker, P. Green, T. O'Brien, S. Levitus, and B. J. Le Boeuf. 2001. Autonomous pinniped environmental samplers: using instrumented animals as oceanographic data collectors. Journal of Atmospheric and Oceanic Technology 18:1882-1893.

Boehme, L., P. Lovell, M. Biuw, F. Roquet, J. Nicholson, S. E. Thorpe, M. P. Meredith, and M. Fedak. 2009. Animal-borne CTD-Satellite Relay Data Loggers for real-time oceanographic data collection. Ocean Science 5:685-695.

Bolker, B. M., M. E. Brooks, C. J. Clark, S. W. Geange, J. R. Poulsen, M. H. H. Stevens, and J. S. White. 2009. Generalized linear mixed models: a practical guide for ecology and evolution. Trends in Ecology & Evolution 24:127-135.

Bon, C., A. Della Penna, F. d'Ovidio, J. Y. P. Arnould, T. Poupart, and C. Bost. 2015. Influence of oceanographic structures on foraging strategies: Macaroni penguins at Crozet Islands. Movement Ecology 3:32.

Boness, D.J., W.D. Bowen, and O.T. Oftedal. 1994. Evidence of a maternal foraging cycle resembling that of otariid seals in a small phocid, the harbour seal. Behavioural Ecology and Sociobiology 34:95-104.

Bowen, W., and G. Harrison. 2007. Seasonal and interannual variability in grey seal diets on Sable Island, eastern Scotian Shelf. NAMMCO Scientific Publications 6:123-134.

Bowen, W. D., C. E. den Heyer, J. I. McMillan, and S. J. Iverson. 2015. Offspring size at weaning affects survival to recruitment and reproductive performance of primiparous gray seals. Ecology and Evolution 5:1412-1424.

Bowen, W. D., J. I. McMillan, and W. Blanchard. 2007. Reduced population growth of gray seals at Sable Island: Evidence from pup production and age of primiparity. Marine Mammal Science 23:48-64.

Bowen, W. D., J. McMillan, and R. Mohn. 2003. Sustained exponential population growth of grey seals at Sable Island, Nova Scotia. ICES Journal of Marine Science 60:1265-1274.

Bowen, W., C. Beck, and S. Iverson. 1999. Bioelectrical impedance analysis as a means of estimating total body water in grey seals. Canadian Journal of Zoology-Revue Canadienne De Zoologie 77:418-422.

Bowen, W., O. Oftedal, and D. Boness. 1992. Mass and Energy-Transfer during Lactation in a Small Phocid, the Harbor Seal (Phoca-Vitulina). Physiological Zoology 65:844-866.

Bowers, D., G. Harker, and B. Stephan. 1996. Absorption spectra of inorganic particles in the Irish Sea and their relevance to remote sensing of chlorophyll. International Journal of Remote Sensing 17:2449-2460.

Boyd, P. W., C. E. Cornwall, A. Davison, S. C. Doney, M. Fourquez, C. L. Hurd, I. D. Lima, and A. McMinn. 2016. Biological responses to environmental heterogeneity under future ocean conditions. Global Change Biology 22:2633-2650.

Boyd, I. L. 1984. The Relationship between Body Condition and the Timing of Implantation in Pregnant Grey Seals (Halichoerus-Grypus). Journal of Zoology 203:113-123.

Boyd, I., E. Hawker, M. Brandon, and I. Staniland. 2001. Measurement of ocean temperatures using instruments carried by Antarctic fur seals. Journal of Marine Systems 27:277-288.

Breed, G. A., W. D. Bowen, J. I. McMillan, and M. L. Leonard. 2006. Sexual segregation of seasonal foraging habitats in a non-migratory marine mammal. Proceedings of the Royal Society B-Biological Sciences 273:2319-2326.

Breed, G. A., I. D. Jonsen, R. A. Myers, W. D. Bowen, and M. L. Leonard. 2009. Sex-specific, seasonal foraging tactics of adult grey seals (Halichoerus grypus) revealed by state-space analysis. Ecology 90:3209-3221.

Breeze, H., D.G. Fenton, R.J. Rutherford, and M.A. Silva. 2002. The Scotian Shelf: An ecological overview for ocean planning. Can. Tech. Rep. Fish. Aquat. Sci. 2393: x + 259 pp.

Brennan, C. E., H. Blanchard, and K. Fennel. 2016. Putting temperature and oxygen thresholds of marine animals in context of environmental change: a regional perspective for the Scotian Shelf and Gulf of St. Lawrence. PloS one 11:e0167411.

Breslow, N. 2004. Whither PQL? Pages 1-22 *in* D.Y. Lin and P.J. Heagerty, editors. Proceedings of the Second Seattle Symposium in Biostatistics. Lecture Notes in Statistics, Volume 179. Springer, New York, New, York, USA.

Breslow, N. E., and D. G. Clayton. 1993. Approximate inference in generalized linear mixed models. Journal of the American statistical Association 88:9-25.

Bricaud, A., A. Morel, and L. Prieur. 1981. Absorption by dissolved organic matter of the sea (yellow substance) in the UV and visible domains. Limnology and Oceanography 26:43-53.

Brickman, D., D. Hebert, and Z. Wang. 2018. Mechanism for the recent ocean warming events on the Scotian Shelf of eastern Canada. Continental Shelf Research 156:11-22.

Brodie, P., and B. Beck. 1983. Predation by sharks on the grey seal (Halichoerus grypus) in eastern Canada. Canadian Journal of Fisheries and Aquatic Sciences 40:267-271.

Bryant, E. 2007. 2D location accuracy statistics for Fastloc® cores running firmware versions 2.2 & 2.3. Technical Report TR01. Wildtrack Telemetry Systems Ltd. Leeds, West Yorkshire, England.

Bundy, A., D. Themelis, J. Sperl, and C.E. den Heyer. 2014. Inshore Scotian Shelf Ecosystem Overview Report: Status and Trends. DFO Can. Sci. Advis. Sec. Res. Doc. 2014/065. xii + 213 p.

Bundy, A. 2005. Structure and functioning of the eastern Scotian Shelf ecosystem before and after the collapse of groundfish stocks in the early 1990s. Canadian Journal of Fisheries and Aquatic Sciences 62:1453-1473.

Bundy, A., and L. Fanning. 2005. Can Atlantic cod (Gadus morhua) recover? Exploring trophic explanations for the non-recovery of the cod stock on the eastern Scotian Shelf, Canada. Canadian Journal of Fisheries and Aquatic Sciences 62:1474-1489.

Bundy, A., J. J. Heymans, L. Morissette, and C. Savenkoff. 2009. Seals, cod and forage fish: A comparative exploration of variations in the theme of stock collapse and ecosystem change in four Northwest Atlantic ecosystems. Progress in Oceanography 81:188-206.

Burgman, M. A., and J. C. Fox. 2003. Bias in species range estimates from minimum convex polygons: implications for conservation and options for improved planning. Animal Conservation 6:19-28.

Burns, J., D. Costa, M. Fedak, M. Hindell, C. Bradshaw, N. Gales, B. McDonald, S. Trumble, and D. Crocker. 2004. Winter habitat use and foraging behavior of crabeater seals along the Western Antarctic Peninsula. Deep-Sea Research Part II-Topical Studies in Oceanography 51:2279-2303.

Burton, R. K., and P. L. Koch. 1999. Isotopic tracking of foraging and long-distance migration in northeastern Pacific pinnipeds. Oecologia 119:578-585.

Calenge, C. 2006. The package "adehabitat" for the R software: A tool for the analysis of space and habitat use by animals. Ecological Modelling 197:516-519.

Campagna, C., A. Rivas, and M. Marin. 2000. Temperature and depth profiles recorded during dives of elephant seals reflect distinct ocean environments. Journal of Marine Systems 24:299-312.

Campagna, C., A. R. Piola, M. R. Marin, M. Lewis, and T. Fernandez. 2006. Southern elephant seal trajectories, fronts and eddies in the Brazil/Malvinas Confluence. Deep-Sea Research Part I-Oceanographic Research Papers 53:1907-1924.

Campagna, C., A. R. Piola, M. R. Marin, M. Lewis, U. Zajaczkovski, and T. Fernandez. 2007. Deep divers in shallow seas: Southern elephant seals on the Patagonian shelf. Deep-Sea Research Part I-Oceanographic Research Papers 54:1792-1814.

Carroll, G., M. Cox, R. Harcourt, B. J. Pitcher, D. Slip, and I. Jonsen. 2017. Hierarchical influences of prey distribution on patterns of prey capture by a marine predator. Functional Ecology 31: 1750-1760.

Carroll, G., R. Harcourt, B. J. Pitcher, D. Slip, and I. Jonsen. 2018. Recent prey capture and dynamic habitat quality mediate short-term foraging site fidelity in a seabird. Proceedings of the Royal Society B 285: 20180788.

Carter, M. I. D., K. A. Bennett, C. B. Embling, P. J. Hosegood, and D. J. Russell. 2016. Navigating uncertain waters: a critical review of inferring foraging behaviour from location and dive data in pinnipeds. Movement Ecology 4:25.

Charnov, E. 1976. Optimal Foraging, Marginal Value Theorem. Theoretical Population Biology 9:129-136.

Charrassin, J., M. Hindell, S. R. Rintoul, F. Roquet, S. Sokolov, M. Biuw, D. Costa, L. Boehme, P. Lovell, R. Coleman, R. Timmermann, A. Meijers, M. Meredith, Y. -. Park, F. Bailleul, M. Goebel, Y. Tremblay, C. -. Bost, C. R. McMahon, I. C. Field, M. A. Fedak, and C. Guinet. 2008. Southern Ocean frontal structure and sea-ice formation rates revealed by elephant seals. Proceedings of the National Academy of Sciences of the United States of America 105:11634-11639.

Choi, J., K. Frank, B. Petrie, and W. Leggett. 2005. Integrated assessment of a large marine ecosystem: a case study of the devolution of the Eastern Scotian Shelf, Canada. Pages 57-78 in Oceanography and Marine Biology, CRC Press.

Choi, J. S., K. T. Frank, W. C. Leggett, and K. Drinkwater. 2004. Transition to an alternate state in a continental shelf ecosystem. Canadian Journal of Fisheries and Aquatic Sciences 61:505-510.

Ciotti, Á. M., J. J. Cullen, and M. R. Lewis. 1999. A semi-analytical model of the influence of phytoplankton community structure on the relationship between light attenuation and ocean color. Journal of Geophysical Research: Oceans 104:1559-1578.

Citta, J. J., S. R. Okkonen, L. T. Quakenbush, W. Maslowski, R. Osinski, J. C. George, R. J. Small, H. Brower Jr., M. P. Heide-Jorgensen, and L. A. Harwood. 2018. Oceanographic characteristics associated with autumn movements of bowhead whales in the Chukchi Sea. Deep-Sea Research Part II-Topical Studies in Oceanography 152:121-131.

Costa, D. P. 1993. The secret life of marine mammals. Oceanography 6:120-128.

Costa, D. P., L. A. Huckstadt, D. E. Crocker, B. I. McDonald, M. E. Goebel, and M. A. Fedak. 2010. Approaches to studying climatic change and its role on the habitat selection of Antarctic pinnipeds. Integrative and Comparative Biology 50:1018-1030.

Costa, D. P., J. M. Klinck, E. E. Hofmann, M. S. Dinniman, and J. M. Burns. 2008. Upper ocean variability in west Antarctic Peninsula continental shelf waters as measured using instrumented seals. Deep-Sea Research Part II-Topical Studies in Oceanography 55:323-337.

Cotte, C., F. d'Ovidio, A. Dragon, C. Guinet, and M. Levy. 2015. Flexible preference of southern elephant seals for distinct mesoscale features within the Antarctic Circumpolar Current. Progress in Oceanography 131:46-58.

Cox, S. L., C. B. Embling, P. J. Hosegood, S. C. Votier, and S. N. Ingram. 2018. Oceanographic drivers of marine mammal and seabird habitat-use across shelf-seas: A guide to key features and recommendations for future research and conservation management. Estuarine Coastal and Shelf Science 212:294-310.

Craig, S. E., H. Thomas, C. T. Jones, W. K. Li, B. J. Greenan, E. H. Shadwick, and W. J. Burt. 2015. The effect of seasonality in phytoplankton community composition on CO2 uptake on the Scotian Shelf. Journal of Marine Systems 147:52-60.

Croll, D. A., K. M. Newton, K. Weng, F. Galvan-Magana, J. O'Sullivan, and H. Dewar. 2012. Movement and habitat use by the spine-tail devil ray in the Eastern Pacific Ocean. Marine Ecology Progress Series 465:193-200.

Cullen, J. 1982. The Deep Chlorophyll Maximum - Comparing Vertical Profiles of Chlorophyll-a. Canadian Journal of Fisheries and Aquatic Sciences 39:791-803.

Cullen, J., and M. Lewis. 1995. Biological Processes and Optical Measurements Near the Sea Surface: some Issues Relevant to Remote Sensing. Journal of Geophysical Research-Oceans 100:13255-13266.

Darecki, M., and D. Stramski. 2004. An evaluation of MODIS and SeaWiFS bio-optical algorithms in the Baltic Sea. Remote Sensing of Environment 89:326-350.

Darecki, M., A. Weeks, S. Sagan, P. Kowalczuk, and S. Kaczmarek. 2003. Optical characteristics of two contrasting Case 2 waters and their influence on remote sensing algorithms. Continental Shelf Research 23:237-250.

Davis, D., and S. Browne. 1996. The natural history of Nova Scotia Vol. 2: Theme regions. Nimbus Publishing and the Nova Scotia Museum. Halifax, Nova Scotia, Canada.

Davoren, G. K. 2013. Distribution of marine predator hotspots explained by persistent areas of prey. Marine Biology 160:3043-3058.

de Boyer Montegut, C., G. Madec, A. Fischer, A. Lazar, and D. Iudicone. 2004. Mixed layer depth over the global ocean: An examination of profile data and a profile-based climatology. Journal of Geophysical Research-Oceans 109:C12003.

den Heyer, C.E., S.L.C. Lang, W.D. Bowen, and M.O. Hammill. 2017. Pup Production at Scotian Shelf Grey Seal (*Halichoerus grypus*) Colonies in 2016. DFO Can. Sci. Advis. Sec. Res. Doc. 2017/056. v + 34 p.

Dever, M., D. Hebert, B. J. W. Greenan, J. Sheng, and P. C. Smith. 2016. Hydrography and Coastal Circulation along the Halifax Line and the Connections with the Gulf of St. Lawrence. Atmosphere-Ocean 54:199-217.

Devred, E., C. Fuentes-Yaco, S. Sathyendranath, C. Caverhill, H. Maass, V. Stuart, T. Platt, and G. White. 2005. A semi-analytic seasonal algorithm to retrieve chlorophyll-a concentration in the Northwest Atlantic Ocean from SeaWiFS data. Indian Journal of Marine Sciences 34:356-367.

DFO. 2014. Stock Assessment of Canadian Grey Seals (Halichoerus Grypus). DFO Can. Sci. Advis. Sec. Sci. Advis. Rep. 2014/010.

Dodge, K. L., B. Galuardi, T. J. Miller, and M. E. Lutcavage. 2014. Leatherback Turtle Movements, Dive Behavior, and Habitat Characteristics in Ecoregions of the Northwest Atlantic Ocean. Plos One 9:e91726.

Doerffer, R., and H. Schiller. 2007. The MERIS case 2 water algorithm. International Journal of Remote Sensing 28:517-535.

Doney, S. C., M. Ruckelshaus, J. E. Duffy, J. P. Barry, F. Chan, C. A. English, H. M. Galindo, J. M. Grebmeier, A. B. Hollowed, N. Knowlton, J. Polovina, N. N. Rabalais, W. J. Sydeman, and L. D. Talley. 2012. Climate Change Impacts on Marine Ecosystems. Annual Review of Marine Science 4:11-37.

Dragon, A., A. Bar-Hen, P. Monestiez, and C. Guinet. 2012. Comparative analysis of methods for inferring successful foraging areas from Argos and GPS tracking data. Marine Ecology Progress Series 452:253-267.

Dragon, A., P. Monestiez, A. Bar-Hen, and C. Guinet. 2010. Linking foraging behaviour to physical oceanographic structures: Southern elephant seals and mesoscale eddies east of Kerguelen Islands. Progress in Oceanography 87:61-71.

Dujon, A. M., R. T. Lindstrom, and G. C. Hays. 2014. The accuracy of Fastloc-GPS locations and implications for animal tracking. Methods in Ecology and Evolution 5:1162-1169.

Eckert, S. A., J. E. Moore, D. C. Dunn, R. S. van Buiten, K. L. Eckert, and P. N. Halpin. 2008. Modeling loggerhead turtle movement in the Mediterranean: Importance of body size and oceanography. Ecological Applications 18:290-308.

Fagan, W. F., M. A. Lewis, M. Auger-Methe, T. Avgar, S. Benhamou, G. Breed, L. LaDage, U. E. Schlaegel, W. Tang, Y. P. Papastamatiou, J. Forester, and T. Mueller. 2013. Spatial memory and animal movement. Ecology Letters 16:1316-1329.

Falkowski, P., R. Barber, and V. Smetacek. 1998. Biogeochemical controls and feedbacks on ocean primary production. Science 281:200-206.

Fedak, M. 2004. Marine animals as platforms for oceanographic sampling: a" win/win" situation for biology and operational oceanography. Memoirs of National Institute of Polar Research, Special Issue 58:133-147.

Fedak, M. A. 2013. The impact of animal platforms on polar ocean observation. Deep-Sea Research Part II-Topical Studies in Oceanography 88-89:7-13.

Field, C., M. Behrenfeld, J. Randerson, and P. Falkowski. 1998. Primary production of the biosphere: Integrating terrestrial and oceanic components. Science 281:237-240.

Field, I., M. Hindell, D. Slip, and K. Michael. 2001. Foraging strategies of southern elephant seals (*Mirounga leonina*) in relation to frontal zones and water masses. Antarctic Science 13:371-379.

Frank, K. T., J. E. Carscadden, and J. E. Simon. 1996. Recent excursions of capelin (*Mallotus villosus*) to the Scotian shelf and Flemish cap during anomalous hydrographic conditions. Canadian Journal of Fisheries and Aquatic Sciences 53:1473-1486.

Frank, K. T., B. Petrie, J. S. Choi, and W. C. Leggett. 2005. Trophic cascades in a formerly cod-dominated ecosystem. Science 308:1621-1623.

Frank, K. T., B. Petrie, J. A. D. Fisher, and W. C. Leggett. 2011. Transient dynamics of an altered large marine ecosystem. Nature 477:86-89.

Frankcombe, L. M., A. Von Der Heydt, and H. A. Dijkstra. 2010. North Atlantic multidecadal climate variability: an investigation of dominant time scales and processes. Journal of Climate 23:3626-3638.

Friedl, M. A., D. Sulla-Menashe, B. Tan, A. Schneider, N. Ramankutty, A. Sibley, and X. Huang. 2010. MODIS Collection 5 global land cover: Algorithm refinements and characterization of new datasets. Remote Sensing of Environment 114:168-182.

Friedl, M. A., D. K. McIver, J. C. Hodges, X. Y. Zhang, D. Muchoney, A. H. Strahler, C. E. Woodcock, S. Gopal, A. Schneider, and A. Cooper. 2002. Global land cover mapping from MODIS: algorithms and early results. Remote Sensing of Environment 83:287-302.

Fuentes-Yaco, C., M. King, W.K.W. Li. 2015. Mapping areas of high phytoplankton biomass in the offshore component of the Scotian Shelf Bioregion: A remotely-sensed approach. DFO Can. Sci. Advis. Sec. Res. Doc. 2015/036. iv + 40 p.

Fuentes-Yaco, C., E. Devred, S. Sathyendranath, T. Platt, L. Payzant, C. Caverhill, C. Porter, H. Maass, and G. White. 2005. Comparison of in situ and remotely-sensed (SeaWiFS) chlorophyll-a in the Northwest Atlantic. Indian Journal of Marine Sciences 34:341-355.

Galbraith, P. S., P. Larouche, J. Chassé, and B. Petrie. 2012. Sea-surface temperature in relation to air temperature in the Gulf of St. Lawrence: interdecadal variability and long term trends. Deep Sea Research Part II: Topical Studies in Oceanography 77:10-20.

Galbraith, P. S., and P. Larouche. 2013. Trends and variability in air and sea surface temperatures in eastern Canada. Canadian Technical Report of Fisheries and Aquatic Sciences 3045:1-18.

Gao, B., M. Montes, Z. Ahmad, and C. Davis. 2000. Atmospheric correction algorithm for hyperspectral remote sensing of ocean color from space. Applied Optics 39:887-896.

Gauthier, S. and G. A. Rose. 2002. *In situ* target strength studies on Atlantic redfish (*Sebastes spp.*). ICES Journal of Marine Science 59: 805-815.

Gende, S. M., and M. F. Sigler. 2006. Persistence of forage fish 'hot spots' and its association with foraging Steller sea lions (*Eumetopias jubatus*) southeast Alaska. Deep-Sea Research Part II-Topical Studies in Oceanography 53:432-441.

Gordon, H., and W. McCluney. 1975. Estimation of Depth of Sunlight Penetration in Sea for Remote-Sensing. Applied Optics 14:413-416.

Gordon, H. R., R. C. Smith, and J. R. V. Zaneveld. 1980. Introduction to ocean optics, Proceedings of the Society of Photo-Optical Instrumentation Engineers, 6:1-43.

Greenberg, D., J. Loder, Y. Shen, D. Lynch, and C. Naimie. 1997. Spatial and temporal structure of the barotropic response of the Scotian Shelf and Gulf of Maine to surface wind stress: A model-based study. Journal of Geophysical Research-Oceans 102:20897-20915.

Greene, C. H., A. J. Pershing, T. M. Cronin, and N. Ceci. 2008. Arctic Climate Change and its Impacts on the Ecology of the North Atlantic. Ecology 89:S24-S38.

Grist, J. P., S. A. Josey, L. Boehme, M. P. Meredith, F. J. Davidson, G. B. Stenson, and M. O. Hammill. 2011. Temperature signature of high latitude Atlantic boundary currents revealed by marine mammal-borne sensor and Argo data. Geophysical Research Letters 38:L15601.

Guinet, C., L. Dubroca, M. Lea, S. Goldsworthy, Y. Cherel, G. Duhamel, F. Bonadonna, and J. Donnay. 2001. Spatial distribution of foraging in female Antarctic fur seals *Arctocephalus gazella* in relation to oceanographic variables: a scale-dependent approach using geographic information systems. Marine Ecology Progress Series 219:251-264.

Guinet, C., X. Xing, E. Walker, P. Monestiez, S. Marchand, B. Picard, T. Jaud, M. Authier, C. Cotte, A. C. Dragon, E. Diamond, D. Antoine, P. Lovell, S. Blain, F. D'Ortenzio, and H. Claustre. 2013. Calibration procedures and first dataset of Southern Ocean chlorophyll a profiles collected by elephant seals equipped with a newly developed CTD-fluorescence tags. Earth System Science Data 5:15-29.

Hammill, M.O., C.E. den Heyer, W.D. Bowen, and S.L.C. Lang. 2017a. Grey Seal Population Trends in Canadian Waters, 1960-2016 and harvest advice. DFO Can. Sci. Advis. Sec. Res. Doc. 2017/052. v + 30 p.

Hammill, M.O., J-F. Gosselin, and G.B. Stenson. 2017b. Pup production of Northwest Atlantic grey seals in the Gulf of St. Lawrence. DFO Can. Sci. Advis. Sec. Res. Doc. 2017/043. iv + 14 p.

Han, G. Q., and J. W. Loder. 2003. Three-dimensional seasonal-mean circulation and hydrography on the eastern Scotian Shelf. Journal of Geophysical Research-Oceans 108:3136.

Han, G., J. Loder, and P. Smith. 1999. Seasonal-mean hydrography and circulation in the Gulf of St. Lawrence and on the eastern Scotian and southern Newfoundland shelves. Journal of Physical Oceanography 29:1279-1301.

Hannah, C., J. Shore, J. Loder, and C. Naimie. 2001. Seasonal circulation on the western and central Scotian Shelf. Journal of Physical Oceanography 31:591-615.

Harley, C., A. Hughes, K. Hultgren, B. Miner, C. Sorte, C. Thornber, L. Rodriguez, L. Tomanek, and S. Williams. 2006. The impacts of climate change in coastal marine systems. Ecology Letters 9:228-241.

Hebert, D., R. Pettipas, D. Brickman, and M Dever. 2018. Meteorological, Sea Ice and Physical Oceanographic Conditions on the Scotian Shelf and in the Gulf of Maine during 2016. DFO Can. Sci. Advis. Sec. Res. Doc. 2018/016. v + 53 p.

Heerah, K., M. Hindell, C. Guinet, and J. Charrassin. 2014. A New Method to Quantify within Dive Foraging Behaviour in Marine Predators. Plos One 9:e99329.

Heerah, K., V. Andrews-Goff, G. Williams, E. Sultan, M. Hindell, T. Patterson, and J. Charrassin. 2013. Ecology of Weddell seals during winter: Influence of environmental parameters on their foraging behaviour. Deep-Sea Research Part II-Topical Studies in Oceanography 88-89:23-33.

Heithaus, M. R., and A. Frid. 2003. Optimal diving under the risk of predation. Journal of Theoretical Biology 223:79-92.

Helms, J. R., A. Stubbins, J. D. Ritchie, E. C. Minor, D. J. Kieber, and K. Mopper. 2008. Absorption spectral slopes and slope ratios as indicators of molecular weight, source, and photobleaching of chromophoric dissolved organic matter. Limnology and Oceanography 53:955-969.

Helser, T. E., F. P. Almeida, and D. E. Waldron. 1995. Biology and fisheries of North-west Atlantic hake (silver hake: *M. bilinearis*). Pages 203-237 *in* J. Alheit, and T.J. Pitcher, editors. Hake. Chapman and Hall Fish and Fisheries Series, Volume 15. Springer, Dordrecht, South Holland, Netherlands.

Herman, A. W., and K. L. Denman. 1979. Intrusions and Vertical Mixing at the Shelf-Slope Water Front South of Nova-Scotia. Journal of the Fisheries Research Board of Canada 36:1445-1453.

Hewer, H., and K. Backhouse. 1968. Embryology and foetal growth of the grey seal, *Halichoerus grypus*. Journal of Zoology 155:507-533.

Hindell, M. A., C. R. McMahon, M. N. Bester, L. Boehme, D. Costa, M. A. Fedak, C. Guinet, L. Herraiz-Borreguero, R. G. Harcourt, and L. Huckstadt. 2016. Circumpolar habitat use in the southern elephant seal: implications for foraging success and population trajectories. Ecosphere 7:e01213.

Hindell, M., H. Burton, and D. Slip. 1991. Foraging Areas of Southern Elephant Seals, Mirounga-Leonina, as Inferred from Water Temperature Data. Australian Journal of Marine and Freshwater Research 42:115-128.

Hoegh-Guldberg, O., and J. F. Bruno. 2010. The Impact of Climate Change on the World's Marine Ecosystems. Science 328:1523-1528.

Holm, H., and A. Burger. 2002. Foraging behavior and resource partitioning by diving birds during winter in areas of strong tidal currents. Waterbirds 25:312-325.

Hooker, S. K., and I. L. Boyd. 2003. Salinity sensors on seals: use of marine predators to carry CTD data loggers. Deep Sea Research Part I: Oceanographic Research Papers 50:927-939.

Hooker, S., and I. Boyd. 2003. Salinity sensors on seals: use of marine predators to carry CTD data loggers. Deep-Sea Research Part I-Oceanographic Research Papers 50:927-939.

Horsman, T.L. and N.L. Shackell. 2009. Atlas of important habitat for key fish species of the Scotian Shelf, Canada. Can. Tech. Rep. Fish. Aquat. Sci. 2835: viii + 82 p.

Houston, A. I., and J. M. McNamara. 1985. A general theory of central place foraging for single-prey loaders. Theoretical Population Biology 28:233-262.

Hu, C., K. Carder, and F. Muller-Karger. 2000. Atmospheric correction of SeaWiFS imagery over turbid coastal waters: A practical method. Remote Sensing of Environment 74:195-206.

Iverson, S. J., W. D. Bowen, D. J. Boness, and O. T. Oftedal. 1993. The Effect of Maternal Size and Milk Energy Output on Pup Growth in Gray Seals (Halichoerus-Grypus). Physiological Zoology 66:61-88.

Jaine, F. R. A., C. A. Rohner, S. J. Weeks, L. I. E. Couturier, M. B. Bennett, K. A. Townsend, and A. J. Richardson. 2014. Movements and habitat use of reef manta rays off eastern Australia: offshore excursions, deep diving and eddy affinity revealed by satellite telemetry. Marine Ecology Progress Series 510:73-86.

Jaud, T., A. Dragon, J. V. Garcia, and C. Guinet. 2012. Relationship between Chlorophyll a Concentration, Light Attenuation and Diving Depth of the Southern Elephant Seal Mirounga leonina. Plos One 7:e47444.

Jena, B. 2017. The effect of phytoplankton pigment composition and packaging on the retrieval of chlorophyll-a concentration from satellite observations in the Southern Ocean. International Journal of Remote Sensing 38:3763-3784.

Ji, R., C. S. Davis, C. Chen, D. W. Townsend, D. G. Mountain, and R. C. Beardsley. 2007. Influence of ocean freshening on shelf phytoplankton dynamics. Geophysical Research Letters 34:L24607.

Johnson, C., E. Devred, B. Casault, E. Head, and J. Spry. 2018. Optical, Chemical, and Biological Oceanographic Conditions on the Scotian Shelf and in the Eastern Gulf of Maine in 2016. DFO Can. Sci. Advis. Sec. Res. Doc. 2018/017. v + 58 p.

Johnston, D. W., A. J. Westgate, and A. J. Read. 2005. Effects of fine-scale oceanographic features on the distribution and movements of harbour porpoises *Phocoena phocoena* in the Bay of Fundy. Marine Ecology Progress Series 295:279-293.

Jonsen, I., C. McMahon, T. Patterson, M. Auger-Methe, R. Harcourt, M. Hindell, and S. Bestley. 2018. Movement responses to environment: fast inference of variation among southern elephant seals with a mixed effects model. Ecology 100: UNSP e02566.

Jonsen, I. D., J. M. Flemming, and R. A. Myers. 2005. Robust state–space modeling of animal movement data. Ecology 86:2874-2880.

Kerrigan, E. A., M. Kienast, H. Thomas, and D. W. Wallace. 2017. Using oxygen isotopes to establish freshwater sources in Bedford Basin, Nova Scotia, a Northwestern Atlantic fjord. Estuarine, Coastal and Shelf Science 199:96-104.

Khan, A. H., E. Levac, and G. L. Chmura. 2013. Future sea surface temperatures in Large Marine Ecosystems of the Northwest Atlantic. ICES Journal of Marine Science 70:915-921.

King, M., D. Fenton, J. Aker, and A. Serdynska. 2016. Offshore Ecologically and Biologically Significant Areas in the Scotian Shelf Bioregion. DFO Can. Sci. Advis. Sec. Res. Doc. 2016/007. viii + 92 p.

Kirk, J.T.O. 1994. Light and photosynthesis in aquatic ecosystems. Cambridge University Press, Cambridge, England.

Kovacs, K. M., A. Aguilar, D. Aurioles, V. Burkanov, C. Campagna, N. Gales, T. Gelatt, S. D. Goldsworthy, S. J. Goodman, and G. J. Hofmeyr. 2012. Global threats to pinnipeds. Marine Mammal Science 28:414-436.

Krause, D. J., M. E. Goebel, G. J. Marshall, and K. Abernathy. 2016. Summer diving and haul-out behavior of leopard seals (Hydrurga leptonyx) near mesopredator breeding colonies at Livingston Island, Antarctic Peninsula. Marine Mammal Science 32:839-867.

Kuhn, C. E. 2011. The influence of subsurface thermal structure on the diving behavior of northern fur seals (Callorhinus ursinus) during the breeding season. Marine Biology 158:649-663.

Kuhn, C., B. McDonald, S. Shaffer, J. Barnes, D. Crocker, J. Burns, and D. Costa. 2006. Diving physiology and winter foraging behavior of a juvenile leopard seal (*Hydrurga leptonyx*). Polar Biology 29:303-307.

Lagman, K.B. 2013. Application of frequency-dependent nudging in biogeochemical modeling and assessment of marine animal tag data for ocean observations. MSc Thesis, Dalhousie University, Halifax, NS, Canada.

Laliberté, J., P. Larouche, E. Devred, and S. Craig. 2018. Chlorophyll-a Concentration Retrieval in the Optically Complex Waters of the St. Lawrence Estuary and Gulf Using Principal Component Analysis. Remote Sensing 10:265.

Lander, M. E., T. Lindstrom, M. Rutishauser, A. Franzheim, and M. Holland. 2015. Development and field testing a satellite-linked fluorometer for marine vertebrates. Animal Biotelemetry 3:40.

Le Boeuf, B., D. E. Crocker, D. P. Costa, S. B. Blackwell, P. M. Webb, and D. S. Houser. 2000. Foraging ecology of northern elephant seals. Ecological Monographs 70:353-382.

Le Boeuf, B. J., D. P. Costa, A. C. Huntley, and S. D. Feldkamp. 1988. Continuous, Deep Diving in Female Northern Elephant Seals, *Mirounga Angustirostris*. Canadian Journal of Zoology 66:446-458.

Lee, Z., M. Darecki, K. L. Carder, C. O. Davis, D. Stramski, and W. J. Rhea. 2005a. Diffuse attenuation coefficient of downwelling irradiance: An evaluation of remote sensing methods. Journal of Geophysical Research: Oceans 110:C02017.

Lee, Z., K. Du, and R. Arnone. 2005b. A model for the diffuse attenuation coefficient of downwelling irradiance. Journal of Geophysical Research: Oceans 110:C02016.

Legendre, P. 2018. Model II regression user's guide, R edition. R Vignette.

Lewis, M. R., and T. Platt. 1982. Scales of variability in estuarine ecosystems. Pages 3-20 *in* V.S. Kennedy, editors. Estuarine Comparisons, Academic Press.

Leys, C., C. Ley, O. Klein, P. Bernard, and L. Licata. 2013. Detecting outliers: Do not use standard deviation around the mean, use absolute deviation around the median. Journal of Experimental Social Psychology 49:764-766.

Li, W. K., and W. G. Harrison. 2008. Propagation of an atmospheric climate signal to phytoplankton in a small marine basin. Limnology and Oceanography 53:1734-1745.

Li, W. K., M. R. Lewis, and W. G. Harrison. 2010. Multiscalarity of the nutrient–chlorophyll relationship in coastal phytoplankton. Estuaries and Coasts 33:440-447.

Li, W. K., W. Glen Harrison, and E. J. Head. 2006. Coherent assembly of phytoplankton communities in diverse temperate ocean ecosystems. Proceedings of the Royal Society B: Biological Sciences 273:1953-1960.

Li, Y., P. S. Fratantoni, C. Chen, J. A. Hare, Y. Sun, R. C. Beardsley, and R. Ji. 2015. Spatio-temporal patterns of stratification on the Northwest Atlantic shelf. Progress in Oceanography 134:123-137.

Li, W. K. W., W. G. Harrison, and E. J. H. Head. 2006. Coherent assembly of phytoplankton communities in diverse temperate ocean ecosystems. Proceedings of the Royal Society B: Biological Sciences 273:1953-1960.

Li, W., and P. Dickie. 2001. Monitoring phytoplankton, bacterioplankton, and virioplankton in a coastal inlet (Bedford Basin) by flow cytometry. Cytometry 44:236-246.

Lidgard, D., W. Bowen, and D. Boness. 2012. Longitudinal changes and consistency in male physical and behavioural traits have implications for mating success in the grey seal (*Halichoerus grypus*). Canadian Journal of Zoology 90:849-860.

Lidgard, D. C., W. D. Bowen, I. D. Jonsen, and S. J. Iverson. 2014. Predator-borne acoustic transceivers and GPS tracking reveal spatiotemporal patterns of encounters with acoustically tagged fish in the open ocean. Marine Ecology Progress Series 501:157-168.

Lidgard, D. C., D. J. Boness, W. D. Bowen, and J. I. McMillan. 2005. State-dependent male mating tactics in the grey seal: the importance of body size. Behavioral Ecology 16:541-549.

Lidgard, D. C., D. J. Boness, W. D. Bowen, and J. I. McMillan. 2003. Diving behaviour during the breeding season in the terrestrially breeding male grey seal: implications for alternative mating tactics. Canadian Journal of Zoology-Revue Canadienne De Zoologie 81:1025-1033.

Loder, J. W. 1998. The coastal ocean off northeastern North America: A large-scale view. The Sea 11:105-138.

Loder, J.W., G. Han, P.S. Galbraith, J. Chassé, and A. van der Baaren (Eds.). 2013. Aspects of climate change in the Northwest Atlantic off Canada. Can. Tech. Rep. Fish. Aquat. Sci. 3045: x + 190 p.

Loder, J. W., G. Han, C. G. Hannah, D. A. Greenberg, and P. C. Smith. 1997. Hydrography and baroclinic circulation in the Scotian Shelf region: winter versus summer. Canadian Journal of Fisheries and Aquatic Sciences 54:40-56.

Lonneville, B., P. Oset García, L. Schepers, B. Vanhoorne, F. Hernandez, and J. Mees. 2019. Marine regions. Flanders Marine Institute. www.marineregions.org.

Longhurst, A. 1995. Seasonal cycles of pelagic production and consumption. Progress in Oceanography 36:77-167.

Lowther, A. D., R. G. Harcourt, B. Page, and S. D. Goldsworthy. 2013. Steady as he goes: at-sea movement of adult male Australian sea lions in a dynamic marine environment. PLoS ONE 8(9): e74348.

Lowther, A. D., C. Lydersen, and K. M. Kovacs. 2016. The seasonal evolution of shelf water masses around Bouvetoya, a sub-Antarctic island in the mid-Atlantic sector of the Southern Ocean, determined from an instrumented southern elephant seal. Polar Research 35:28278.

Lucey, S. M., and J. A. Nye. 2010. Shifting species assemblages in the northeast US continental shelf large marine ecosystem. Marine Ecology Progress Series 415:23-33.

Lyamin, O. I., L. M. Mukhametov, and J. M. Siegel. 2017. Sleep in the northern fur seal. Current Opinion in Neurobiology 44:144-151.

Lydersen, C., O. A. Nøst, K. M. Kovacs, and M. A. Fedak. 2004. Temperature data from Norwegian and Russian waters of the northern Barents Sea collected by free-living ringed seals. Journal of Marine Systems 46:99-108.

Macarthur, R. H., and E. R. Pianka. 1966. On Optimal use of a Patchy Environment. American Naturalist 100:603-609.

Mahon, R., and R. Smith. 1989. Demersal Fish Assemblages on the Scotian Shelf, Northwest Atlantic - Spatial-Distribution and Persistence. Canadian Journal of Fisheries and Aquatic Sciences 46:134-152.

Malpress, V., S. Bestley, S. Corney, D. Welsford, S. Labrousse, M. Sumner, and M. Hindell. 2017. Bio-physical characterisation of polynyas as a key foraging habitat for juvenile male southern elephant seals (Mirounga leonina) in Prydz Bay, East Antarctica. Plos One 12:e0184536.

Manov, D., G. Chang, and T. Dickey. 2004. Methods for reducing biofouling of moored optical sensors. Journal of Atmospheric and Oceanic Technology 21:958-968.

McClintock, B. T., D. S. Johnson, M. B. Hooten, J. M. Ver Hoef, and J. M. Morales. 2014. When to be discrete: the importance of time formulation in understanding animal movement. Movement Ecology 2:21.

McConnell, B., C. Chambers, and M. Fedak. 1992. Foraging Ecology of Southern Elephant Seals in Relation to the Bathymetry and Productivity of the Southern-Ocean. Antarctic Science 4:393-398.

McIntyre, T., I. J. Ansorge, H. Bornemann, J. Ploetz, C. A. Tosh, and M. N. Bester. 2011. Elephant seal dive behaviour is influenced by ocean temperature: implications for climate change impacts on an ocean predator. Marine Ecology Progress Series 441:257-272.

Mellish, J. A. E., S. J. Iverson, and W. D. Bowen. 1999. Variation in milk production and lactation performance in grey seals and consequences for pup growth and weaning characteristics. Physiological and Biochemical Zoology 72:677-690.

Methratta, E. T., and J. S. Link. 2006. Seasonal variation in groundfish habitat associations in the Gulf of Maine-Georges Bank region. Marine Ecology Progress Series 326:245-256.

Miller, P. I., K. L. Scales, S. N. Ingram, E. J. Southall, and D. W. Sims. 2015. Basking sharks and oceanographic fronts: quantifying associations in the north-east Atlantic. Functional Ecology 29:1099-1109.

Mohn, R., and W. Bowen. 1996. Grey seal predation on the eastern Scotian Shelf: Modelling the impact on Atlantic cod. Canadian Journal of Fisheries and Aquatic Sciences 53:2722-2738.

Montes-Hugo, M., S. C. Doney, H. W. Ducklow, W. Fraser, D. Martinson, S. E. Stammerjohn, and O. Schofield. 2009. Recent Changes in Phytoplankton Communities Associated with Rapid Regional Climate Change Along the Western Antarctic Peninsula. Science 323:1470-1473.

Moore, S.E. 2008. Marine mammals as ecosystem sentinels. Journal of Mammalogy 89:534-540.

Moore, J. K., W. Fu, F. Primeau, G. L. Britten, K. Lindsay, M. Long, S. C. Doney, N. Mahowald, F. Hoffman, and J. T. Randerson. 2018. Sustained climate warming drives declining marine biological productivity. Science 359:1139-1142.

Moore, T. S., J. W. Campbell, and M. D. Dowell. 2009. A class-based approach to characterizing and mapping the uncertainty of the MODIS ocean chlorophyll product. Remote Sensing of Environment 113:2424-2430.

Morales, J. M., D. T. Haydon, J. Frair, K. E. Holsinger, and J. M. Fryxell. 2004. Extracting more out of relocation data: building movement models as mixtures of random walks. Ecology 85:2436-2445.

Morel, A. 1988. Optical modeling of the upper ocean in relation to its biogenous matter content (case I waters). Journal of Geophysical Research: oceans 93:10749-10768.

Morel, A., and S. Maritorena. 2001. Bio-optical properties of oceanic waters: A reappraisal. Journal of Geophysical Research-Oceans 106:7163-7180.

Morel, A., and H. Loisel. 1998. Apparent optical properties of oceanic water: dependence on the molecular scattering contribution. Applied Optics 37:4765-4776.

Morel, A., and A. Bricaud. 1981. Theoretical Results Concerning Light-Absorption in a Discrete Medium, and Application to Specific Absorption of Phytoplankton. Deep-Sea Research Part A-Oceanographic Research Papers 28:1375-1393.

Morel, A., and L. Prieur. 1977. Analysis of Variations in Ocean Color. Limnology and Oceanography 22:709-722.

Morel, A., B. Gentili, M. Chami, and J. Ras. 2006. Bio-optical properties of high chlorophyll Case 1 waters and of yellow-substance-dominated Case 2 waters. Deep-Sea Research Part I-Oceanographic Research Papers 53:1439-1459.

Moses, W. J., A. A. Gitelson, S. Berdnikov, and V. Povazhnyy. 2009. Estimation of chlorophyll-a concentration in case II waters using MODIS and MERIS data-successes and challenges. Environmental Research Letters 4:045005.

Muller-Karger, F. E., R. Varela, R. Thunell, R. Luerssen, C. Hu, and J. J. Walsh. 2005. The importance of continental margins in the global carbon cycle. Geophysical Research Letters 32:L01602.

Nakanowatari, T., K. I. Ohshima, V. Mensah, Y. Mitani, K. Hattori, M. Kobayashi, F. Roquet, Y. Sakurai, H. Mitsudera, and M. Wakatsuchi. 2017. Hydrographic observations by instrumented marine mammals in the Sea of Okhotsk. Polar Science 13:56-65.

Neuenhoff, R. D., D. P. Swain, S. P. Cox, M. K. McAllister, A. W. Trites, C. J. Walters, and M. O. Hammill. 2018. Continued decline of a collapsed population of Atlantic cod (Gadus morhua) due to predation-driven Allee effects. Canadian Journal of Fisheries and Aquatic Sciences 76:168-184.

Nordstrom, C.A., B.C. Battaile, C. Cotté, and A.W. Trites. 2013a. Foraging habits of lactating northern fur seals are structured by thermocline depths and submesoscale fronts in the eastern Bering Sea. Deep-Sea Research II 88-89:78-96.

Nordstrom, C. A., K. J. Benoit-Bird, B. C. Battaile, and A. W. Trites. 2013b. Northern fur seals augment ship-derived ocean temperatures with higher temporal and spatial resolution data in the eastern Bering Sea. Deep Sea Research Part II: Topical Studies in Oceanography 94:257-273.

Nye, J. A., J. S. Link, J. A. Hare, and W. J. Overholtz. 2009. Changing spatial distribution of fish stocks in relation to climate and population size on the Northeast United States continental shelf. Marine Ecology Progress Series 393:111-129.

Nye, J. A., A. Bundy, N. Shackell, K. D. Friedland, and J. S. Link. 2010. Coherent trends in contiguous survey time-series of major ecological and commercial fish species in the Gulf of Maine ecosystem. ICES Journal of Marine Science 67:26-40.

O'Boyle, R., and M. Sinclair. 2012. Seal-cod interactions on the Eastern Scotian Shelf: Reconsideration of modelling assumptions. Fisheries Research 115:1-13.

Ohashi, K., and J. Sheng 2013. Influence of St. Lawrence River discharge on the circulation and hydrography in Canadian Atlantic waters. Continental Shelf Research 58:32-49.

Ohashi, K., J. Sheng, K. R. Thompson, C. G. Hannah, and H. Ritchie. 2009. Numerical study of three-dimensional shelf circulation on the Scotian Shelf using a shelf circulation model. Continental Shelf Research 29:2138-2156.

O'Reilly, J. E., S. Maritorena, B. G. Mitchell, D. A. Siegel, K. L. Carder, S. A. Garver, M. Kahru, and C. McClain. 1998. Ocean color chlorophyll algorithms for SeaWiFS. Journal of Geophysical Research: Oceans 103:24937-24953.

Orians, G. H. and N.E. Pearson. 1979. On the theory of central place foraging. Pages 155-177 *in* J. Horn, G.R. Stairs, and R.D. Mitchell, editors. Analysis of Ecological Systems. Ohio State Press, Columbus, Ohio, USA.

O'Toole, M. D., M. Lea, C. Guinet, R. Schick, and M. A. Hindell. 2015. Foraging strategy switch of a top marine predator according to seasonal resource differences. Frontiers in Marine Science 2:21.

O'Toole, M. D., M. Lea, C. Guinet, and M. A. Hindell. 2014. Estimating Trans-Seasonal Variability in Water Column Biomass for a Highly Migratory, Deep Diving Predator. Plos One 9:e113171.

Padman, L., D. P. Costa, S. T. Bolmer, M. E. Goebel, L. A. Huckstadt, A. Jenkins, B. I. McDonald, and D. R. Shoosmith. 2010. Seals map bathymetry of the Antarctic continental shelf. Geophysical Research Letters 37:L21601.

Panteleev, G., B. de Young, M. Luneva, C. Reiss, and E. Semenov. 2004. Modeling the circulation of Western Bank on the Scotian Shelf through sequential application of a variational algorithm and a nonlinear model. Journal of Geophysical Research: Oceans 109:C02003.

Patterson, T. A., B. J. McConnell, M. A. Fedak, M. V. Bravington, and M. A. Hindell. 2010. Using GPS data to evaluate the accuracy of state-space methods for correction of Argos satellite telemetry error. Ecology 91:273-285.

Perry, R. I., and S. J. Smith. 1994. Identifying habitat associations of marine fishes using survey data: an application to the Northwest Atlantic. Canadian Journal of Fisheries and Aquatic Sciences 51:589-602.

Petrie, B., P. Yeats and P. Strain. 1999. Nitrate, silicate and phosphate atlas for the Scotian Shelf and the Gulf of Maine. Can. Tech. Rep. Hydrogr. Ocean Sci. 203, vii + 96 pp.

Petrie, 8., K. Drinkwater, D. Gregory, R. Pettipas and A. Sandstrom. 1996. Temperature and salinity atlas for the Scotian Shelf and the Gulf of Maine. Can. Tech. Rep. Hydrogr. Ocean Sci. 171: v + 398 pp.

Petrie, B. 2007. Does the North Atlantic Oscillation affect hydrographic properties on the Canadian Atlantic continental shelf? Atmosphere-Ocean 45:141-151.

Platt, T., A. Prakash, and B. Irwin. 1972. Phytoplankton nutrients and flushing of inlets on the coast of Nova Scotia. Naturaliste Canadien 99: 253-261.

Platt, T., and A. W. Herman. 1983. Remote sensing of phytoplankton in the sea: surface-layer chlorophyll as an estimate of water-column chlorophyll and primary production. International Journal of Remote Sensing 4:343-351.

Platt, T., S. Sathyendranath, M. Forget, G. N. White III, C. Caverhill, H. Bouman, E. Devred, and S. Son. 2008. Operational estimation of primary production at large geographical scales. Remote Sensing of Environment 112:3437-3448.

Platt, T., C. Fuentes-Yaco, and K. T. Frank. 2003. Spring algal bloom and larval fish survival. Nature 423:398-399.

Polovina, J. J., G. H. Balazs, E. A. Howell, D. M. Parker, M. P. Seki, and P. H. Dutton. 2004. Forage and migration habitat of loggerhead (*Caretta caretta*) and olive ridley (*Lepidochelys olivacea*) sea turtles in the central North Pacific Ocean. Fisheries Oceanography 13:36-51.

Prieur, L., and S. Sathyendranath. 1981. An optical classification of coastal and oceanic waters based on the specific spectral absorption curves of phytoplankton pigments, dissolved organic matter, and other particulate materials 1. Limnology and Oceanography 26:671-689.

Prince, S. D., and S. N. Goward. 1995. Global primary production: a remote sensing approach. Journal of Biogeography 22:815-835.

R Core Team. 2018. R: A language and environment for statistical computing. R Foundation for Statistical Computing, Vienna.

Ream, R. R., J. T. Sterling, and T. R. Loughlin. 2005. Oceanographic features related to northern fur seal migratory movements. Deep-Sea Research Part II-Topical Studies in Oceanography 52:823-843.

Remer, L. A., Y. J. Kaufman, D. Tanre, S. Mattoo, D. A. Chu, J. V. Martins, R. R. Li, C. Ichoku, R. C. Levy, R. G. Kleidman, T. F. Eck, E. Vermote, and B. N. Holben. 2005. The MODIS aerosol algorithm, products, and validation. Journal of the Atmospheric Sciences 62:947-973.

Ricard, D., and Shackell, N. L. 2013. Population status (abundance/ biomass, geographic extent, body size and condition), preferred habitat, depth, temperature and salinity preferences of marine fish and invertebrates on the Scotian Shelf and Bay of Fundy (1970-2012). Can. Tech. Rep. Fish. Aquat. Sci., 3012: vii + 181 p.

Richardson, K., A. W. Visser, and F. B. Pedersen. 2000. Subsurface phytoplankton blooms fuel pelagic production in the North Sea. Journal of Plankton Research 22:1663-1671.

Richaud, B., Y. Kwon, T. M. Joyce, P. S. Fratantoni, and S. J. Lentz. 2016. Surface and bottom temperature and salinity climatology along the continental shelf off the Canadian and US East Coasts. Continental Shelf Research 124:165-181.

Riser, S. C., H. J. Freeland, D. Roemmich, S. Wijffels, A. Troisi, M. Belbéoch, D. Gilbert, J. Xu, S. Pouliquen, A. Thresher, P. Le Traon, G. Maze, B. Klein, M. Ravichandran, F. Grant, P. Poulain, T. Suga, B. Lim, A. Sterl, P. Sutton, K. Mork, P. J. Vélez-Belchi, I. Ansorge, B. King, J. Turton, M. Baringer, and S. R. Jayne. 2016. Fifteen years of ocean observations with the global Argo array. Nature Climate Change 6: 145-153.

Robinson, P. W., S. E. Simmons, D. E. Crocker, and D. P. Costa. 2010. Measurements of foraging success in a highly pelagic marine predator, the northern elephant seal. Journal of Animal Ecology 79:1146-1156.

Rochelle-Newall, E., and T. Fisher. 2002. Production of chromophoric dissolved organic matter fluorescence in marine and estuarine environments: an investigation into the role of phytoplankton. Marine Chemistry 77:7-21.

Roemmich, D., G.C. Johnson, S. Riser, R. Davis, J. Gilson, W.B. Owens, S.L. Garzoli, C. Schmid, and M. Ignaszewski. 2009. The Argo Program: Observing the global ocean with profiling floats. Oceanography 22:34–43.

Roquet, F., J. Charrassin, S. Marchand, L. Boehme, M. Fedak, G. Reverdin, and C. Guinet. 2011. Delayed-mode calibration of hydrographic data obtained from animal-borne satellite relay data loggers. Journal of Atmospheric and Oceanic Technology 28:787-801.

Roquet, F., G. Williams, M. A. Hindell, R. Harcourt, C. McMahon, C. Guinet, J. Charrassin, G. Reverdin, L. Boehme, P. Lovell, and M. Fedak. 2014. A Southern Indian Ocean database of hydrographic profiles obtained with instrumented elephant seals. Scientific Data 1:140028.

Roquet, F., C. Wunsch, G. Forget, P. Heimbach, C. Guinet, G. Reverdin, J. Charrassin, F. Bailleul, D. P. Costa, L. A. Huckstadt, K. T. Goetz, K. M. Kovacs, C. Lydersen, M. Biuw, O. A. Nost, H. Bornemann, J. Ploetz, M. N. Bester, T. McIntyre, M. C. Muelbert, M. A. Hindell, C. R. McMahon, G. Williams, R. Harcourt, I. C. Field, L. Chafik, K. W. Nicholls, L. Boehme, and M. A. Fedak. 2013. Estimates of the Southern Ocean general circulation improved by animal-borne instruments. Geophysical Research Letters 40:6176-6180.

Ross, T., S. E. Craig, A. Comeau, R. Davis, M. Dever, and M. Beck. 2017. Blooms and subsurface phytoplankton layers on the Scotian Shelf: Insights from profiling gliders. Journal of Marine Systems 172:118-127.

Sarmiento, J., T. Hughes, R. Stouffer, and S. Manabe. 1998. Simulated response of the ocean carbon cycle to anthropogenic climate warming. Nature 393:245-249.

Sarmiento, J., R. Slater, R. Barber, L. Bopp, S. Doney, A. Hirst, J. Kleypas, R. Matear, U. Mikolajewicz, P. Monfray, V. Soldatov, S. Spall, and R. Stouffer. 2004. Response of ocean ecosystems to climate warming. Global Biogeochemical Cycles 18:GB3003.

Sathyendranath, S., A. Longhurst, C. M. Caverhill, and T. Platt. 1995. Regionally and seasonally differentiated primary production in the North Atlantic. Deep Sea Research Part I: Oceanographic Research Papers 42:1773-1802.

Saunders, R., and K. Kriebel. 1988. An Improved Method for Detecting Clear Sky and Cloudy Radiances from Avhrr Data. International Journal of Remote Sensing 9:123-150.

Sauzede, R., H. Lavigne, H. Claustre, J. Uitz, C. Schmechtig, F. D'Ortenzio, C. Guinet, and S. Pesant. 2015. Vertical distribution of chlorophyll a concentration and phytoplankton community composition from in situ fluorescence profiles: a first database for the global oceanVertical distribution of chlorophyll a concentration and phytoplankton community composition from in situ fluorescence profiles: a first database for the global ocean. Earth System Science Data 7:261-273.

Scales, K. L., E. L. Hazen, M. G. Jacox, C. A. Edwards, A. M. Boustany, M. J. Oliver, and S. J. Bograd. 2017. Scale of inference: on the sensitivity of habitat models for wide-ranging marine predators to the resolution of environmental data. Ecography 40:210-220.

Scales, K. L., P. I. Miller, C. B. Embling, S. N. Ingram, E. Pirotta, and S. C. Votier. 2014. Mesoscale fronts as foraging habitats: composite front mapping reveals oceanographic drivers of habitat use for a pelagic seabird. Journal of the Royal Society Interface 11:UNSP 20140679.

Schroeder, T., I. Behnert, M. Schaale, J. Fischer, and R. Doerffer. 2007. Atmospheric correction algorithm for MERIS above case-2 waters. International Journal of Remote Sensing 28:1469-1486.

Scott, J. S. 1982. Depth Temperature and Salinity Preferences of Common Fishes of the Scotian Shelf Canada. Journal of Northwest Atlantic Fishery Science 3:29-40.

Scott, W. B. and M. G. Scott. 1988. Atlantic fishes of Canada. Canadian Bulletin of Fisheries and Aquatic Sciences 219.

Shackell, N. L., and K. T. Frank. 2007. Compensation in exploited marine fish communities on the Scotian Shelf, Canada. Marine Ecology Progress Series 336:235-247.

Shackell, N. L., D. Ricard, and C. Stortini. 2014. Thermal habitat index of many Northwest Atlantic temperate species stays neutral under warming projected for 2030 but changes radically by 2060. PLoS One 9:e90662.

Shackell, N. L., A. Bundy, J. A. Nye, and J. S. Link. 2012. Common large-scale responses to climate and fishing across Northwest Atlantic ecosystems. ICES Journal of Marine Science 69:151-162.

Shackell, N. L., K. T. Frank, J. A. Fisher, B. Petrie, and W. C. Leggett. 2009. Decline in top predator body size and changing climate alter trophic structure in an oceanic ecosystem. Proceedings of the Royal Society B: Biological Sciences 277:1353-1360.

Shan, S., and J. Sheng. 2012. Examination of circulation, flushing time and dispersion in Halifax Harbour of Nova Scotia. Water Quality Research Journal of Canada 47:353-374.

Shan, S., J. Sheng, K. R. Thompson, and D. A. Greenberg. 2011. Simulating the three-dimensional circulation and hydrography of Halifax Harbour using a multi-nested coastal ocean circulation model. Ocean Dynamics 61:951-976.

Sheng, J. 2001. Dynamics of a buoyancy-driven coastal jet: The Gaspe Current. Journal of Physical Oceanography 31:3146-3162.

Siegel, D., S. Maritorena, N. Nelson, M. Behrenfeld, and C. McClain. 2005. Colored dissolved organic matter and its influence on the satellite-based characterization of the ocean biosphere. Geophysical Research Letters 32:L20605.

Siemann, L. A., C. J. Huntsberger, J. S. Leavitt, and R. J. Smolowitz. 2018. Summering on the bank: Seasonal distribution and abundance of monkfish on Georges Bank. Plos One 13:e0206829.

Simmons, S. E., Y. Tremblay, and D. P. Costa. 2009. Pinnipeds as ocean-temperature samplers: calibrations, validations, and data quality. Limnology and Oceanography-Methods 7:648-656.

Simpson, J. H., and J. Sharples. 2012. Introduction to the physical and biological oceanography of shelf seas. Cambridge University Press, Cambridge, England.

Sims, D. W., E. J. Southall, N. E. Humphries, G. C. Hays, C. J. Bradshaw, J. W. Pitchford, A. James, M. Z. Ahmed, A. S. Brierley, and M. A. Hindell. 2008. Scaling laws of marine predator search behaviour. Nature 451:1098.

Sinclair, M., M. Power, E. Head, W. K. W. Li, M. McMahon, R. Mohn, R. O'Boyle, D. Swain, and J. Tremblay. 2015. Eastern Scotian Shelf trophic dynamics: A review of the evidence for diverse hypotheses. Progress in Oceanography 138:305-321.

Sinclair, M., and T. D. Iles. 1985. Atlantic Herring (*Clupea-Harengus*) Distributions in the Gulf of Maine Scotian Shelf Area in Relation to Oceanographic Features. Canadian Journal of Fisheries and Aquatic Sciences 42:880-887.

Sinclair, M., M. Power, E. Head, W. K. W. Li, M. McMahon, R. Mohn, R. O'Boyle, D. Swain, and J. Tremblay. 2015. Eastern Scotian Shelf trophic dynamics: A review of the evidence for diverse hypotheses. Progress in Oceanography 138:305-321.

Smith, R. C., and K. S. Baker. 1981. Optical properties of the clearest natural waters (200–800 nm). Applied Optics 20:177-184.

Smith, P., and F. Schwing. 1991. Mean Circulation and Variability on the Eastern Canadian Continental-Shelf. Continental Shelf Research 11:977-1012.

Smith, R., and K. Baker. 1978. Optical Classification of Natural-Waters. Limnology and Oceanography 23:260-267.

Song, H., R. Ji, C. Stock, and Z. Wang. 2010. Phenology of phytoplankton blooms in the Nova Scotian Shelf–Gulf of Maine region: remote sensing and modeling analysis. Journal of Plankton Research 32:1485-1499.

Sousa, L. L., N. Queiroz, G. Mucientes, N. E. Humphries, and D. W. Sims. 2016. Environmental influence on the seasonal movements of satellite-tracked ocean sunfish *Mola mola* in the north-east Atlantic. Animal Biotelemetry 4:7.

Springer, A. M., D. G. Roseneau, E. C. Murphy, and M. I. Springer. 1984. Environmental Controls of Marine Food Webs - Food-Habits of Seabirds in the Eastern Chukchi Sea. Canadian Journal of Fisheries and Aquatic Sciences 41:1202-1215.

Sterling, J. T., A. M. Springer, S. J. Iverson, S. P. Johnson, N. A. Pelland, D. S. Johnson, M. Lea, and N. A. Bond. 2014. The Sun, Moon, Wind, and Biological Imperative-Shaping Contrasting Wintertime Migration and Foraging Strategies of Adult Male and Female Northern Fur Seals (Callorhinus ursinus). Plos One 9:e93068.

Stevick, P. T., L. S. Incze, S. D. Kraus, S. Rosen, N. Wolff, and A. Baukus. 2008. Trophic relationships and oceanography on and around a small offshore bank. Marine Ecology Progress Series 363:15-28.

Stobo, W. T., B. Beck, and J. K. Horne. 1990. Seasonal movements of grey seals (*Halichoerus grypus*) in the Northwest Atlantic. Canadian Bulletin of Fisheries and Aquatic Sciences 222:199-213.

Stortini, C. H., N. L. Shackell, P. Tyedmers, and K. Beazley. 2015. Assessing marine species vulnerability to projected warming on the Scotian Shelf, Canada. ICES Journal of Marine Science 72:1731-1743.

Strain, P. M., and P. A. Yeats. 2005. Nutrients in The Gully, Scotian Shelf, Canada. Atmosphere-Ocean 43:145-161.

Strickland, J.D.H. 1965. Phytoplankton and Marine Primary Production. Annual Review of Microbiology 19:127-162.

Sumner, M., K. Michael, C. Bradshaw, and M. Hindell. 2003. Remote sensing of Southern Ocean sea surface temperature: implications for marine biophysical models. Remote Sensing of Environment 84:161-173.

Sverdrup, H.U. 1953. On conditions for the vernal blooming of phytoplankton. ICES Journal of Marine Science 18:287-295.

Swain, D. P., G. A. Chouinard, R. Morin, and K. F. Drinkwater. 1998. Seasonal variation in the habitat associations of Atlantic cod (Gadus morhua) and American plaice (*Hippoglossoides platessoides*) from the southern Gulf of St. Lawrence. Canadian Journal of Fisheries and Aquatic Sciences 55:2548-2561.

Sydeman, W. J., R. D. Brodeur, C. B. Grimes, A. S. Bychkov, and S. McKinnell. 2006. Marine habitat "hotspots" and their use by migratory species and top predators in the North Pacific Ocean: Introduction. Deep-Sea Research Part II-Topical Studies in Oceanography 53:247-249.

Teo, S. L. H., R. M. Kudela, A. Rais, C. Perle, D. P. Costa, and B. A. Block. 2009. Estimating chlorophyll profiles from electronic tags deployed on pelagic animals. Aquatic Biology 5:195-207.

Thompson, D., P. Hammond, K. Nicholas, and M. Fedak. 1991. Movements, Diving and Foraging Behavior of Gray Seals (Halichoerus-Grypus). Journal of Zoology 224:223-232.

Thys, T. M., J. P. Ryan, H. Dewar, C. R. Perle, K. Lyons, J. O'Sullivan, C. Farwell, M. J. Howard, K. C. Weng, B. E. Lavaniegos, G. Gaxiola-Castro, L. E. Miranda Bojorquez, E. L. Hazen, and S. J. Bograd. 2015. Ecology of the Ocean Sunfish, *Mola mola*, in the southern California Current System. Journal of Experimental Marine Biology and Ecology 471:64-76.

Treasure, A. M., F. Roquet, I. J. Ansorge, M. N. Bester, L. Boehme, H. Bornemann, J. Charrassin, D. Chevallier, D. P. Costa, and M. A. Fedak. 2017. Marine mammals exploring the oceans pole to pole: a review of the MEOP consortium. Oceanography 30:132-138.

Trzcinski, M. K., R. Mohn, and W. D. Bowen. 2006. Continued decline of an Atlantic cod population: How important is gray seal predation? Ecological Applications 16:2276-2292.

Tucker, S., W. D. Bowen, and S. J. Iverson. 2007. Dimensions of diet segregation in grey seals Halichoerus grypus revealed through stable isotopes of carbon (delta C-13) and nitrogen (delta N-15). Marine Ecology Progress Series 339:271-282.

Tuszynski, J. 2014. Tools: moving window statistics, GIF, Base64, ROC AUC, etc. R Package Version 1.17.1.2

Twardowski, M. S., E. Boss, J. M. Sullivan, and P. L. Donaghay. 2004. Modeling the spectral shape of absorption by chromophoric dissolved organic matter. Marine Chemistry 89: 69-88.

Vacquie-Garcia, J., C. Guinet, C. Laurent, and F. Bailleul. 2015. Delineation of the southern elephant seal's main foraging environments defined by temperature and light conditions. Deep-Sea Research Part II-Topical Studies in Oceanography 113:145-153.

Vacquie-Garcia, J., J. Mallefet, F. Bailleul, B. Picard, and C. Guinet. 2017. Marine Bioluminescence: Measurement by a Classical Light Sensor and Related Foraging Behavior of a Deep Diving Predator. Photochemistry and Photobiology 93:1312-1319.

Venables, W. N. and Ripley, B. D. (2002) Modern Applied Statistics with S. Fourth Edition. Springer, New York. ISBN 0-387-95457-0.

Walther, G., E. Post, P. Convey, A. Menzel, C. Parmesan, T. Beebee, J. Fromentin, O. Hoegh-Guldberg, and F. Bairlein. 2002. Ecological responses to recent climate change. Nature 416:389-395.

Wang, M., and W. Shi. 2007. The NIR-SWIR combined atmospheric correction approach for MODIS ocean color data processing. Optics Express 15:15722-15733.

Welschmeyer, N. A. 1994. Fluorometric analysis of chlorophyll a in the presence of chlorophyll b and pheopigments. Limnology and Oceanography 39:1985-1992.

Whittingham, M. J., P. A. Stephens, R. B. Bradbury, and R. P. Freckleton. 2006. Why do we still use stepwise modelling in ecology and behaviour? Journal of Animal Ecology 75:1182-1189.

Whoriskey, K., with contributions from C. M. Albertsen. 2017. swim: Switching Markov Movement Models. R package version 0.2.4.

Whoriskey, K., M. Auger-Methe, C. M. Albertsen, F. G. Whoriskey, T. R. Binder, C. C. Krueger, and J. Mills Flemming. 2017. A hidden Markov movement model for rapidly identifying behavioral states from animal tracks. Ecology and Evolution 7:2112-2121.

Worcester, T., and M. Parker. 2010. Ecosystem Status and Trends Report for the Gulf of Maine and Scotian Shelf. DFO Can. Sci. Advis. Sec. Res. Doc. 2010/070. vi + 59 p.

Wynn, R. B., V. A. Huvenne, T. P. Le Bas, B. J. Murton, D. P. Connelly, B. J. Bett, H. A. Ruhl, K. J. Morris, J. Peakall, and D. R. Parsons. 2014. Autonomous Underwater Vehicles (AUVs): Their past, present and future contributions to the advancement of marine geoscience. Marine Geology 352:451-468.

Xie, H., C. Aubry, S. Bélanger, and G. Song. 2012. The dynamics of absorption coefficients of CDOM and particles in the St. Lawrence estuarine system: Biogeochemical and physical implications. Marine Chemistry 128:44-56.

Xing, X., H. Claustre, S. Blain, F. D'Ortenzio, D. Antoine, J. Ras, and C. Guinet. 2012. Quenching correction for in vivo chlorophyll fluorescence acquired by autonomous platforms: A case study with instrumented elephant seals in the Kerguelen region (Southern Ocean). Limnology and Oceanography: Methods 10:483-495.

Yen, P. P. W., W. J. Sydeman, S. J. Bograd, and K. D. Hyrenbach. 2006. Spring-time distributions of migratory marine birds in the southern California Current: Oceanic eddy associations and coastal habitat hotspots over 17 years. Deep-Sea Research Part II-Topical Studies in Oceanography 53:399-418.

Zhou, J., J. Wang, A. Baudon, and A. T. Chow. 2013. Improved Fluorescence Excitation-Emission Matrix Regional Integration to Quantify Spectra for Fluorescent Dissolved Organic Matter. Journal of Environmental Quality 42:925-930.

Zwanenburg, K. 2000. The effects of fishing on demersal fish communities of the Scotian Shelf. ICES Journal of Marine Science 57:503-509.

APPENDIX A: SUPPLEMENTAL TABLES

Table A.1 Total number of locations where (a) sea surface temperature (SST; ºC), (b) upper-water column temperature (T_{50}; ºC), (c) mixed layer depth (MLD; m), and (d) chlorophyll-*a* concentration (chl-*a*; mg m^{-3}) were measured by month and by year of deployment; totals do not include observations made in January.

(a) SST

	Jun	**Jul**	**Aug**	**Sep**	**Oct**	**Nov**	**Dec**	**Total**
2009	0	0	0	0	12741	31080	27772	71593
2010	0	0	0	11728	31898	35561	26887	106074
2011	7939	12449	9305	9687	16004	16296	13180	84860
2012	795	4732	4467	4302	4075	4084	3981	26436
2013	1433	15714	14756	14691	17075	19134	15554	98357
2014	9860	19047	15720	16230	21485	24801	18430	125573
2015	4918	9904	6820	7699	10129	12736	11881	64087

(b) T_{50}

	Jun	**Jul**	**Aug**	**Sep**	**Oct**	**Nov**	**Dec**	**Total**
2009	0	0	0	0	7719	15931	15572	39222
2010	0	0	0	7648	24193	20241	18418	70500
2011	6263	9356	4894	6138	11072	8245	8120	54088
2012	273	2667	2770	3245	2454	2063	1478	14950
2013	916	10668	9208	9026	11618	12630	10015	64081
2014	7623	14058	8260	8001	14370	16386	7748	76446
2015	5967	12280	4614	7173	11263	11713	10409	63419

(c) MLD

	Jun	Jul	Aug	Sep	Oct	Nov	Dec	Total
2009	0	0	0	0	8913	17860	13517	40290
2010	0	0	0	10091	29905	22922	17168	80086
2011	6971	10783	7189	8141	14239	10665	7390	65378
2012	559	3904	3786	3918	3626	2519	1285	19597
2013	1111	13499	13070	12931	15741	15142	7686	79180
2014	8671	17146	12930	12479	17368	19655	7841	96090
2015	6920	14012	7296	8756	12334	13178	9438	71934

(d) Chl-*a*

	Jun	Jul	Aug	Sep	Oct	Nov	Dec	Total
2009	0	0	0	0	649	1246	815	2710
2010	0	0	0	1042	3814	3660	3217	11733
2011	708	1084	683	848	1381	1267	1527	7498
2012	45	360	353	438	290	374	166	2026
2013	140	1659	1400	1381	1751	2071	1671	10073
2014	1151	2259	1252	1104	2339	2951	1321	12377
2015	366	669	168	176	317	437	291	2424

Table A.2 Sample mean and standard deviations of oceanographic properties measured by grey seals (n = 79) including chlorophyll-*a* concentration (chl-*a*; mg m^{-3}), upper-water column temperature (T_{50}; ºC), bottom temperature (ºC), bottom depth (m), and bottom duration (s) used in the Water Column Model (Model 1) and Bottom Conditions Model (Model 2); values are separated by season, sex, and behavioural states estimated by hidden Markov movement models.

	Transiting				**Foraging**			
	Male		**Female**		**Male**		**Female**	
	Summer	**Fall**	**Summer**	**Fall**	**Summer**	**Fall**	**Summer**	**Fall**
Chl-*a*	0.52	0.39	0.41	0.36	0.54	0.42	0.39	0.38
σ	0.16	0.23	0.19	0.20	0.19	0.22	0.16	0.20
T_{50}	9.38	8.77	8.78	9.28	8.84	9.02	8.68	9.06
σ	2.11	2.37	2.25	2.66	1.76	2.36	2.28	2.44
Bottom Temperature	5.42	6.50	5.35	6.07	5.34	6.50	6.05	5.77
σ	4.12	3.52	3.24	3.08	4.86	4.00	4.33	3.32
Bottom Depth	59.63	63.21	67.32	65.29	60.42	60.44	63.90	64.17
σ	35.76	39.78	39.56	37.74	37.24	39.14	36.38	33.57
Bottom Duration	209.16	211.47	303.35	269.41	216.17	198.95	297.63	259.29
σ	95.40	89.61	142.47	111.41	104.33	95.87	154.17	120.67